MOBILE 24-INCH SATELLITE PHOTOMETRIC OBSERVATORY

Final Report

Distribution of this report is provided in the interest of information exchange. Responsibility for the contents resides in the author or organization that prepared it.

14 October 1966

Prepared under Contract NAS 1-5580
by Goodyear Aerospace Corporation
Akron, Ohio

for

NATIONAL AERONAUTICS & SPACE ADMINISTRATION

CONTENTS

ILLUSTRATIONS

# MOBILE 24-INCH SATELLITE PHOTOMETRIC OBSERVATORY

SUMMARY

The objective of this contract was to design, fabricate, check out, and field test a transportable ground-based photometric facility for satellite observation and measurement. This was accomplished by providing an f/20 Cassegrainian telescope with a 24-inch aperture housed in a truck-mounted van. The forward compartment of the van houses the optical and electronic equipment, and the aft compartment deploys to form an observation deck. The self-supporting observatory contains electrical power generating equipment, air conditioning and heating equipment, control equipment, and instrumentation equipment. The facility was tested by measuring the light intensity of satellites in orbit and calibrated by measurements of the intensity of known stars.

INTRODUCTION

The requirements for this program were generated under a previous contract, NAS 1-4669, entitled "Program Definition Study for Evaluating Satellite Materials by Ground-Based Photometry." Phase I of that program determined the fundamental aspects of ground-based photometric techniques for evaluating the stability of satellite materials.

It was concluded that a satellite's material characteristics could be determined by measuring and analyzing the optical field scattered from the satellite. Phase II outlined a plan for the design, fabrication, and testing of a mobile 24-inch telescope and associated equipment. Phase III described the use of the proposed equipment for observation of satellites in orbit. The present contract, NAS 1-5580, implemented Phase II of the study.

This report will describe the design, fabrication, and testing of the ground-based photometric equipment for satellite observation and measurement. The system consists of a mobile 24-inch telescope instrumented for the measurement of optical field intensity, intensity distribution versus wave length, and intensity versus polarization. The sketch shows the principles applied in the development of the system. The optical field generated by sunlight scattered from an artificial earth satellite is precisely determined by the satellite's material characteristics, configuration, and composition, and by its orientation and position with respect to the sun and earth. As the satellite orbits about the earth, the optical field intensity and the degree of polarization of the reflected light can be measured by an observer.
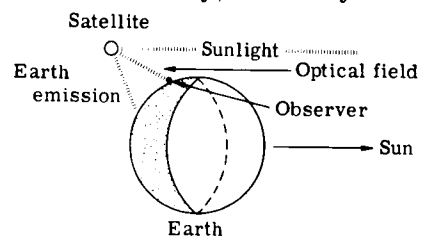
The photometric equipment consists of a transportable 24-inch telescope instrumented for sequential measurements of the optical field intensity and the degree of polarization in each of three spectral bands. Photoelectric methods are used to measure the intensity of light passing through known field apertures mounted at the focal plane of the 24-inch telescope. The spectral band is determined by appropriate filters inserted in the optical path. To determine the degree of polarization, a rotating analyzer is placed in the optical path. A detailed discussion of the parameters that can be established by the use of ground-based photometric measurements is presented in Appendix A.

SYMBOLS

A	weighting coefficient for specular reflection	I_{max}	plane polarized light intensity, maximum, lm
A_T	aperture of telescope	I_{min}	plane polarized light intensity, minimum, lm
B	weighting coefficient for diffuse reflection; also, standard light transmission in the blue spectrum; number of degrees per cycle of ripple	J_T	total inertia of the load, lb-ft-sec^2
		K_A	amplifier gain
D	satellite distance, feet; also, diameter of camera aperture; ripple voltage ratio	K_B	back EMF, volts/rad/sec
		K_F	tachometer voltage sensitivity, volts/rad/sec
d	field stop diameter	K_M	operator's gain
E	energy density incident on camera, lm/cm^2	K_T	torque sensitivity, lb-ft/amp
		k	extinction coefficient
E_d	diffuse component of illuminance, lm/cm^2	L_M	armature inductance, henries
E_0	illuminance value at zero stellar magnitude, lm/cm^2	M	photometric system sensitivity margin for a 10th magnitude visual band input
E_M	input voltage to motor, volts	m	measured (apparent) magnitude
E_I	input to the velocity loop, volts	m_0	extra-atmospheric stellar magnitude
E_s	solar illuminance on the satellite, lm/cm^2	m_{sp}	specular component of satellite magnitude
E_{sp}	specular component of illuminance, lm/cm^2	m_v	extra-atmospheric stellar magnitude in the visible spectrum
E_v	light energy density in the visible spectrum, lm/cm^2	$m_\odot$	solar magnitude
e_i	amplifier input, volts	P	degree of polarization
e_o	amplifier output, volts	P_{mag}	polarization magnitude
F	intercepted light flux, lm	P%	percent polarization
f	f number of camera	pfm	photographic figure of merit
fl	focal length	R	satellite radius, feet
$f(\psi)$	Russell phase function	R_A	amplifier output resistance, ohms
G_1	photomultiplier cathode sensitivity, microamperes/lm	R_c	radius of curvature, feet
		R_M	motor armature resistance, ohms
G_2	photomultiplier gain	R_s	reflection of light at an optical surface
HA	hour angle of the star		
I	image diameter	R_{s1}	reflection coefficient of primary mirror
I_c	cathode current of photomultiplier, amp	R_{s2}	reflection coefficient of secondary mirror
I_p	plate current of photomultiplier, amp		

R_{S3}	reflection at surface of field lens	U	standard light transmission in the ultraviolet spectrum
R_T	total resistance in armature circuit, ohms	V	standard light transmission in the visible spectrum
R_W	wiring resistance, ohms		
r	total solar reflectance	W	energy from a field or a satellite, watts
s	specularity	X	air mass, No. of zenith atmospheres
S	Laplace operator	Z	zenith distance, deg
S_1	photometer maximum sensitivity, amp	γ	specular reflectance
S.R.	slant range, feet	$\Delta\theta$	peak ripple amplitude, deg
T_a	apparent transmissivity	δ	declination of the star, deg
T_{a1}	transmission through atmosphere	θ	observer's latitude, deg
T_{a2}	transmission through field lens	θ_i	input displacement, deg
T_{a3}	transmission through filters	θ_o	output displacement, deg
T_{a4}	transmission through compensating plate	θ_T	telescope displacement, deg
		τ_E	electrical time constant, sec
T_{a5}	transmission through Lyot depolarizer	τ_M	mechanical time constant, sec
		ϕ	angle describing an imaged field, deg
T_D	torque disturbance, lb-ft	ψ	phase angle, deg
T_f	transmittance of field lens	Ω	angular velocity of satellite relative to observer, deg/sec

DESIGN PARAMETERS

The contract lists equipment to be provided and design parameters as follows:

(1)   Provide a vehicle with the required stability to permit operation at improved or un-improved sites which have reasonably stable soil conditions. Transient excursions of less than 1 second of time constant are not to exceed a few seconds of arc under normal operating conditions, including such disturbances as those caused by the movement of personnel and wind variations up to 20 mph. The chassis is to be a 10 by 8 tandem type with rear tandem drive, capable of maintaining a minimum road speed of 60 mph when loaded and traveling on a level expressway. The wheel base and spring specification will be determined with due consideration to weight and equipment layout.

(2)   Provide a telescope with a large aperture (approximately 24 inches in diameter). Primary emphasis of the design is to be placed on light-gathering capabilities for effectiveness in photometric performance, rather than on image resolution.

(3)   Provide appropriate sensors and sensing devices so that the system is capable of reliable and repeatable photometric measurements of satellites as faint as an apparent visual magnitude of +8.

(4)   Provide electronic instrumentation and equipment to process and record the sensor signals, as well as other pertinent and necessary data.

(5)   Conduct a complete test and check-out operation to verify the proper operation of the complete unit and all of its parts.

(6)   Conduct a trial field test as an acceptance test to verify the operational readiness of the system under realistic operating conditions.

DESCRIPTION OF EQUIPMENT

The Truck and Van

General. - The NASA Satellite Photometric Observatory (fig. 1) is a self-propelled, self-supporting mobile observatory consisting of a telescope complex, electrical power-generating equipment, air conditioning and heating equipment, hydraulic equipment, control equipment, photometric equipment, and auxiliary telescope equipment housed in a truck-mounted van. A system of jacks and leveling indicators permits the entire van and truck frame to be elevated and leveled as required for an observation mission.

The observatory has a road weight of 32 000 pounds, including truck weight. In the transport configuration, the complete unit is 28 feet long, 8 feet wide, and 12.5 feet high. In the deployed configuration, the unit is 32 feet long, 25 feet wide (maximum width), and 12.5 feet high (with telescope horizontal).

The truck. - The truck provides a mobile platform for the observatory van. It is a truck chassis with ten wheels and a 92-inch conventional cab. The truck has special springs to provide a "soft" ride for the observatory van. Operating and equipment specifications for the truck are listed below.

(1)   Truck suitable for mounting a special van approximately 20 feet long x 8 feet wide x 112-1/2 inches high (including 1/2-inch thick wood strips on chassis frame). Nominal frame height, with the loads specified below, 37-1/2 inches.

(2)   Total weight of the van (including all contents and attachments but excluding any part of the truck) constant at 21 000 pounds, ±2000 pounds, with the center of gravity approximately 11 feet behind the cab. A 6000-pound telescope, included in the 21 000 pound total, will be 14 feet behind the cab.

(3)   The vehicle will operate on primary or secondary roads in continental United States at altitudes up to 12 000 feet and to adjacent off-road field sites normally negotiable by a standard automobile.

(4)   The cruising speed on a level highway will be not less than 60 mph.

(5)   The cab will accommodate the driver and two passengers.

(6)   The dynamic loading of the truck to the telescope under normal road conditions will be a maximum of 1-1/2 g's vertically and 1-g along any other orthogonal axis. These loadings may occur simultaneously. Vertical loadings may range to a maximum of
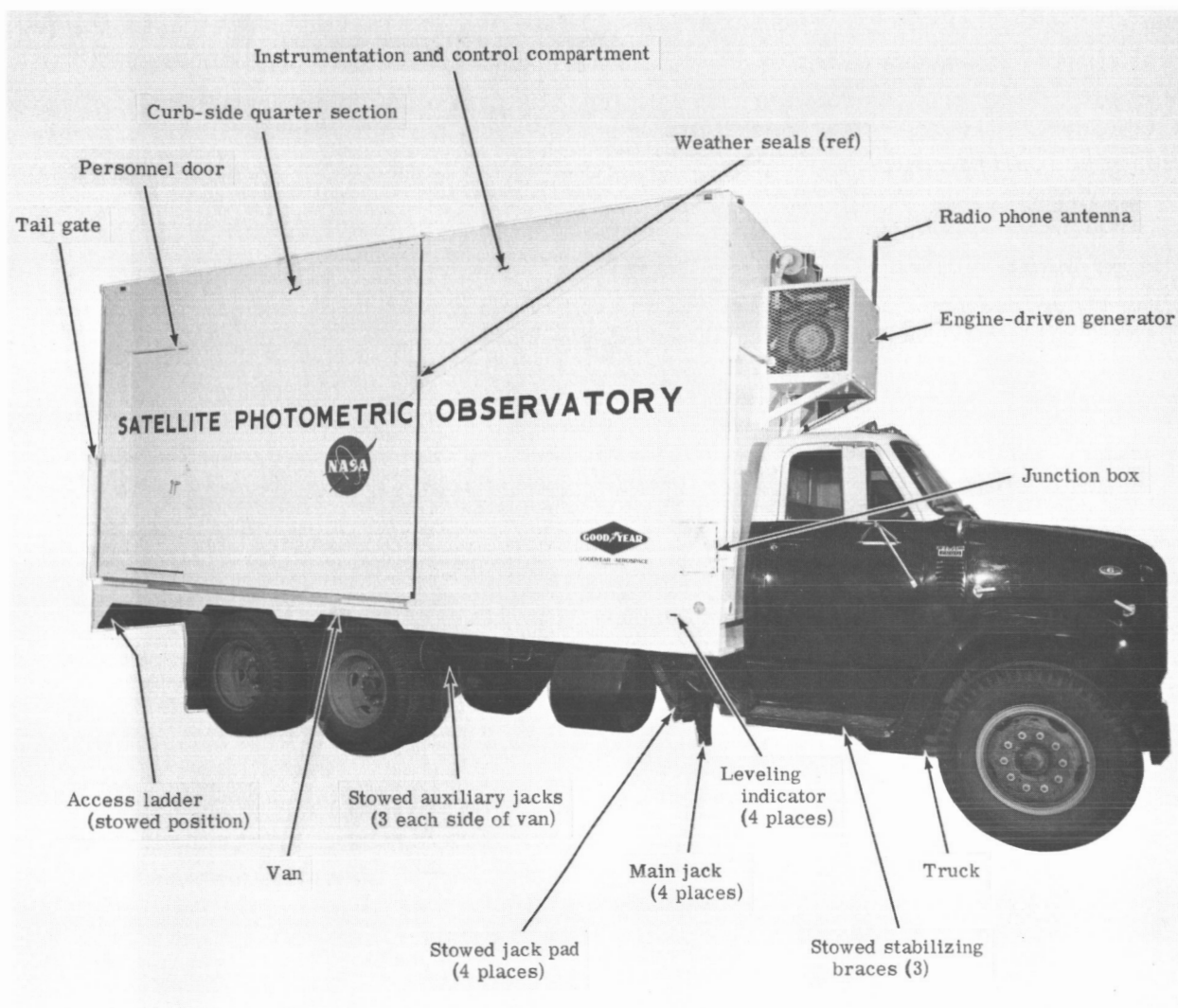
Figure 1. - NASA Mobile Photometric Observatory in transport configuration.

2-1/2 g's on rare occasions for extreme conditions not normally anticipated. The vertical loadings of 1-1/2 g's and 2-1/2 g's are interpreted as 1/2 and 1-1/2 g's respectively in addition to the weight of the telescope. The telescope will be mounted on a rigid van floor structure, which will be attached to the truck frame in a conventional manner.

The van. - The van (fig. 1) houses the telescope complex, the associated controlling and monitoring equipment, and miscellaneous auxiliary equipment. In the transport configuration the van is 20 feet long, 8 feet wide, and 9 feet 3 inches high. A personnel door is located near the aft end of the curb-side wall. The van will be described as consisting of two parts: the forward housing, called the instrumentation and control compartment; and an expandable aft housing, called the observation deck.

Instrumentation and control compartment: The instrumentation and control compartment

5

(also referred to as "forward compartment" and "equipment compartment") is a rectangular enclosure at the forward end of the van. The enclosure covers a deck area 8 feet long and 8 feet wide. A personnel door in the aft wall permits entry and exit of personnel between the compartment and the observation deck. The compartment contains the operating, controlling, monitoring, and recording equipment associated with the telescope complex, plus storage cupboards and miscellaneous auxiliary equipment. Location of the equipment is shown in figures 2 and 3. Mounted at the aft end of the streetside wall, but not visible in figure 2, is a light switch panel and the deployment control panel.

Observation deck: The aft 12-foot length of the van encloses the telescope complex when the unit is in the transport configuration. When the unit is in the deployed configuration, a system of parting lines and hinges permits the rear wall and the aft 12-foot length of the side-walls to swing outward and down to the horizontal position to form an observation deck 25 feet wide by 16 feet long (see fig. 4). Weather-tight seals at the parting lines prevent entry of dust and water when the van is in the transport configuration. Four hydraulic cylinders, two for each wall, are used to raise and lower the two side wall sections.

Van descriptions. - Detailed descriptions of the structure and equipment are given in the following paragraphs.

The primary floor structure is a weldment of steel structural channel members and plates, including the mounting surface for the telescope and the hard points for the lifting jacks. This structure provides all the strength and stiffness required in the floor for satisfactory operation of the telescope when elevated by the jacks to an unsprung height. Except for the telescope mounting pads, the upper surface of the floor consists of one-fourth-inch steel plates in one plane throughout the interior length and width of the van. The floor is capable of withstanding a general loading of 300 lb/ft^2 and a minimum concentrated loading of 200 $lb/in.^2$ The entire floor, except for the telescope mounting pads, has a non-skid surface. Two 2-inch conduits are installed between the telescope and the aft right corner of the closed portion of the van.

The walls and roof are of standard commercial custom van construction, nominally two inches thick. They are composed of a steel framework, two inches of fiberglass insulation, and aluminum or steel skins.

The aft compartment of the van converts to an open platform by pivoting each side wall (with half the top and half the rear wall) outward about a hinge line at the floor level. Adjustable posts support the lowered side walls from the ground at approximately the same level as the van floor. Each extended side wall is capable of supporting two 200-pound men walking on its surface, without causing permanent deformation. The two rear wall panels are hinged to the side walls and can be lowered to form additional floor surface. Floor surface at the rear of the van spans the area between the rear wall panels.

A personnel access door is provided on the curb side near the rear wall. A partition across the aft end of the forward 8-foot portion of the van encloses the operations area, obscuring all lighting in that area from the telescope. This partition is a rigid wall with a 30 by 75-inch sliding door. Removable access steps at the rear of the van permit access from the ground.

When the van is closed for travel or for storage, the interior is completely sealed against road dust and driving rain.

Four leveling jacks are provided with the van. Each jack attachment to the primary structure spans the two structural channels so that the direct column load is taken by the

6
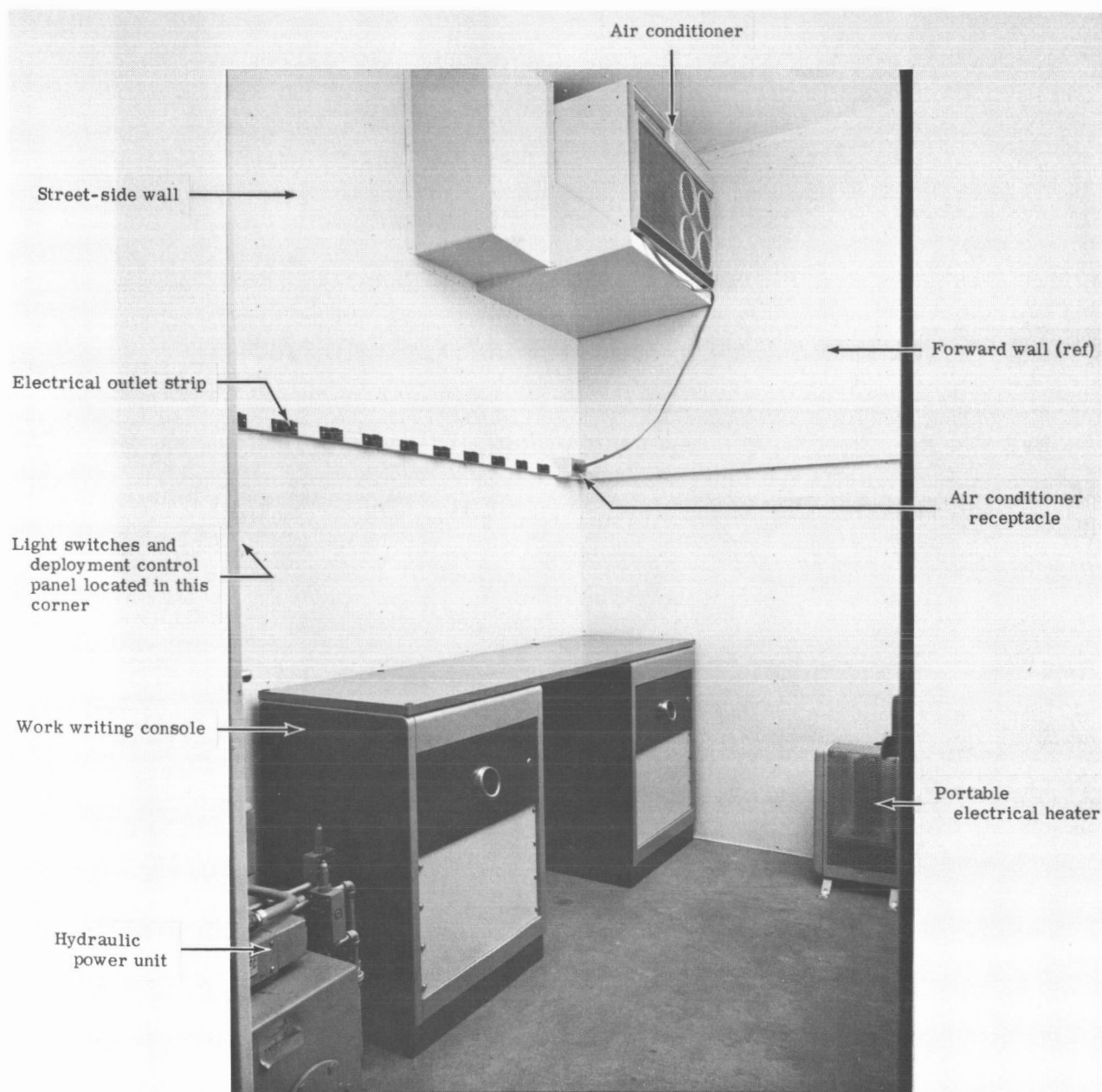
Figure 2. - Street-side wall of forward compartment (overhead storage cabinets not shown).

Power circuit breaker box

Generator control panel

Forward wall (ref)

Radio receiver

Tape recorder

Photometer

Operational amplifier assembly

Video monitor

Control assembly

Monitor assembly

Recording oscillograph

Manual control

Power amplifier (polar servo)

Power amplifier (declination servo)

28 Vdc power supply

Connector assembly (behind panel)

Terminal strip (behind panel)
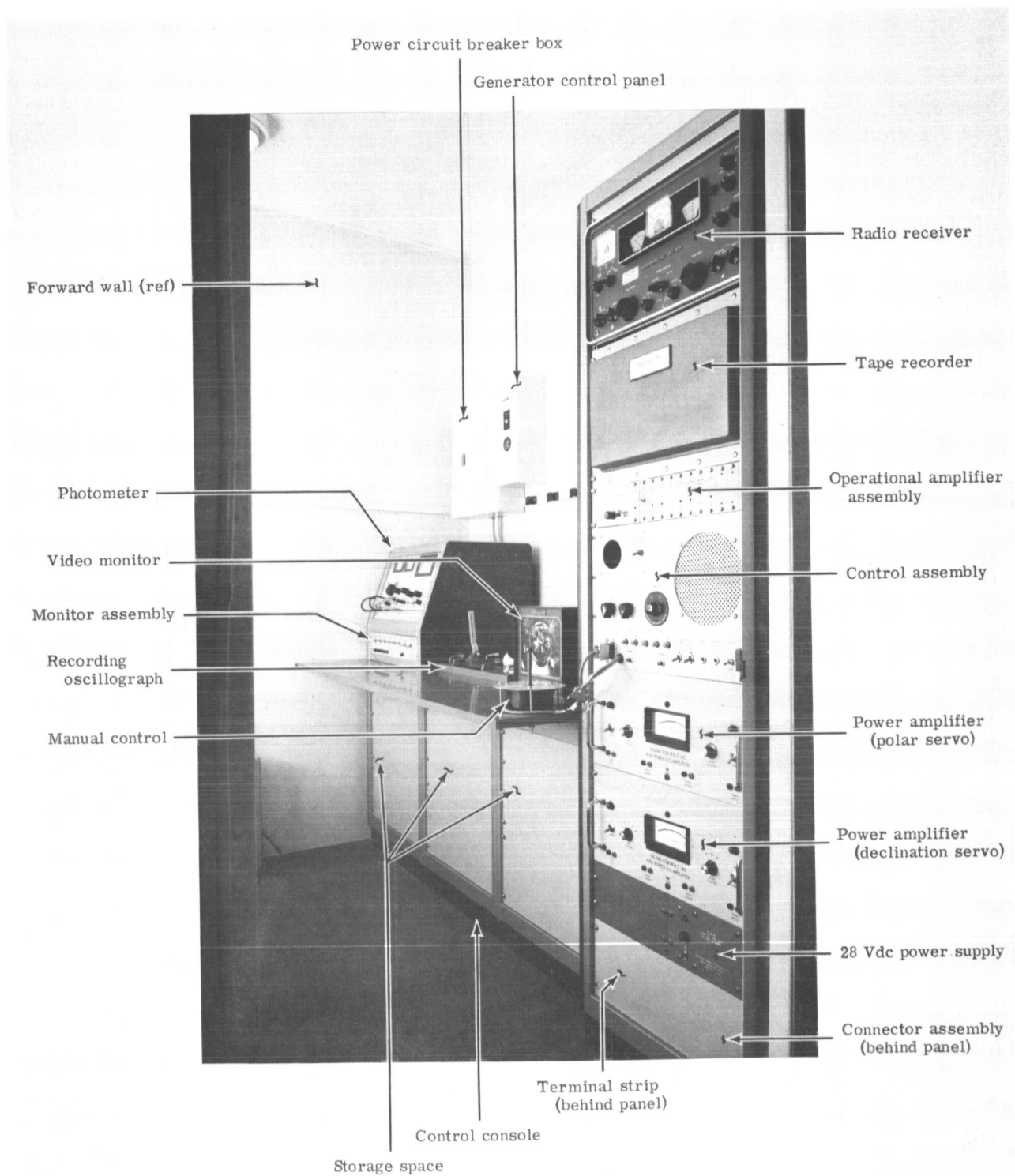
Control console

Storage space

Figure 3. - Curb-side wall of forward compartment (overhead storage cabinets not shown).
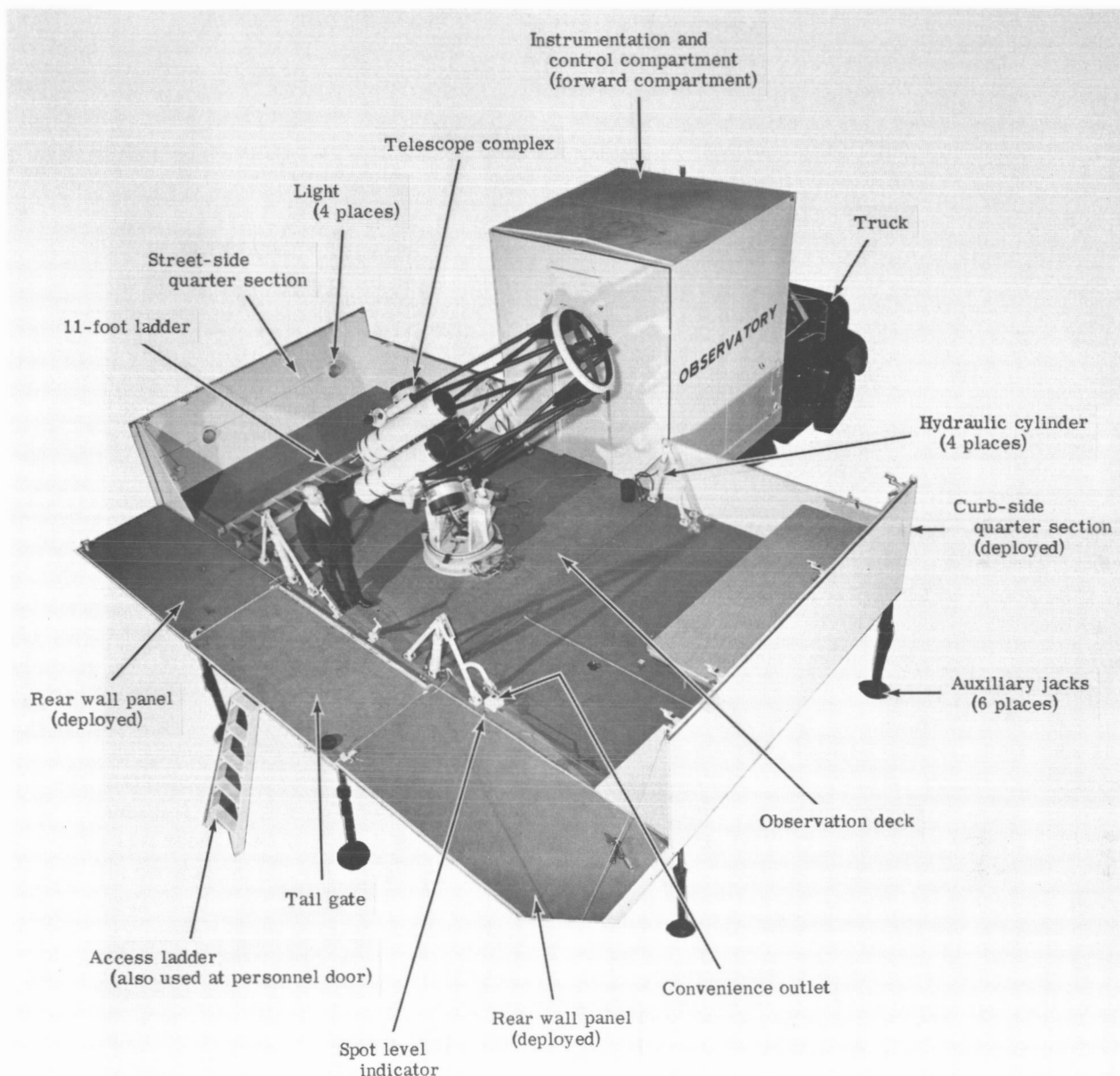
Figure 4. - Mobile photometric observatory in deployed configuration.

channels. Two additional jacks provided for use under the front bumper prevent cantilevering the cab end of the truck when leveling the van floor. The gear-type leveling jacks are crank-operated, two-speed, retractable, and with removable 18-inch-square, self-aligning bases. The two front jacks are standard commercial type. Any combination of three jacks is capable of supporting the combined load of the truck, van, and contents (32 000 pounds maximum). The jacks have sufficient elevation range to level the assembly at an unsprung height on ground slopes up to 2-1/2° lengthwise or 5° crosswise.

A hydraulic van conversion actuator system, operable only from inside the van, opens and closes the observation deck. The actuator system is equipped with safety features to

prevent damage if all latches are not released. The power unit is capable of 1.5 gallons per minute, contains two four-way valves, and is driven by a 1-hp electric motor. Primary power for the motor is 110 volts, 60 Hz.

The van air conditioner is a commercial window unit rated at 11 000 Btu. The unit operates on 115 volts and consumes 1340 watts. Two fan speeds are provided. When recirculating air, the unit is rated at 270 or 240 ft^3/min. When using external air, the unit moves 90 or 75 ft^3/min. Exterior openings are provided with covers to be applied when the air conditioner is not in use.

An engine generator is mounted over the cab in a special compartment attached to the front wall of the van. The single phase, two-wire unit is rated at 10 000 watts, 120 volts, 60 Hz. Vibration isolators attach the unit to the floor of the compartment. Acoustical materials minimize the transmission of noise and vibration to the inside of the van. A residential type muffler is installed on the engine exhaust pipe above the compartment. Ignition wiring is extended to the truck's battery, and fuel is supplied from the truck's fuel tank by an electric fuel pump. Controls for remote operation of the generator are panel-mounted on the inside right wall, close to the forward end of the van.

The heater is equipped with a built-in thermostatic control, and is a radiant convection electric heater rated at 1500 watts.

A power distribution panel is provided and located on the right side wall. The circuit breaker numbers and their functions are:

1 - Main	7 - Control assembly
2 - Air conditioner	8 - Lights
3 - Main	9 - Telescope power
4 - Curb-side receptacles	10 - Convenience outlets (in console)
5 - Road-side receptacles	11 - Plug strip (in cabinet)
6 - Hydraulic power unit	12 - Spare

Plug-in strips with duplex outlets are installed on both side walls and extend the entire length of the forward compartment. A weatherproof receptacle connected to the distribution panel is installed on the outside of the van to receive either the 120-volt output of the generator or 120-volt power from a remote source (not both at one time). The receptacle and associated wiring are capable of handling the load normally derived from the generator.

Two combination 120- and 12-volt ceiling lights are installed in the forward housing of the van and four in the aft housing (observation deck). The forward lights are operated by a switch in the forward area near the door frame. The rear lights are operated by three-way switches, one located inside the van, adjacent to the rear door, and one in the forward area, beside the switch for the forward lights. Relays are provided to actuate the 12-volt lighting system when 120-volt power is not available.

The generator control box contains the start/stop switch for the motor-generator set, a run time meter, and a charging ammeter.

Items provided for emergency use on the highway include (1) three fuse-type warning flares, (2) three warning flags, (3) one warning reflector pack, (4) two CO_2-type fire

extinguishers, (5) one sealed-beam headlamp, (6) two type 1034 lamp bulbs, (7) two type 1073 lamp bulbs, and (8) two type 67 lamp bulbs.

Control System Equipment

General. - The polar and declination axes of the telescope are manually controlled by two identical control systems. Figure 5 is a block diagram of one of the systems. Each loop consists of one axis of a hand control, hand control excitation power module, demodulator, compensation amplifiers, power amplifiers, and the drive torquer-tachometer unit.

Manual control. - A two-axis hand control is provided for controlling the polar and declination axes of the telescope. It is an a-c excited stiff-stick transducer, which produces phase reversing voltages proportional to applied force. The d-c demodulators are built into the base of the control. Ten pounds of force produce approximately 0.9 volt d-c output with 8 volts, 400 Hz excitation.

Power module. - The excitation for the hand control is obtained from a 400-Hz sine wave power module. The input to this module is unregulated 28 Vdc. It provides a regulated 115 volt, 400-Hz output. This in turn is stepped down to 8 volts, 400 Hz through a small power transformer. The power module and step-down transformer are both located on the control assembly chassis. A small power resistor is connected to the terminals of the step-down transformer to provide a continuous minimum load.

Operational amplifier assembly. - The preamplifiers for the control system are chopper-stabilized, d-c operational amplifiers. They have the following open loop characteristics: input impedance, 0.5 MΩ; voltage gain, 160 dB; gain stability versus temperature, 0.1 dB/^{o}C; gain stability versus supply, 0.2 dB/%; gain bandwidth product, 30 Mc/sec; output impedance, 0.5 kilohm; rated output voltage, ±10 volts; rated output current, ±20 mA; and specification temperature range, -25 to +80°C. Six of these amplifier modules and the associated compensation circuit modules are mounted in a rack mount adapter which has a self-contained plus and minus 15 Vdc power supply. Line and load regulation for this supply is 0.1 percent, and noise and ripple are less than 100 microvolts rms.

Power amplifiers. - The polar and declination servos use identical power amplifiers. These units are high-power D-C amplifiers designed for operation with the torquer motors and tachometers installed in the telescope mount. This is a completely solid-state unit, rated at 500 watts at a peak voltage of ±56 Vdc. By switch resistors in the feedback path, fixed gains of 10, 20, 50, 100 and 200 V/V can be selected. At minimum gain of 10, the amplifier bandwidth is 10 kc; at the maximum gain of 200, the bandwidth is 1 kc. A magnetically regulated power supply operating from 115 Vac is integrally packaged with the amplifier.

Control assembly. - The control assembly provides the control functions for the polar and declination axes. This unit contains the power switch that controls power to the operational amplifier assembly and the power amplifiers, the polar and declination brake switches, the limit of travel and level unit indicators, rate controls for the two axes, and the connector for the hand control. Also on this unit is the speaker for the receiver, the time signal demodulator, the time signal and mike audio mixers, the signal modulated tone generator, and a video switch for camera 1 or 2 selection for the monitor.

28 Vdc power supply. - A 28-volt power supply furnishes non-regulated voltage for relay
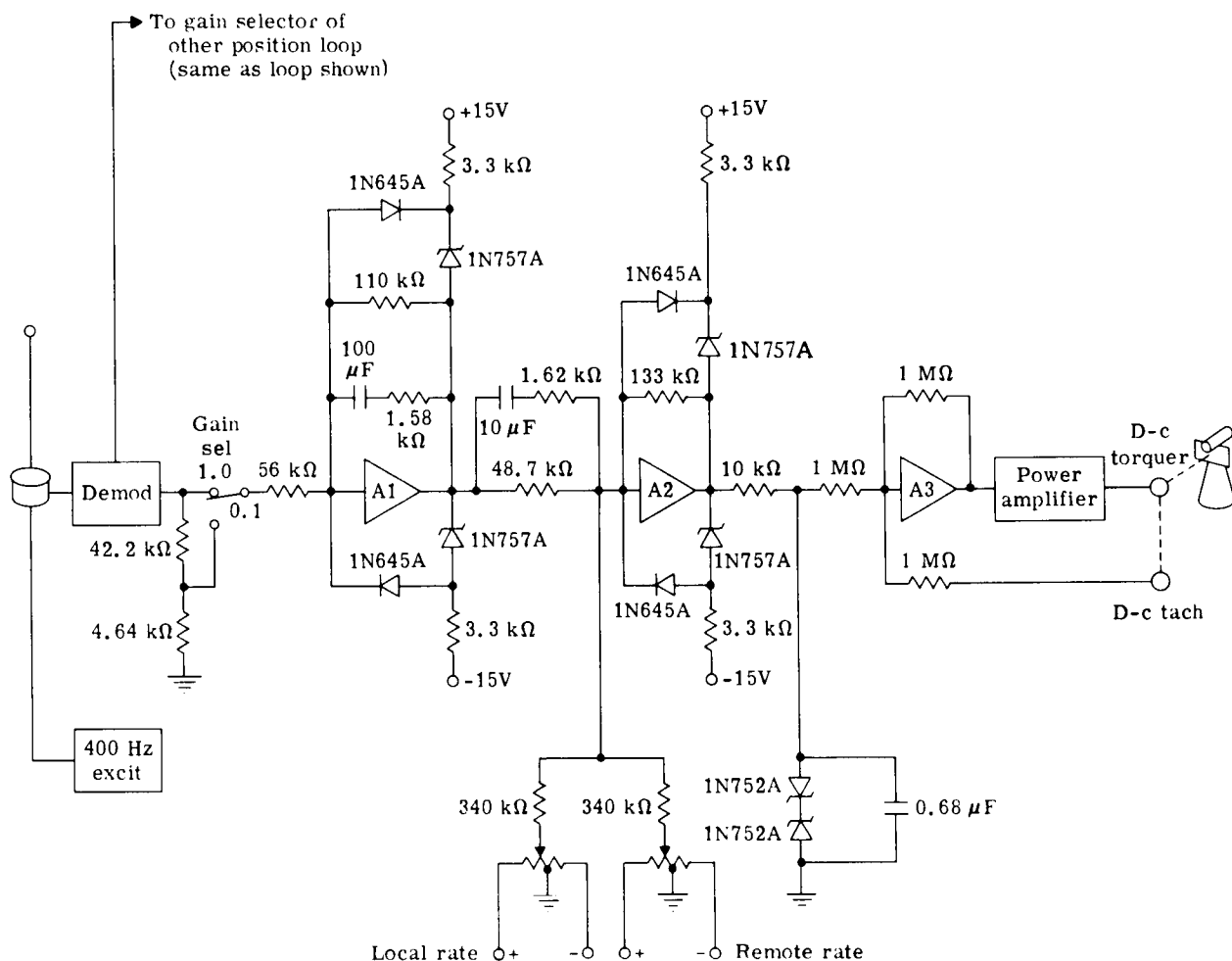
Figure 5. - Control system block diagram.

and solenoid operations. The unit contains silicon rectifiers in a full-wave rectifier circuit and RC filtering. The ripple voltage is less than 1 volt rms and the internal impedance is less than 0.4 ohm.

Drive system. - The drives are gearless d-c torquer-tachometer units. They are built into the axes, thus eliminating the gearing. The torquer has the following characteristics: peak torque 22 lb-ft, voltage of peak torque 51 volts, current at peak torque 9.6 amperes, and a torque sensitivity of 2.3 lb-ft/A. The tachometer has a sensitivity of 105 volts/radian/ second, 0.25 percent ripple maximum, and 279 ripple cycles per revolution.

Control box. - The rate potentiometers for servo control of the polar and declination axes are repeated on this portable unit, as are provisions for mounting the hand control.

12

Instrumentation System Equipment

General. - The instrumentation system is the heart of the photometric facility. The system accepts the light from the star or satellite, determines the frequency band by the use of filters, determines the polarization, converts the light to an electrical signal, records the signal, determines and records the time reference, and records other auxiliary signals.

The system comprises the 24-inch telescope, the instrumentation assembly, a photometer, a monitor assembly, a signal-modulated tone generator, a recording oscillograph, a receiver, and a tape recorder.

System description. - A simplified block diagram of the system is shown in figure 6.

The light from the satellite is gathered by the 24-inch Cassegrainian telescope, passed through a polarizer and a color filter, and focused at the aperture plate. The polarizer filter is driven by a 12 steps/revolution digimotor through a 3 to 1 gear ratio. The polarizer assembly is so constructed that the polarizer lens can be manually folded out of the light path. Three filter bands are contained in the instrumentation assembly: the U band in the 3600 Å region, the B band in the 4200 Å region, and the V band in the 5300 Å region. Two sets of these filters are arranged on a wheel, which is driven by a 12 steps/revolution digimotor. Two pulses are required to step from filter to filter. The order of the filters is B-U-V-B-U-V. The sequence can be started with any filter. The aperture slide contains apertures of 4, 2, 1 and 0.5 minutes of arc. Except for the largest aperture, the apertures are in pairs. Two solenoid-actuated shutters control the action of the apertures.

The image aperture is controlled by a normally open shutter, and the adjacent aperture (sky background) by a normally closed shutter. This is the normal position for recording photometric data. By closing the normally open shutter on the image aperture and opening the normally closed shutter, a measurement is made of the sky background adjacent to the satellite. Closing both shutters gives a measurement of the photomultiplier dark current.

The light from the aperture is passed through a condensing lens and a depolarizer filter and impinges on the photosensitive cathode of the photomultiplier. The depolarizer filter eliminates the slightly polarized sensitivity of the photomultiplier. The condensing lens collimates the light on a large area of the cathode of the photomultiplier. This eliminates any variations due to supersensitive spots on the cathode.

The output of the photomultiplier is amplified by the photometer and recorded on an oscillograph. The high voltage for the photomultiplier is also generated by the photometer.

The signal output of the photometer is also provided to the signal modulated tone generator. This is a voltage-sensitive transistor oscillator, with an audio signal that decreases in pitch when a signal is present. This tone is used by the tracking operator to aurally verify that the satellite is within the aperture of the instrumentation system.

To correlate the photometric data with orbital parameters, calibration stars, zenith angles, etc, a time signal from Station WWV is received and demodulated for recording on the oscillograph trace. The signal is also mixed with spoken commands for tape recordings.

Telescope complex description. - The telescope complex (see fig. 7) is mounted on the observation deck. The complex consists of a main telescope and three auxiliary telescopes mounted on a four-axis pedestal.
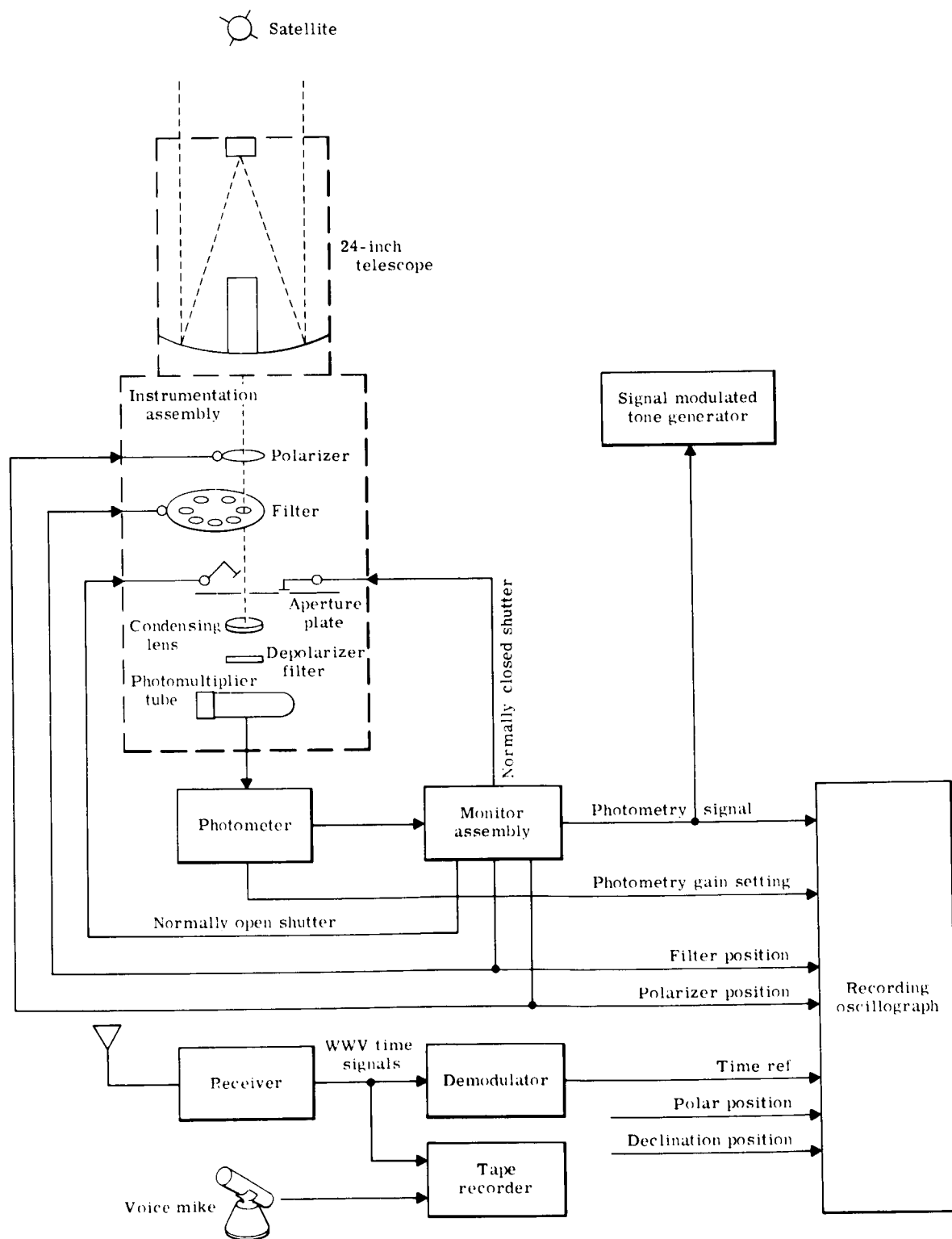
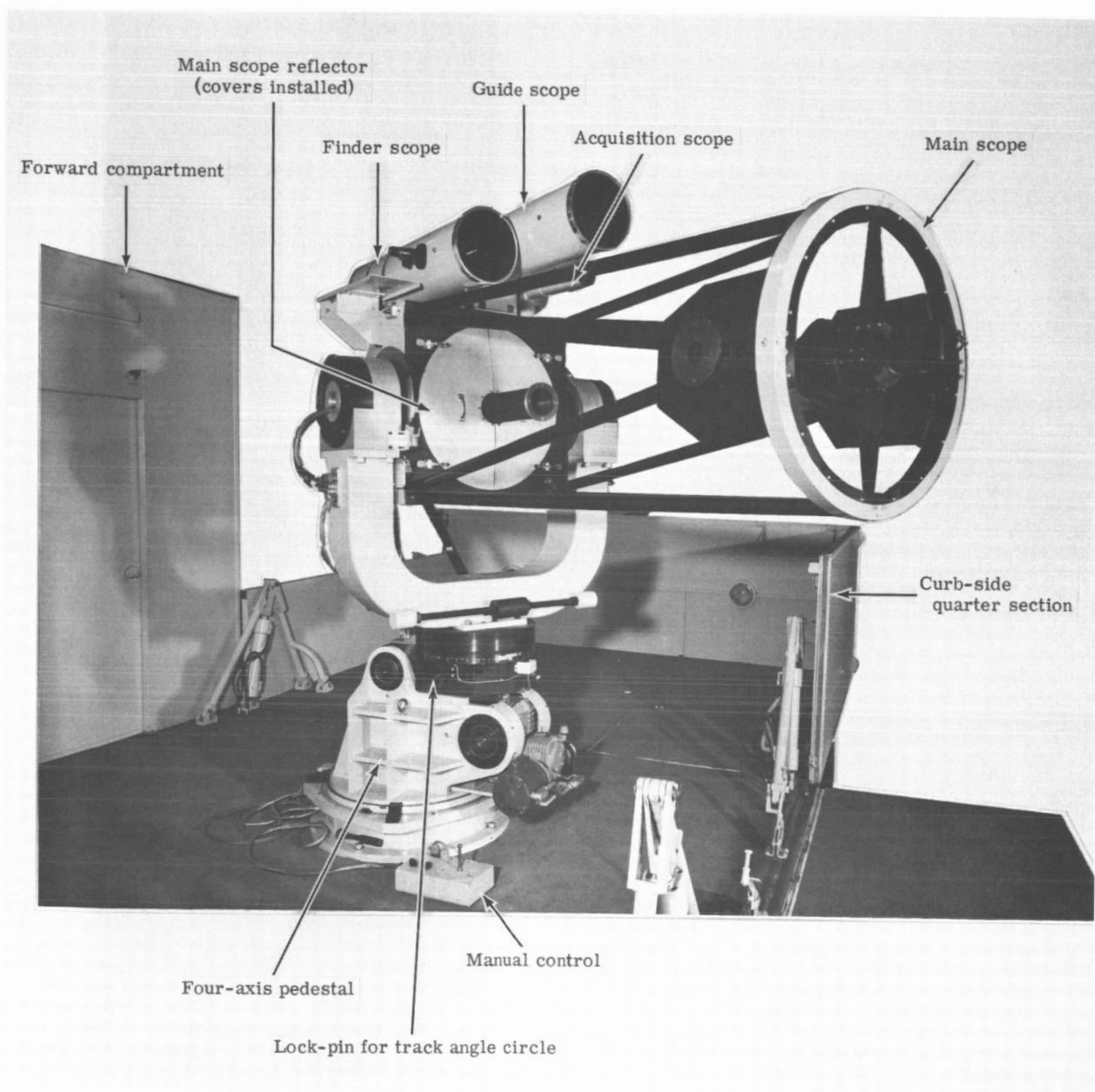Figure 6. - Instrumentation system block diagram.

Figure 7. - Telescope complex.

Main telescope: The telescope and mount were manufactured to Goodyear Aerospace specifications by Joseph Nunn and Associates. The telescope is of the reflector type, the primary mirror being 24 inches in diameter, with optical performance accurate to 1/10th wave length of sodium light. The focal ratio of the primary mirror is f/4, providing an f/4 Newtonian mode. In the Cassegrain mode, the secondary mirror provides a magnification of 5, resulting in an overall focal ratio of f/20. All the optical surfaces are overcoated and aluminized. An Erfle type eyepiece is provided for the main telescope. The Cassegrain focus is approximately 14.5 inches behind the primary reflecting surface.

The telescope mounting is the English fork type. Starting from the base, the mount has an azimuth axis with ±270° travel, a latitude axis with 0 to 90° travel, a polar axis with ±180° travel, and a declination axis with ±45° travel. All axes are graduated in at least 1/2° intervals. Angular pick-off potentiometers are mounted on all but the azimuth axis. All axes can be locked for stowage.

Acquisition telescope: The acquisition telescope is a wide-field, low-magnification visual telescope used for initial acquisition of the satellite track. After the sighting has been attained on the acquisition telescope, sightings are taken in succession with the finder telescope and the guide telescope to narrow the field of observation and establish the tracking field for the main telescope. Specifications for the acquisition scope are as follows:

(1) A 3-inch aperture objective and a 6° true field view.

(2) An Erfle eyepiece with mounting and aligning provisions capable of being attached at two positions around the main telescope.

(3) An illuminated reticle with cross hairs and one-degree true field circle.

Finder telescope: The finder telescope is an 8-inch Newtonian scope used for the second stage of establishing the tracking pattern. A platform is provided for attachment of a TV camera. Specifications for the scope are as follows:

(1) Focal ratio is f/4

(2) True field view is 1 degree.

(3) Power is 43X, with a 3/4-inch, or 20mm, effective focal length orthoscopic eyepiece.

(4) Illuminated reticle with cross line and 8.5 minutes of arc true field circle.

Guide telescope: The guide telescope is a narrow-field, high magnification, 8-inch Cassegrain reflector type scope used in the third stage of establishing the tracking pattern for the main telescope. The scope is a visual type, with provisions for vidicon camera operation. Specifications for the scope are as follows:

(1) Focal ratio is f/20.

(2) True field view is 8.5 minutes.

(3) One-half inch, or 12 mm, effective focal length orthoscopic eyepiece.

(4) Illuminated reticle having cross hairs and a one-minute arc true field circle.

16

Instrumentation assembly. - The instrumentation assembly is mounted on the main telescope. It consists of a photomultiplier, a depolarizer, a condensing lens, an aperture slide, shutters for opening and closing the apertures, a wheel containing six UBV filters, and a polarizer disc. Digimotors are used to step the filter wheel through the six positions and to rotate the polarizer disc in 10° steps. The aperture slide contains stop sizes of 4, 2, 1, and 0.5 minutes. Except for the 4-minute position, adjacent apertures are provided for quick measurement of sky background. With both apertures closed, the dark current of the photomultiplier is determined. The photomultiplier has an S4 spectral response (3000-65 000 Å region). The U filter (3600 Å) is a Corning 9863. The B filter (4200 Å) is a Corning 5030 cemented to a 2-mm-thick Schott GG-13. The V filter (5300 Å) is a Corning 3384.

Photometer. - Specifications for the photometer are as follows:

(1) Current Sensitivity - 17 ranges in overlapping 1 and 3 sequence, from 10 milliamperes to 100 picoamperes full scale. The sensitivity vernier located below the range selector switch allows continuous adjustment of sensitivity in all selectable ranges.

(2) Accuracy - Within 3 percent of full scale on all ranges from 10 milliamperes to 10 nanoamperes, and within 4 percent of full scale from 3 to 0.1 nanoamperes. Linearity better than 0.5 percent.

(3) Zero Drift - Less than 2 percent in any 24 hour period after a 10-minute warm-up.

(4) Meter - Linear transmittance scale from 0 to 100 percent in 1 percent steps, and a logarithmic density scale from 0 to 2.

(5) Output - A 5-volt output at up to 10 milliamperes is provided for full-scale meter deflections with sensitivity vernier control at maximum sensitivity position (full cw). The output terminals may be connected directly to high impedance recording devices. A series resistor is necessary when driving a milliampere recorder or a mirror galvanometer.

(6) Response - The speed of response of the instrument is specified as not slower than 0.2 second for 67 percent of full-scale deflection, and with capacities no greater than 5000 pF.

(7) Dark Current Control - Ten-turn potentiometer allowing compensation to be made for counteracting normal amounts of dark current delivered by the photomultiplier.

(8) Power Supply - Regulated, continuously variable, high-voltage power supply with an output range from 0 to 2000 volts at 0 to 5 milliamperes. Line and load regulation is better than 0.05 percent with line variations from 100 to 130 volts. This supply can be used independently and has its positive termination at ground potential. Ripple and noise all less than 0.05 percent.

Monitor assembly. - The monitor assembly contains the solid-state sequence driver circuitry for controlling the automatic sequencing of the UBV filters and polarizer in the instrumentation assembly. These functions are also manually controllable from the monitor assembly. Indicator lights give the status and provide signals for recording. The sky background and dark current solenoids in the instrumentation assembly are controlled from this unit.

Recording oscillograph. - A recording oscillograph is mounted in the console with the

front panel horizontal to the writing surface. Notes can easily be made on the recording paper as data is being taken. The oscillograph has 18 data channels, although only five are active with the present instrumentation. Dynamic measurements from dc to 13 kc are possible, depending on the galvanometer and paper selection. Five speeds are selectable by pushbuttons: 0.25, 1, 4, 16, and 64 inches per second. The record paper width is 7 inches, and the length is compatible with a 3-inch diameter roll or 200 feet of thin base paper. The unit is equipped with a trace identification system, which prints the channel number in the margin and interrupts the corresponding trace. The galvanometers furnished with the system have a flat frequency range of 0 - 125 cps and a system voltage sensitivity of 8.40 mV/inch at 11.5 inch optical arm. Also provided is a unit which, by heating and the application of actinic light, produces a completely latensified oscillogram at recording speeds up to 4 inches per second.

Receiver. - To provide timing signals, the system employs a commercially available short wave receiver which covers the frequency range of 0.54 to 30 Mc in six bands and provides a 10 dB signal-to-noise ratio of 1.5 microvolts AM. The 18 tube triple conversion superheterodyne circuit provides for the reception of AM, SSD, and CW signals. Other features are vernier tuning, adjustable bandwidth, adjustable AVC, heat frequency oscillator, noise limiting, and an S meter.

Tape recorder. - The tape recorded installed is a 1/2 trace, 4 speed (15/16, 1-7/8, 3-3/4, and 7-1/2 in/s) monophonic tape recorder/reproducer. It is fully transistorized, including the 3-watt audio output amplifier. The frequency response is 40 to 17 000 cps, ±3 dB, at 7-1/2 in/s; 40 to 10 000 cps ±3 dB, at 3-3/4 in/s. Wow and flutter is less than 0.25 at 7-1/2 in/s and less than 0.3 percent at 3-3/4 in/s.

Binoculars. - Two pairs of 7 x 50 wide angle binoculars are supplied with the facility. The field of view is 530 feet at 1000 yards. The binoculars feature coated optics, center focusing, and a 7-mm exit pupil for bright images during night viewing.

Camera and tripod. - The 35 mm camera provided features an f/2 lens, diaphragm scales of 2, 2.8, 4, 5.6, 8, 11, 16, an electronic shutter with speeds of 30 seconds to 1/500 second automatic and 1/30 second manual, motor-driven film advance at the rate of one frame per second, and quick rewind by electric motor. A quick-set tripod is furnished for mounting the camera. This camera is used to take sky photographs which are time-correlated to the photometric data.

TV System Equipment

General. - The TV system is used for remote tracking of the satellite from inside the equipment compartment. It consists of two TV cameras, an eight-inch TV monitor, and a coaxial switch (camera selector switch located on the control assembly).

TV cameras. - Two commercial transistorized television cameras are supplied for attachment to the 8-inch auxiliary telescopes. The electrical characteristics are: horizontal center resolution of 700 lines minimum video output and 300 lines minimum rf output; random interlace scanning of 15 750 cycles horizontal (crystal controlled) and 60 cycles vertical; video output of 1.5 volts peak-to-peak composite with 75-ohm termination; and temperature operating range of -20 to 70°C.

The TV cameras are mounted on the telescope structure and are optically coupled to the

eight-inch Cassegrain guide scope. Each camera consists of a vidicon tube, the sweep generator circuits used to form the raster, the video amplifier and sync circuits, and output stages for matching the coaxial cables. The cameras produce a composite video-sync signal, which is routed to the TV monitor via the selector switch on the control assembly.

Video monitor. - As a tracking aid, an 8-inch TV monitor is mounted on the console surface. The unit can be used with either composite video input or with separate video and sync. A composite video input of 0.25 to 1.2 volts is required for full contrast. The video bandwidth is in excess of 10 Mc (3 dB down) permitting 800 lines resolution. The monitor includes d-c restoration for stable black reference.

The TV monitor receives the composite video-sync signal from the TV camera selected by the operator, separates the sync signal from the video, and generates the vertical and horizontal sweeps for the 8-inch picture tube. A horizontal flyback transformer generates the picture tube high voltage. The video signal is amplified and applied to the grid of the cathode ray tube. The circuitry is very similar to a commercial television receiver.

The satellite is first visually acquired on the acquisition scope, using the control box rate controls. With the camera selector switch set to position "1" (Newtonian finder scope camera), the image should appear on the monitor. The hand stick is used to center the image, and then the monitor is switched to the guide scope camera. The image is centered and the satellite tracked with the hand stick.

TEST PROGRAM

General

The test program was designed to provide assurance that all component and subsystem elements going into the system were evaluated, and confirm that the overall system performance was in accordance with requirements and objectives. A further purpose was to obtain test data that could be used as a guide in future design.

The test program consisted of two parts, which will be separately treated in this report. These two parts are the component and subsystem tests and the acceptance tests for the overall system. The tests were conducted as a normal part of the GAC equipment development process and were part of the control procedures. The acceptance tests were witnessed by NASA representatives.

Both parts of the test program were carried out by following a Development Test Instruction (DTI) generated for each separate test. All data were recorded on a test data form and made a part of each DTI. The major subcontractors were required to perform similar tests prior to acceptance of parts.

Component and Subsystem Tests

The component and subsystem tests are listed below by test instruction number (TI), with a short statement of the purpose and results and a description of the tests and the suitability of the equipment tested.

Operational amplifier assembly test (TI GN351-1). - The purpose of this test was to balance the operational amplifiers and to measure the response of the servo compensation components. The response curves are included in this report with the analysis of the control system.

The test consisted of three parts: balancing each of the six amplifiers, static gain tests of the polar and declination preamplifiers, and dynamic response tests.

Balancing was accomplished by applying power, grounding the input terminals, and connecting a sensitive d-c voltmeter to the signal output terminals of each amplifier during balancing. After ample warm-up time for the amplifiers to stabilize (2 minutes or more), they were balanced in succession by means of the zero control on the front of each amplifier. The adjustments brought the voltage to less than one tenth of a millivolt for each amplifier, which was recorded on the DTI test report form, thus demonstrating a very satisfactory operating condition.

The static gain tests for both the polar and declination preamplifiers consisted of applying various input voltages (from 0.75 to 6.0 volts), using both gain positions, measuring the output, and thereby calculating and recording the resulting gain for each. For proper performance, these must all be within ±10 percent of their nominal design values, as listed for reference on the DTI test report form for this DTI. Actual recorded values show that all measured gains had variations from nominal on the order of 1 percent or less, except for the low gain mode of the polar preamplifier, which had a gain of 4 percent below nominal. This demonstrated the gain characteristics to be well within acceptable limits for good performance.

The dynamic response tests on both the polar and declination amplifiers consisted of connecting them with a servo analyzer and oscilloscope. The input voltage (output of the servo analyzer) is adjusted to a 0.5-volt peak or less (avoid saturation), and frequency response data is taken over the range of 0.1 to 40 c/s, recording frequency, phase, and gain data. Plots of gain versus frequency and phase versus frequency were made from this data.

The dynamic responses of both the polar and declination amplifiers were very similar, and their response curves were nearly identical. The curves obtained for the polar axis are given in figure B9 (Appendix B), demonstrating that the response is well within acceptable limits for good performance.

Based on these tests, the operational amplifier assembly was deemed acceptable and fully satisfactory.

High-power d-c amplifier test (TI GN351-2). - The gain of both the polar and declination axis amplifiers was measured at frequencies of 5, 10, and 100 c/s with the gain selector set at 100. At a frequency of 5 c/s, the gain was checked at settings of 200, 50, 20, and 10. Gains measured the same as indicated by the gain selector.

After the balancing adjustment/check, the test consisted of connecting an oscillator to the amplifier input and an oscilloscope to the output in parallel with a 10-ohm load resistor. Gain settings and frequencies were then varied over the values indicated above, and the resulting measured gain was compared with the gain settings. Acceptability limits were ±10 percent. The measured gains were found to agree with the settings in all cases except for a gain setting of 50, where the gain was 0.4 percent low (actual measured gain of 49.8).

The other amplifier was tested in the same manner, and was also found to agree with the settings to within 2 percent. The amplifiers were therefore considered acceptable.

Control assembly and hand control test (TI GN351-3). - For this test, excitation was applied to the hand control and the sensitivity on each axis was measured by applying force and measuring the output voltage. The voltage swing was greater than the +0.8 to -0.8 volt established as the minimum.

To perform this test, power is applied to the control assembly, and the 400-cycle excitation voltage on pins A and C of the receptacle for the hand controller (J6) was checked before plugging in the hand controller. A voltmeter was used across the output to read the voltage swing either way as corresponding forces were applied to the stick along that axis (and the same across the other output channel for stick forces applied orthogonally). By applying modest forces (of a few pounds) to the stick in both directions, it should be possible to obtain a voltage swing (on both axes) of at least +0.8 to -0.8 volt on the voltmeter.

The test results showed that the excitation voltage was 8 volts (nominal 8 volts, ± 10 percent) and the detector output ranged from +1.0 to -1.0 volt on both axes. Therefore, the equipment was deemed acceptable.

Communications receiver test (TI GN351-4). - The input voltage required from a signal generator at the antenna terminals to give a 10-dB signal-to-noise ratio as seen on an oscilloscope was measured at 2.5, 5, and 10 MHz. The value was always less than 0.5μ V (0.4, 0.3, and 0.2μ V, respectively). In addition, the rf calibration of the tuning dials and other alignments were checked in the instrument lab against the manufacturer's specified values for the receiver and found to be satisfactory.

Audio tape recorder test (TI GN351-5). - The record, playback, and erase functions of the recorder were tested by using an audio oscillator to generate audio inputs to the microphone and observing the playback output on an oscilloscope. Operation was checked at 100, 1000, and 10 000 Hz and at tape speeds of 7-1/2, 3-3/4, 1-7/8, and 15/16 inches per second. Use of the radio/phono input was also checked, and performance was found to be in satisfactory conformance with the manufacturer's specification. All of the functions and controls (start, stop, record lock, rewind, speaker switch, volume, pause, counter, etc) were also checked for proper operation. Based on these tests, the unit was found to be acceptable.

28-volt d-c supply test (TI GN351-6). - Measurements were made of the no load and loaded voltage, the ripple voltage, and the total output impedance. For loading the supply, a 3-ohm, 300-watt resistor was used. The resulting voltage change was less than 10 percent (32.4 and 29.05 volts). Ripple voltage was 0.5 volt rms, and the supply internal impedance was 0.294 ohm (compared to a requirement of less than 0.4 ohm). Accordingly, the unit was found acceptable.

TV camera and monitor test (TI GN351-7). - The TV system (cameras and monitor unit) were tested for proper performance by operating with both a general scene and an RETMA resolution chart. The camera and monitor were properly interconnected, plugged in, and allowed a warm-up period (approximately 5 minutes). The RETMA resolution chart was then placed in the camera field of view such that with the camera focused, the chart area covered the monitor screen properly. With brightness and contrast adjusted properly, the chart image on the monitor was observed and measured to determine the system performance characteristics with respect to resolution, vertical linearity and size, horizontal size, vertical and horizontal centering, and uniformity of screen brightness and contrast. The equipment met RETMA standards in all these respects and was therefore considered acceptable.

Oscillographic recorder test (TI GN351-8). - Functional and operational checks of the recorder consisted of making an input to the recorder from an audio oscillator and checking the quality of recording performed up to the galvanometer response frequency and at all chart paper speeds.

Four 100-c/s response galvanometer units were inserted in the recorder in accordance with the instructions in the operating manual and then aligned. The oscillator was hooked up as parallel inputs to all four channels through identical damping pads (7.5 - 121 ohm resistor pad) to give a signal attenuation to about 6 percent of the oscillator output. By using precision (±1 percent) resistors, identical inputs were assured. The recorder was then turned on and operated in accordance with the operating manual in all modes over the frequency range. The recorded traces were observed and measured for the following:

(1) Identity and uniformity of traces.

(2) Accuracy of paper speeds, as shown by the pitch of the recorded signal traces.

(3) Response fidelity of the recording, as revealed by the shape of the signal trace.

All functions were checked including controls, trace positioning, fixing (by the UV and heat platen fixing accessory provided), overload release, etc to determine that the equipment operated properly and in accordance with the manufacturer's specifications. The tests indicated the units to be satisfactory in all these respects.

Photometer test (TI GN351-9). - This test and the following test (TI GN351-10) were actually performed simultaneously as a matter of expediency, since a photomultiplier such as that in the photometer instrumentation head is required to activate the photometer unit (and vice versa).

The purpose of this test is to ascertain that the unit functions properly in supplying the high voltage to the photomultiplier and in handling the photomultiplier output to provide precision measurement capability. This was accomplished by connecting the photometer to the instrumentation head and its photomultiplier and operating in accordance with the manufacturer's instructions for the photometer. Zero check and dark current adjustments were made satisfactorily under "no-light" conditions on the photomultiplier. Then by various discrete lighting increments, the gain switch was advanced to check the gain ratios, which were alternately 3 and 3-1/3 throughout the range (one decade, or 10 for every two gain steps). Stability of the system was checked by repeating to note any drift occurring with time, either in photomultiplier output or gain or in dark current adjustments. The instrument was found to conform to the manufacturer's specifications(see page 17)in all respects and was therefore considered satisfactory.

Photometer head test (TI GN351-10). - This test was performed in conjunction with test TI GN351-9. The test included a check of all the required functions provided in this unit in addition to the basic electro-optical performance of the lenses, filters, photomultiplier, etc. The test consisted of the following checks:

(1) Check of the photomultiplier output under constant lighting conditions as a function of field slide stop bar position to verify proportional outputs (4 to 1 between stops).

(2) Check of the proper action of the shutters when actuating voltages are applied to proper pins (or proper monitor switch, if monitor assembly is connected).

(3) Check of the filter wheel actuation and position indication through proper pins (or proper switches and indicating lights, if monitor is connected).

(4) Same check as item 3 for Polaroid filter unit position.

(5) Eyepiece focus and synthetic field stop illumination check with field stop slide bar in corresponding position. This is the end position (with the 45° mirror on the optical

axis), and eyepiece focusing capability was considered satisfactory by ascertaining that in observing the synthetic field stop through the eyepiece, the focus adjustment could be made smoothly and extended both ways from the "in-focus" position. Actuation of the momentary switch provided proper illumination of the synthetic field stop.

(6) Check of the Fabry lens action, accomplished by moving the small point light source about in the field or field stop opening. Photomultiplier current is non-varying when axial distance and light intensity are kept constant, despite other movements of the light source in the field, when the Fabry lens action is proper.

For establishment of performance of the photomultiplier output versus light level/field stop position (item 1), photometer meter readings were recorded on the DTI test report form. For the polarization filter wheel position monitoring voltage output (item 4), the voltage reading for each position was recorded.

The accomplishment of these tests with the units interconnected with 25-foot long coaxial cables (to assure system compatibility when hooked together in the complete installation) demonstrated satisfactory performance capabilities.

Monitor assembly test (TI GN351-11). - This test was used to assure that the automatic sequencing of the shutters, filter wheel, and polarizer operated correctly.

The test consisted of three main steps:

(1) A continuity check to verify continuity of key circuit elements by following the tabulated continuity check points on the test report form.

(2) Checking the operation of the monitor unit's automatic sequencing system and output corresponding to the various control switch positions as specified in the test instructions, and checking the sequencing rates as specified.

(3) Connecting the monitor assembly to the photometer instrumentation head unit and checking out the control functions and monitoring indications (indicator lights) as specified. This included shutters, filters, and polarization wheel.

Some difficulty was experienced with the sequencing of the filter wheel, since two pulses were required to advance from one filter position to the next. The circuitry was modified to correct the difficulty. After correction of the difficulty, the assembly performed satisfactorily and checked out properly in all respects.

35 mm sky field camera and cable test (TI GN351-12). - This test was primarily a check of the mechanical features of the camera to verify its proper performance and compatibility with this system. The test consisted of three steps:

(1) Checking that the exposure control always kept the shutter open for more than 30 seconds with a dark sky field target. The actual exposure times (a total of 10), as tabulated on the test form, ranged from a minimum of 65 seconds to a maximum of 80 seconds.

(2) Checking that the iris opens to the full specified diameter when set to f/2.

(3) Demonstrating that the automatic frame advance and frame counter mechanism functions properly after loading the camera with film.

These tests, along with picture-taking ability, demonstrated the suitability of the camera for its intended use with this system.

7X 50 binoculars test (TI GN351-13). - This test was performed primarily to verify the optical quality, 9-degree field of view, and functional (focusing etc) suitability of the equipment, as well as to verify the proper complement of lens covers, carrying strap, case, etc. The test consisted of:

(1) Checking the focusing on both near (less than 50 feet) and far fields (stars, moon, planets).

(2) Checking the field of view by measuring its subtent (on a star field), and verifying usable images to the edges. Two stars 9 degrees apart were viewed for this test.

(3) Checking the binocular magnification (7X).

The equipment was found to be satisfactory in all these respects and was therefore considered acceptable.

Servo subsystem test (TI GN351-14). - The purpose of this test was to measure the closed velocity loop response at normal speeds and record performance at sidereal rate for both drive axes. It consisted of the following individual tests of the subsystem:

(1) Open tachometer loop tests were performed to check proper polarity of the tachometer output connection (and reverse the connection, if necessary) for balancing the rate control voltage. This was carried out on both axes (polar and declination).

(2) Closed loop test measurements were made to obtain the velocity loop response on both axes. The test consisted of connecting input and output of the system (each axis separately) to a servo analyzer with an oscilloscope and operating over a frequency range from 0.5 to 20 c/s. The phase and gain for each frequency were recorded. The resulting plots for the polar and declination axes are given in figures B10 and B11, respectively, in Appendix B.

(3) Sidereal rate performance tests were performed by driving the axis under test at sidereal rate with a recorder connected to the tachometer output terminals. The level should be about 8 millivolts for sidereal rate, and it should be possible to record smooth motion at this rate for some period of time to as close as the resolution of the test input signal or rate control potentiometer will allow. The resulting signal recordings for the polar and declination axes are shown in figures B12A and B12B, respectively, in Appendix B. The rate could also be controlled down to substantially less than one half the sidereal rate in both axes (see recordings).

(4) Maximum rate tests were made to verify performance out to values utilizing input control signals of from 5.5 to 6.6 volts in both directions. Values obtained for the polar axis were +6.0 and -5.6, and those obtained for the declination axis were +5.56 and -5.6 volts.

(5) Limit system tests were performed to verify the proper functioning of all parts of the limit system on both axes. It consisted of driving toward and slowly into one of the limits, noting the position of cutoff and stopping, and noting that the proper limit light went on. Then it was driven off the limit by use of the reset switch. This was repeated for all the limits, and demonstrated proper functioning of the system.

(6) Position loop hand control tests were performed by verifying that a force on the hand control in either direction would cause a voltage swing of at least ±3.8 volts. Voltage swings of approximately ±5 volts on both axes were obtained.

Since the system met the requirements of all of the tests satisfactorily, it was considered acceptable.

TV and guide scope subsystem test (TI GN351-15). - This test was for the purpose of determining the TV/guide scope compatibility and evaluating the performance characteristics. The performance of the individual elements was separately determined from test TI GN351-7 (described earlier in this section) and the telescope acceptance tests (described later in this section). This test consisted of mounting the TV cameras on the telescope, coupling optically by means of eyepiece prisms, and connecting electrically to permit evaluation of the electro-optical coupling. The following checks were made:

(1) Focus was checked by first aiming at a convenient near field of sufficient illumination and adjusting the focus (and electrical controls) as necessary to obtain an image on the monitor screen. Then the telescope was aimed at a far field object (bright star, planet, or the moon) and focused for a sharp image on the monitor screen.

(2) The system stability check consisted of guiding away from or moving to other directions or objects and back, to determine that focus and other adjustments did not change or drift excessively.

(3) Sensitivity was checked by aiming the focused and adjusted system at various stellar objects. Stars of 1.26 magnitude were viewed successfully, but stars of 2.22 and 2.46 magnitudes were not distinguishable on the monitor.

(4) Balance was demonstrated by adjustment and addition of balance weights to provide balanced condition.

These system tests verified compatibility, function, and capability to operate on between 1st and 2nd magnitude stars.

Instrumentation subsystem test (TI GN351-16). - The primary purpose of this test was to evaluate the accuracy of the instrumentation system and demonstrate an accuracy of better than 2 percent. Previous tests have demonstrated the functional suitability of the various elements of the system (see tests TI GN351-6 and TI GN351-8 through TI GN351-11). In this test, therefore, these elements were operated together to determine overall accuracy in measuring discrete steady light sources.

For this test, which called for 10 or more stars to be measured in each color band, 40 measurements were taken (on 10 stars) so that gain switching in as many levels as possible could be evaluated in addition to the three color bands. Typically, for a given star (e.g., the fourth one used, BS 8665), five measurements were made:

(1) In V band at gain settings of 10 and 9
(2) In V band at gain settings of 9 and 8
(3) In B band at gain settings of 10 and 9
(4) In B band at gain settings of 9 and 8
(5) In U band at gain settings of 11 and 10

In the case of BS 8905, six measurements were made - two in each band.

These measurements, taken for several stars of different color indices and different magnitudes (brightness levels), thus permitted gain ratios over the most useful range of the

instrumentation system which would be applicable to the entire range, based on the gain measurements of a previous DTI described above.

Since every measurement was made at two gain levels, a gain ratio could be calculated. These were normalized by dividing the ratio by 1.1111 whenever the higher of the two gains was an even number (thus accommodating the alternate ratios of 3 and 3.3333, with a product of 10 for each pair of gain steps). Then, to obtain the mean value, these normalized values were squared, summed, and divided by the number added (averaged); then after subtracting 3 from the value obtained, the result was divided by 3 and multiplied by 100 to give the mean percentage error of the system (required to be less than 2 percent). The result obtained from this test was 1.52 percent. Then, to obtain the percentage coefficient of variation (required to be less than 1 percent), the square root was taken of the sum of the measured values minus the square of the averaged sum of the squares obtained above. The result, divided by 3 and multiplied by 100, is the percentage coefficient of variation, and the value obtained from these test measurements was 0.64 percent.

These values were within the requirements and were considered to be conservative as far as the system performance was concerned, since data reduction errors would be included in the above results. The instrumentation subsystem was therefore considered to be satisfactory and acceptable.

Performance and alignment tests on the telescopes (TI GN351-17). - The purpose of this test was to check the focus and optical alignment of the main telescope after delivery and installation on the van and to check the parallelism between the main and auxiliary scopes. The auxiliary scopes had to be adjusted to make their optical axes alignment parallel to that of the main telescope.

This test consisted of using the star Polaris (to avoid the need for continuous track while checking and aligning) as a target, and checking for clarity of focused image (compatible with prevailing seeing conditions), out of focus diffraction pattern concentricity, and any other discrepancies or anomalies (color, edge of field distortion, etc). In addition, a lensless cross-hair test jig fitted over the front end of the light tube through the primary mirror served as a means of checking concentric alignment of the primary and secondary mirrors. (Tilt of either mirror could be adjusted, if necessary, to correct any discrepancy.)

Polaris was used to check parallelism of auxiliary and main scopes by determining the image relationship to the cross hairs of each auxiliary scope with the main scope centered on the star. Any displacement from the intersection of the cross hairs was removed by the boresighting mount adjustments provided on the base of each scope. This proved to be somewhat difficult at first, and some shifting occurred, until later improvements to the mounts and eyepieces alleviated this problem. As a result of these tests and adjustments, the telescopes were considered acceptable.

Van tests. - The van manufacturer performed van acceptance tests with GAC monitoring prior to its acceptance by GAC. This was an extensive series of tests of all the van components and subsystems set forth in an 11-page test procedure, which was followed completely. It included specified functional tests of the motor generator set, air conditioner, power distribution system, lighting, heater, hydraulic deployment system, and the leveling and stabilizing system. The truck and van were road tested for mobility, suspension effectiveness, and braking with a dummy load installed, and the entire system was given a rain test. The only significant problems occurred in the rain test, when leaks discovered along the telescope compartment roof line and at the bottom of the curbside door required remedial treatment.

In addition to an inspection of the entire system for design conformance and workmanship, the test included a functional check of every system, such as deployment of the jacks and leveling

system, operating the sides to open to a deployed platform and to close to a road configuration, etc. The integrally installed units, such as generator, air conditioner, heater, hydraulics, were performance checked and measured for conformance to the specifications furnished by the manufacturers. Functioning of the power distribution system, van mounting, and van/truck interface compatibility (such as motor generator electric fuel pump and tank connection, truck/van/motor generator electrical systems interconnections, van mounting to the truck chassis) were checked.

The road test of the complete unit, which preceded the rain test and other functional tests, was made at full gross weight of 32 390 pounds, achieved by mounting a dummy equivalent load at the telescope mounting pad. The road test consisted of a 31-mile run over a selected course and at speeds covering the specified operating range for driving and road conditions.

In addition, the unit was checked for overall external dimensions, specified internal clearance dimensions, axle load distribution, and full complement of specified auxiliary equipment (ladders, covers, etc), as well as required safety equipment and equipment stowage provisions.

Since the results of these tests and inspections showed the van and associated equipment, together with its installation,to be satisfactory, it was considered acceptable.

Telescope tests. - The manufacturer performed acceptance tests on the telescope prior to its acceptance by GAC.

General inspection: The entire telescope system, which includes the main telescope assembly, the four-axis mount, and the three auxiliary telescopes, was inspected visually to determine compliance with general requirements, workmanship, finish, provision of all required features, etc. The system was measured to determine overall dimensional conformance, and was found to meet all requirements. Measurements are as follows:

(1) Height - 98-1/2 inches (requirement: less than 100 inches)

(2) Width - 57-3/4 inches, including 9-inch wiring projection on sides (requirement: under 84 inches)

(3) Length - 119-1/2 inches, including allowance of 20 inches for instrumentation package (requirement: under 126 inches)

(4) Weight - 4750 lb, approx. (requirement: 4000 to 6000 lb)

Optical characteristics: Optical qualities were determined by three separate checks:

(1) Check of uncoated main optics assembled in telescope

(2) Optical check of primary and secondary mirrors of the main telescope at the optical manufacturer's plant

(3) Final optical performance check of all telescopes (main and auxiliary) after final assembly, including alignment, boresighting, etc

For the check of uncoated optics, system tests of the unaluminized optics on stars were conducted at the telescope manufacturer's plant at Pasadena, California on the night of 22 March 1966. Although these tests were made under adverse conditions, including poor atmospheric "seeing" and high sky and ambient light levels, they indicated satisfactory performance of the various telescopes. The "eyepiece test" of the equal secondary shadow size at the same distances inside and outside of focus, when pointed at the star Polaris, evidenced good optical figures for both the primary and secondary mirrors, and this was further indicated

from the diffraction pattern. Light grasp, magnification, field of view, and (where provided) the reticle scale were found to be satisfactory for each telescope.

Careful testing of the primary and secondary mirror system elements of the main telescope was carried out by the optical manufacturer to determine characteristics and insure quality. The tests included "focograms", knife-edge cut-off, and pinhole diffraction ring tests.

Figure 8 presents a focogram made on Polaroid film at the Cassegrain (f/20) focus of the 24-inch telescope's optical system. A schematic diagram of the autocollimated Foucault test setup for this focogram is shown in figure 9. Although this focogram does not provide precise quantitative information, the delicate shading throughout the circular field is objective evidence of the good optical figures for the system's components, and supports the conclusions from the far more sensitive visual tests.

The critical tests were the visual inspection of the uniform cut-off of the intensity as a knife-edge intercepted the reflected beam at the f/20 focus, and the visual inspection of the sharpness of the f/20 image of the pinhole light source at high magnification. Microscopic vibrations at the test tunnel made it impossible to take successful photographs (which require appreciable exposure time) of these more sensitive tests, including those showing the linearity of diffraction interference fringes. The optical technician who performed the laboratory tests concluded that the optical system was accurate to 1/20 wave, or about 300 angstroms, which is double the accuracy required by the specification (see appendix F).

The main telescope optical system was checked for general conditions, alignment, and performance. As one such check, a test was made of its ability to resolve the components of Polaris. Results were satisfactory. The boresighting alignment in two positions between the auxiliary and main scopes was checked, and showed variations up to 15 arc seconds. The focal length was checked and adjusted to bring the focal plane approximately 7 inches behind the back face of the telescope.

Mechanical tests: The purpose of the mechanical tests was to verify the proper mechanical functioning of the telescope. They included checks of the focusing mechanics, travel and stop positioning for all four axes, brakes and locks, limit switches, actuators, setting circles, and telescope balancing provisions. The tests showed the telescope to be mechanically satisfactory. Measured results are shown in Table 1.

TABLE 1. - TELESCOPE MECHANICAL MEASUREMENTS

Axis	Travel		Setting circle interval	
	Specification	Measured	Specification	Measured
Azimuth	±270°	±271°	1/2°	1/2° (with vernier)
Latitude	0 to 60°	10 min to 89° 45 min [a]	1/2°	1/2° (with vernier)
Polar	±180°	181-1/2 to 182°	1/2° and 2 min of hour angle	1° and 4 min of hour angle [b]
Declination	±45°	+45-1/2 to -45° 10 min	1/2°	1/2° (with vernier)

[a] Manually to 0° and 90° with hand wheel

[b] With vernier to 15 min of arc and 1 min of hour angle

28

Figure 8. - Focogram showing quality of optical figures of the primary and secondary mirrors.

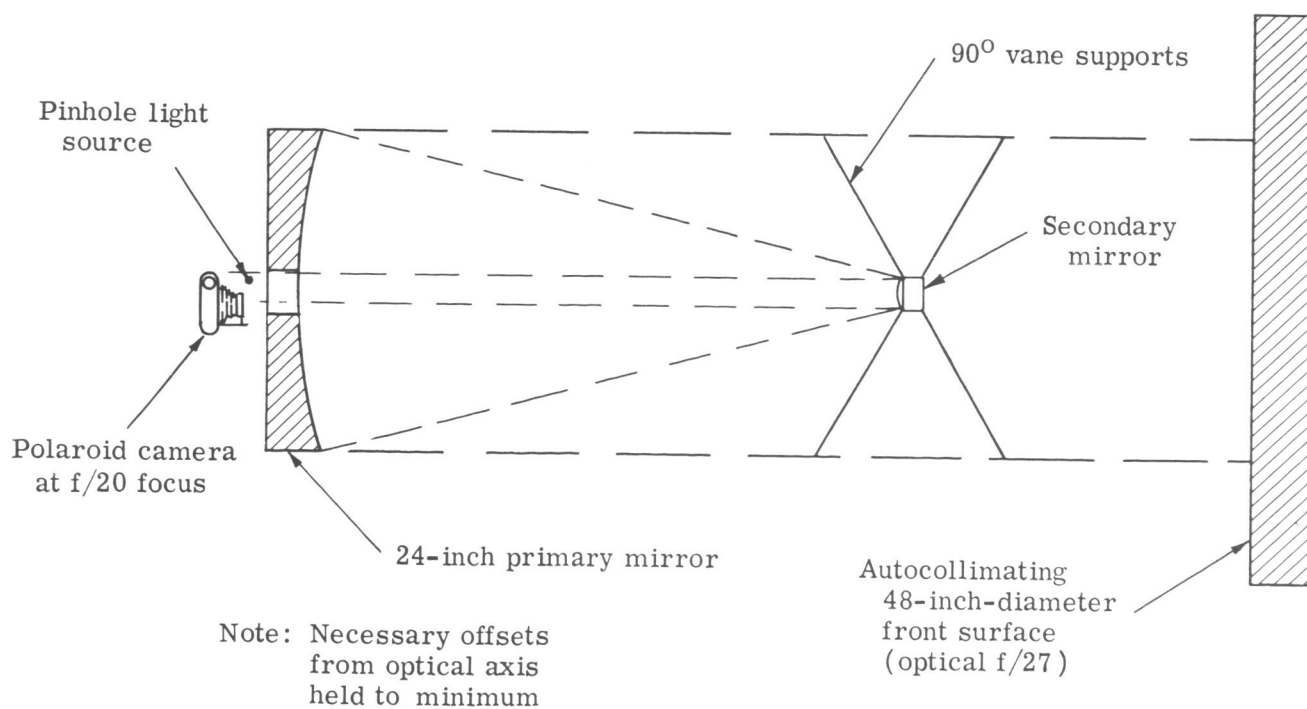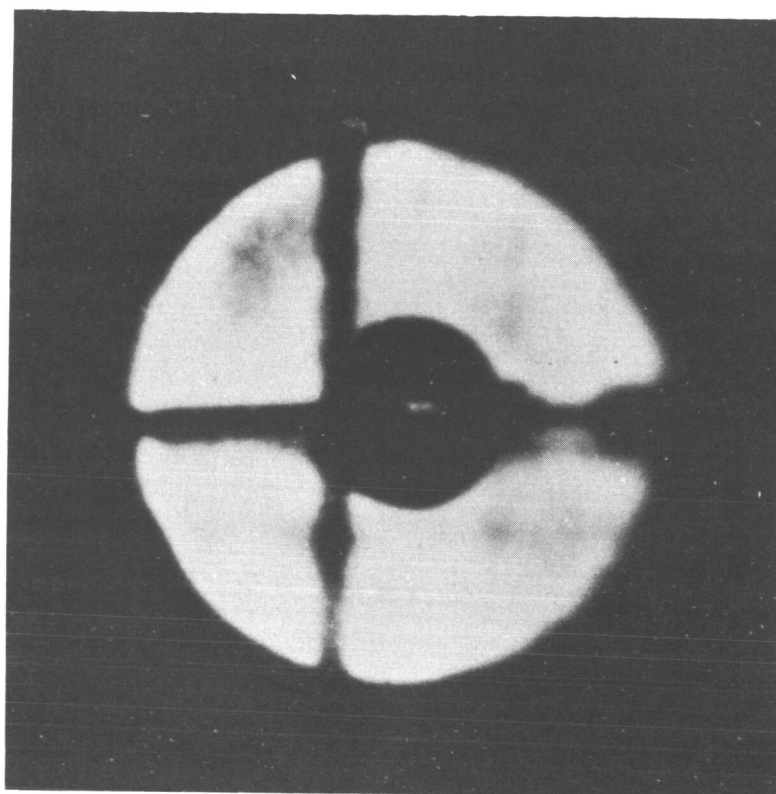
Note: Necessary offsets from optical axis held to minimum

Figure 9. - Setup for taking Focogram at f/20 Cassegrain focus.

In addition, the torques required to move the telescope about each of the tracking axes were measured with brakes on and off, with the telescope in various positions representing the attitude extremes. The loads were applied with scales at the forward ring, orthogonally with respect to the axis being measured, and the brakes set to desired values. Following are the measured results:

	Brake off	Brake on
Polar	10 to 35 oz	48 to 56 oz
Declination	7 to 25 oz	40 to 59 oz

The highest of these loads were measured with the latitude axis on the 0° setting.

Electrical tests: Electrical tests were performed to demonstrate proper functioning of all electrical circuits and equipment. This included the drives, limit switches, setting circle illumination, reticle illumination, and axis position-indicating potentiometers. These tests demonstrated satisfactory conformance. Measured results are given in the following paragraphs.

The drive motors were hooked up open loop to a 12-volt storage battery through a rheostat at the telescope base plug connectors. Both polar and declination motors drove satisfactorily. Then the tachometer outputs were checked (at the base plug connector) with a voltmeter while the telescope was moved at steady rates. For a rate of about 1° per second, the reading was between 1-3/4 and 2 volts; for approximately 3° per second, the readings were 5 to 5-1/2 volts. The latitude drive rate was measured as 24° 15 min per minute up, and 25° 40 min per minute down. (Specification requirement was between 20° and 35° per minute each way.)

The limit switches cut off properly at the following points:

Polar	$+176^{\circ}$, -178°
Declination	$+41^{\circ}$ 30 min, -42°

The level cut-off switch actuated at approximately 0° of telescope axis elevation above the horizontal, regardless of aspect.

Potentiometer measured values were as follows:

Polar

180° E	3400 ohms
90° E	2500 ohms
0°	1740 ohms
90° W	900 ohms
180° W	80 ohms

Declination

$+45^{\circ}$	2600 ohms
0°	1340 ohms
-45°	120 ohms

Latitude

90°	2550 ohms
60°	1770 ohms
30°	860 ohms
0°	50 ohms

These measured values were all within acceptable limits. The telescope electrical circuits were also checked from the connector pins for continuity and shorts, and found satisfactory.

Acceptance Testing

General. - Acceptance testing consisted of the following tests, listed by test instruction number:

TI GN351-18-1	Site selection
TI GN351-18-2	Vehicle acceptance
TI GN351-18-3	Jack and van deployment and rigidity
TI GN351-18-4	Electric generator
TI GN351-18-5	Sky camera and tape recording
TI GN351-18-6	Telescope optical alignment and focusing
TI GN351-18-7	Control system
TI GN351-18-8	Reception and recording time (WWV)
TI GN351-18-9	Signal-modulated time generator performance
TI GN351-18-10	Azimuth and latitude orientation
TI GN351-18-11	Second-order extinction coefficients
TI GN351-18-12	Scale factors
TI GN351-18-13	Primary extinction coefficients and zero point terms
TI GN351-18-14	Acquisition of a 7th magnitude satellite
TI GN351-18-15	Polarization data on Echo Satellite
TI GN351-18-16	Sensitivity and accuracy of each data mode
TI GN351-18-17	Absolute intensity calibration in each data mode

Because of the tight schedule, this testing was carried out concurrently with the final assembly and checkout operation, and with operations involving preparation of the unit for its departure to Palomar Mountain, California, on its first assignment. This first assignment was photometric surveillance of the PAGEOS satellite following its June 23rd launch, under contract NAS 1-6189.

The field-verification trials, which were called for as the final contract requirement, were also carried out as a part of the acceptance test program. The entire program was performed by GAC in accordance with DTI's developed by GAC to determine and complete overall system compliance with requirements. The major portion of the acceptance test program (including the field-verification trials) was carried out at the contractor's Akron, Ohio plant and at the Knoll Site of the GAC radar test range complex at Wingfoot Lake. Some items, several of which required clear skies, were completed at the operating site on Palomar Mountain on a non-interference basis with the PAGEOS surveillance mission. The tests demonstrated conformance with contract requirements. Descriptions and results of the tests are covered in the following paragraphs. (For procedures employed, see ref. 1.)

Site selection (TI GN351-18-1). - The purpose of this test was to exercise, verify or improve, and firmly establish the site selection criteria and processes so that they could be

employed with confidence for future operations. The test used the previously established site selection criteria and survey procedures, which emphasized the following aspects:

(1) Communication between site and main plant (logistic support, data exchange, computer lab)

(2) Good photometric viewing and environment - absence of city lights, smoke, etc.

(3) Adequate horizon viewing - e.g., to permit 7th magnitude satellite acquisition below 15°

(4) Continuous security of site for operation and equipment.

The site selection for field verification trials involved consideration of several alternatives, which included the following:

(1) A suitable location on the apron or edge of the Akron municipal airport

(2) Old Guggenheim Airship Institute grounds (GAC Plant H, Life Sciences laboratory)

(3) Goodyear tract occupied by Zeppelin Rifle Club at north edge of Akron-Canton Airport (former Smithsonian Astrophysical Observatory Site No. 0053)

(4) Knoll Site of radar test range, Wingfoot Lake (WFL)

(5) Point Site of radar test range, Wingfoot Lake (site where the initial photometric work was carried out)

(6) Landing strip area or other location at the main plant area at Wingfoot Lake

Results of the site selection process are tabulated in Table 2.

TABLE 2. - SITE EVALUATIONS

Site	Communi-cation	Sky condition	Horizon view	Security	Other[a]	Rating
Akron airport	S	U	S	S	S	6
Plant H (Guggenheim Airship Institute)	S	U	S	S	E	5
Rifle Range	S	S	S	S	S	3
Knoll Site, WFL	E	E	E	E	E	1
Point site, WFL	E	E	S	E	E	2
Air Strip, WFL	S	E	P	E	S	4
Remote rural site	P	E	E	U	P	7

Code

| E | excellent | P | poor |
| S | satisfactory | U | unsatisfactory |

[a]Other factors included access, facilities such as shelter, tables, work bench, etc

The Knoll Site of the radar test range at Wingfoot Lake was selected, and proved to be quite satisfactory for the acceptance tests, as well as appropriate for the initial field verification trials for the equipment and associated processes and techniques. For communication, there was a GAC extension phone already installed in the shack and the truck radio mobile phone worked well from this high, unobstructed location. Sky conditions, as well as the horizon view, were good at this high point away from the city. The chain-link fence around the shack and adjacent area provided excellent security. The uneven, graveled area gave a good evaluation of the mobile observatory's stability capabilities.

Vehicle acceptance (T I GN351-18-2). - The purpose of this test was to demonstrate the suitability of the primary vehicle (truck and van body combination) as a mobile platform, both from the standpoint of mobility and that of a protective environment for the telescope and associated equipment. The test covered the following aspects:

(1) Primary vehicle road and off-road performance

(2) Vehicle auxiliary and safety equipment performance

(3) Post-road-test inspection to determine that all protective functions were effective, both during and after the road tests.

Vehicle performance: The mobile observatory was driven a total of 14 miles on turnpikes, highways, secondary roads, and off-road to determine all of its road characteristics and capabilities. During these tests the level road speed, suspension system "ride" qualities, stability, off-road mobility, and maneuverability capabilities were measured or otherwise determined, as appropriate. They were found to conform to the specified design objectives.

Following the road testing, a thorough inspection of all seams, latches, cabinet doors, locks, and equipment in the observatory showed no signs of damage or inadequacies. The observatory equipment was also operated following these road tests, further confirming the suitability of the mobility characteristics.

All accessory equipment was also checked, including lights, mirrors, heaters, defrosters, gauges, horns, and windshield wipers. Service and operating equipment, such as jacks, tools, manuals, visors, etc were checked, as well as all safety equipment, including flares, first aid kit, brake, flashers, etc. These checks determined that all required equipment was provided and that it was in proper working order.

The tests demonstrated satisfactory conformance of the vehicle to design objectives and performance requirements. These results were amply confirmed by subsequent experience in the operational utilization of the equipment for the PAGEOS surveillance.

Jack and van deployment and rigidity (TI GN351-18-3). - The purpose of this test was to demonstrate the performance adequacy of the jack and leveling system and the van conversion deployment system. These play a major role in providing a precision level rigid operating platform for the observatory telescope. This test consisted of three main steps:

(1) Deploying the jacking and leveling system to elevate and level the observatory in operating configuration

(2) Lowering and extending the side of the van to provide the full operating platform, checking all operating systems (electrical, hydraulic, and heating and air conditioning), and recycling to closed again.

(3) Checking stability of the deployed observatory van and platform by noting the maximum disturbance-induced excursions of the stellar image on the main telescope optical axis.

This test, which was carried out at the selected test site after the road tests were completed, demonstrated satisfactory compliance with system design objectives. Results are discussed in the following paragraphs.

Elevating and stabilizing system tests: The location and orientation selected at the test site for optimum photometric aspects was a fairly uneven graveled surface, and in addition there were some adjacent higher black-top paved surfaces. Since no attempt was made to modify or level the surface (the jacks were simply extended and the observatory elevated), this represented some challenge to the system in accommodating irregular surface conditions. However, the system handled the situation quite well. The system was elevated to operating configuration and leveled without incident, and the sway bracing anchored to provide full stabilization . Everything functioned satisfactorily.

Van platform deployment and systems check: Van sides were lowered and auxiliary jacks placed without incident, again despite the challenge offered by still further and larger irregularities in the surface at the locations for these jacks. The system was energized by means of its own motor-generator; it was also checked later under shore power connection with the cable provided. The electrical, hydraulic, heating and air conditioning, and all other systems functioned satisfactorily.

Stability of optical axis of system: The telescope was aimed at Polaris, and image motion was viewed for the effects of movement of operating personnel, wind gusts, and vibrations of the motor-generator set under power. The largest effect was that of movements of the personnel. Although this varied considerably with the vigor of such movements, it was determined that normal operating movements caused observed maximum image excursions of from 10 to 14 arc seconds, peak to peak (that is, ±5 to 7 arc seconds from the static mean position). The maximum effect observed in wind gusts of up to approximately 20 mph was about 2/3 of this amount. The effect of the motor-generator set was barely visible (almost completely masked by normal scintillation) regardless of power level. There was no discernible difference with the motor-generator set on or off (equipment operating on shore power).

Generator acceptance test (TI GN351-18-4). - The purpose of this test was to verify the adequacy and suitability of the generator installation performance and other characteristics. It consisted essentially of evaluating power output level and regulation, starting and charging characteristics, vibration and noise output level, and any other characteristics affecting system operation. The results of the test, which demonstrated the system to be entirely satisfactory, are discussed in detail below.

Power output level and regulation: With all systems drawing power simultaneously, the generator functioned satisfactorily and regulation remained within required limits:

No-load voltage 125 volts

Maximum load voltage 112 volts

It should be noted that this considerably exceeded any load that would be encountered in actual operation; for instance, two of the heaviest loads (heater and air conditioner) would never occur simultaneously. Likewise, during normal operation of the control system for satellite tracking and observation, the main lights and the hydraulic system would be off. There was also no appreciable change in rpm.

34

Starting and charging characteristics: The engine started smoothly every time, and delivered power demanded as soon as it reached operating speed (a matter of a few seconds). It also kept the battery fully charged when operated sufficiently to do so. The electrical system was modified so that the generator could supply power to recharge the truck battery.

Noise and vibration level: The noise and vibration level were both low and considered to be satisfactory. The noise level, while significant, was tolerable after a few minutes of operation and the vibration (as observed in the preceding test) was scarcely observable in the optic system.

Sky camera and tape recording (TI GN351-18-5). - One of the primary purposes of the sky camera and the tape recorder is to obtain a record of the satellite orbit on each pass. An ephemeris reference data point is obtained from which corrections to the orbital elements can be made for use in making accurate computer reduction and analysis of the photometric data obtained on that same pass. The equipment elements also perform other important functions, and it is the purpose of this test to demonstrate that they are capable of performing in the required manner.

For this purpose, the performance verification test consisted of making camera film exposure frames, which are time-synchronized by audio tape recording of shutter "open" and "closed" time for that frame superimposed on a concurrent audio recording of the National Bureau of Standards WWV radio time signal, all made during a standard operational sequence. The test thus consisted of adjusting the radio receiver for time signal reception; setting up the camera with orientation to include satellite passage in the frames; adjusting the tape recorder for the proper time signal and voice recording; and exposing the sky camera frames, coordinating shutter "open" and "closed" time recording.

The test results were as follows:

(1) Adjusting radio receiver for time signal reception. This was readily accomplished, using the capability described under the corresponding acceptance test.

(2) Camera setup and orientation. The proper camera setup is demonstrated by the framing of the satellite track between shutter open and close points in figure 10.

(3) Audio tape recorder operation. Inputs to the tape recorder include a microphone placed to pick up the voices of the operators on the rear platform and other crew members. It makes clear, concurrent audio recordings of radio time signal; camera operations, including shutter open and closed and frame identification announcements; other operating signals from the crew members (such as calling for satellite or adjacent sky background tracking orientation); and any other significant observations voiced either deliberately or spontaneously (such as bright star side-swipe, satellite crossing of identifiable described position in star field, moonlight or thin cloud interference with satellite sky background intensity level, etc). These voice recordings were of good quality, and when played back afterwards it was easily possible to make a precision reduction of the shutter open and close times from the WWV time signal reference (accuracy was between ±0.1 and 0.2 second). Repeated playback with a stop watch permitted improvement of accuracy.

(4) Sky camera film frame exposures. The frames are exposed by opening the shutter after the satellite has entered the camera field and letting it remain open until a short time before leaving the field, when the shutter is closed. Then the camera is reoriented to the next overlapping field along the satellite path, so that when the shutter is opened, the satellite has entered the new field, etc. The camera performance and its operation is demonstrated by figure 10, which is one of the frames so exposed during this test showing the trail of the PAGEOS satellite.

Figure 10. - Sky camera frame
showing satellite track.

The sensitivity of the camera in showing faint clouds or other aberrations is indicated by
the silhouetting of the trees against the dark Palomar sky, which, despite the full darkness,
shows clearly on the frame below the satellite track. The brightest star trail on this frame is
that of β Ceti. By taking the right ascension and declination of the satellite trail ends, mea-
suring their position on the recorded star field, and coordinating with the WWV time for shutter
opening and closing on the audio recording, a precise determination of the orbital element cor-
rection for the actual satellite position in orbit can be made.

Also clearly visible on the satellite trail in figure 10 is the regular pulsing and other
variations of intensity of the light reflected from the satellite. By proper techniques, this can
be read out photoelectrically from the film with a photodensitometer to give a time-correlated
signal trace corresponding fully to that obtained on the oscillograph. However, even with care-
ful application of such photographic photometry techniques, it will lack the amplitude precision
and frequency response available from the direct photoelectric measurement obtained with the
photomultiplier.

As can be seen from the above discussion and from the quality of the photographic record
shown in figure 10, the tests fully demonstrated the capability of the equipment to meet per-
formance requirements.

Telescope optical alignment and focusing (TI GN351-18-6). - The general purpose of the telescope alignment and focusing test is to determine the adequacy of the mechanical functions and characteristics associated with the optical geometry of the system to meet system performance requirements. The test consists of the following steps:

(1) Check and/or adjust the optical alignment of the main telescope mirrors

(2) Check the complete optical alignment of all telescopes through the eyepieces

(3) Check and/or adjust the parallelism (bore-sighting) of all telescopes (main and auxiliary)

(4) Check the focusing range adjustment.

Specifically, this test is intended to determine whether the complete optical system is fully aligned in all of these aspects, or to assure that the mechanical adjustments provided will permit such alignment. The results of the test are discussed below.

Optical alignment of main telescope mirrors: The basic alignment of the primary and secondary mirrors was checked by visually observing the centering of mirrors and overall concentricity. To do this, a test jig equipped with cross hairs was inserted in the eyepiece adapter tube. Concentricity was good, with no perceptible misalignment.

Complete optical alignment of all telescopes: With the eyepiece in the optical train of the main telescope, it was pointed toward a star of appropriate magnitude (3rd or 4th for the main telescope), so that with the eyepiece drawn to a slightly out-of-focus position, clear diffraction rings were formed. These rings were checked for concentricity. After examining their general alignment with the eyepieces removed, the same diffraction ring concentricity check was made with the auxiliary telescopes. All were found to be in good alignment, apparently having been properly adjusted by the manufacturer prior to delivery. Checks were also made of some of the adjustments provided to test their effectiveness. They were found to operate properly.

Parallelism (or bore-sighting) check: After individual alignments were established, the alignments of the telescopes with each other were checked by pointing at a star (Polaris) and noting whether its image was aligned with the reticle cross hairs of all telescopes simultaneously. They were found to be considerably out of alignment, but were brought into alignment by the adjustments provided. Then the telescope latitude and azimuth axes were reset to a different position, representing an opposite extreme of the latitude axis, and the telescope was pointed to Polaris and again checked for alignment among the various telescopes. They were found to be out of line by over 30 seconds of arc. Modifications of the supporting alignment and adjusting provisions and associated parts (by both GAC and the manufacturer) were required to bring this "sag" of the various optical axes with respect to each other for different attitudes down to acceptable limits. When this was done, it was possible to bore-sight-align all telescopes so that their departure in the various attitudes remained within 10 to 15 seconds of arc, which does not seriously interfere with the tracking capability for the field stop sizes incorporated (4 minutes to 30 seconds), and was therefore considered satisfactory.

Focusing: The focusing range of each of the telescopes was checked to ensure that a satisfactorily sharp focus could be obtained within the range of mechanical adjustment provided. The main telescope clearly resolved the components of Polaris, but would not focus on objects at a distance of less than a few miles; this was considered satisfactory. The auxiliary telescopes also exhibited a satisfactory focusing range, from infinity down to within a few miles for the 8-inch Cassegrain guide scope, and closer for the other two.

Tracking servo control system (TI GN351-18-7). - The purpose of this test was to demonstrate the proper functioning of the system and its ability to accurately and satisfactorily track (1) stars at very low (sidereal) rates; and (2) satellites at the much higher angular rates involved. The system must function with respect to motion about both the polar and declination axes. This operating test includes verification of the following:

(1) Rate control action of axis controls, both on the main control panel and on the portable hand-held control box.

(2) Hand stick control effectiveness, both at the main control panel and the hand-held control box.

(3) Star tracking at sidereal rate.

(4) Satellite tracking.

Rate controls: The rate controls were first used to bring the meter readings to zero on each axis control amplifier, prior to switching on the output to engage the control loop for that axis. The action of the rate control for each axis was checked at the control panel, and then zeroed to make both axes stationary. The rate controls on the hand-held control box were similarly tested and used to bring the telescope around to various desired attitudes. The cutout action of the limit switches was also verified by bringing the telescope toward the various limits.

Hand stick control: Following reset by moving away from the limit switches, the telescope was brought to a suitable attitude clear of obstructions or limits and at a low rate. The hand control effectiveness was checked while plugged in at the main control panel station and was found to be satisfactory. This test was tried in both gain settings. It was then tried out using the hand-held control box, where its function was equally satisfactory.

Star (sidereal rate) tracking control: With the latitude and azimuth axis set in non-equatorial configuration, so that tracking action was required in both axes, the operator brought the telescope around to a star of low declination by use of the rate control knobs on the hand-held control box. Then, looking in the acquisition scope, he used the same controls to bring the star toward the center of the field, carefully adjusting each to kill most of the apparent drift. He then switched to the stick for fine control of displacement in the field, and brought the image over toward the reticle cross hair intersection.

As the image reached the center region, corresponding to the main field stop in the photometer head on the main telescope, the photometer output meter indicated momentary acquisition and the tone generator pitch depressed in coincidence. The operator then switched to the eyepiece of the 8-inch scope for finer control, and again guided the image toward the center region, where the photometer output and tone generator again signalled acquisition. The operator then maneuvered the image with the stick to maintain the tone generator pitch depressed to indicate tracking, with the photometric signal recording a high percentage of the time. After a few minutes practice, he was able to hold continuous track. This was with the 4-minute field stop. Tracking tests were later repeated with the 2-minute and 1-minute field stop. (During later field use, good tracking was accomplished with the 30-second field stop, though there was seldom any need for this. Refer to the description of the system sensitivity and accuracy for each data mode, TI GN351-18-16.)

Following this, tracking was tried successfully on a high declination star, where the sidereal rates are very low in such a non-equatorial configuration of the two lower (setting) axes. Slight bumping of the stick was sometimes required here.

Satellite tracking: The Echo I satellite was used as a target of opportunity for this test, since it is typical in rate and other characteristics (except brightness, which has relatively little effect on tracking). For this test the azimuth and elevation (latitude) axes were set to orient the polar axis to the pole of the satellite track. Then the telescope was rotated on the polar axis to bring it down to a point corresponding to approximately a 10° altitude above the horizon, with the declination set to the value corresponding to that hour angle on the polar axis, as predicted from the orbit ephemeris. The telescope was held at this acquisition attitude from a few minutes prior to predicted time until actual acquisition. The acquisition star field was confirmed in the acquisition scope and the area scanned both in the acquisition scope field and direct.

When the satellite was spotted, the operator watching in the acquisition scope first used the rate potentiometer control knobs on his hand control box to "catch" the satellite and bring it toward the cross hairs, killing most of the apparent drift of the satellite image with respect to the cross hairs. He then switched to the stick for fine control, to bring it into the "squealer" (tone generator) response region corresponding to the photometric acquisition in the field stop, and then to the 8-inch scope for even finer control.

Once this stage had been reached, with rate control potentiometers adjusted to eliminate drift and image position held by the stick, tracking control behavior was almost identical to that with a star, except for the fact that the slowly changing angular rate of the satellite's motion required readjustment of the rate control potentiometers from time to time in order to prevent build-up of excessive stick control forces. Also, in satellite tracking the satellite remains relatively still in the field while the entire star field drifts slowly by in the background like a moving, star-studded, black curtain.

The eyepiece, since it is on the telescope, is itself slowly and continuously moving, so that the operator has to follow it to watch the satellite. If the path and access provisions have been properly established ahead of time by a prior "swing through," then this presents no difficulty.

The operator was able to maintain track; although, again, it took a few minutes of practice for a new operator to acquire the knack of steady continuous tracking. (During this test all the operators were new.) Track was maintained for approximately 14 minutes, until the satellite became obscured. It was soon demonstrated that with a small amount of experience an operator can maintain good satellite tracking under normal conditions, and the control system was demonstrated to be performing properly. (For percent track maintainable with satellites, refer to figure 15.)

Reception and recording of time signals (TI GN351-18-8). - The purpose of this test was to demonstrate satisfactory performance of the communication-type radio receiver installation in this system, and its capability to receive and produce an output signal of sufficiently good quality to provide a readable recording under normal operating conditions. The test consisted of:

(1) Checking the receiver's functions

(2) Reception of time signal on several bands

(3) Recording the demodulated signal on the oscillograph (and the audio on the tape recorder)

To make the tests valid for other locations where a better antenna might be needed, as proved to be the case at Palomar (see fig. 11) a simple, short, single-wire antenna was used

Figure 11. - Radio antenna array for time signal receiver at
Palomar Mountain (triple dipole).

for this test at the Akron Wingfoot Lake Knoll test site.   Results of the test were as follows:

All receiver functions (band spread, SSB, variable AGC rate, narrow bandpass control, etc) checked out satisfactorily.   National Bureau of Standards station WWV was successfully tuned in on 2-1/2, 5, 10, and 20 megacycles.   By making use of the various available features it was possible to obtain a signal of acceptable quality on each of these frequencies.   The modulation of the WWV carrier signal was fed directly in audio form to the tape recorder. However, the signal was demodulated before it was fed to the oscillograph.   This gave sufficient signal for legible recording on the oscillograph charts (see fig. 12). To summarize, the tests verified that performance conformed to the specifications, and that satisfactory time signal recording capability is provided.

Signal-modulated tone generator performance (TI GN351-18-9). - The purpose of this test was to demonstrate proper functioning of the tone generator modulation by the photometer output signal level.   The test was a simple one, involving turning on the generator and photometer, adjusting the speaker volume control, and pointing the telescope toward a light source to increase photometer output so corresponding pitch depression could be noted.

The results of the test were equally simple.   The controls functioned properly, and the

Figure 12. – Typical time signal oscillograph record.

pitch depression proportional to light intensity into the telescope was observed. As the light intensity into the telescope was decreased, the pitch rose again, and when the light was removed the tone generator pitch returned to its original (high) level. The test demonstrated that the tone generator performance is satisfactory.

Precision of azimuth and latitude and polar and declination axes and protractors (TI GN351-18-10). - The purpose of this test was to determine whether the accuracy of alignment of each of the four axes and their protractors was sufficient to permit orientation of the telescope to the specified accuracy (specification requirement: within 0.4 degree).

The test consisted of placing the telescope in its sidereal mode, using an "astro-compass" procedure, and then using that sidereal setup to acquire, within 0.4 degree, several stars by regular astronomic coordinate (local hour angle, declination) procedure. The results were as follows.

The astro-compass procedure was repeated on several stars. Since all indicated the same azimuth setting, it was then clamped at the azimuth and used for star acquisition of six different stars by polar and declination axis settings. All six were well inside the 1° reticle circle in the acquisition scope, thus demonstrating an accuracy within 0.4 degree. The settings were as shown in Table 3 for the Palomar Mountain site (W 116° 51 min, N 33° 19 min) on 23 June 1966 U.T. The test indicated the accuracy of the 4-axis mount to be in accordance with requirements.

TABLE 3. - SETTINGS FOR CHECKING ALIGNMENT
PRECISION BY STAR TRACKING

| Star | U.T. time | Circle readings | |
		LHA	Declination
72 Ophiuchus	8 hr 28 min	0:40 W	+ 9°, 33 min
η Hercules	8 hr 35 min	0:54 E	+ 30°, 12 min
α Serpens	8 hr 55 min	3:30 W	+ 6°, 33 min
BS 5859	9 hr 59 min	4:33 W	+ 5°, 34 min
ξ Hercules	10 hr 32 min	2:53 W	+ 29°, 15 min
71 Ophiuchus	10 hr 39 min	2:51 W	+ 8°, 43 min

Second-Order extinction coefficient (TI GN351-18-11). - This is the first test exercising the photometric capabilities of the system, and the first test to involve integrated employment of all elements of the photometric observatory system. The purpose of the test is to utilize this system and the associated procedures developed to determine the 2nd order U-B-V photometric extinction coefficients for the test site location (Palomar Mountain, California). The tests consisted of the following:

(1) Standard 2nd order extinction coefficient photometric calibration data procedure, using three or more close pairs of stars. (Procedure is described in reference 1.)

(2) Reducing the oscillographic data recordings to digital form.

(3) Using the computer programs developed for this purpose to reduce and analyze this data and derive coefficients.

Measurements were made of the following six stars, consisting of close pairs of widely different colors, in the U, B, and V bands:

Pair No. 1   BS 5854 and 5859

Pair No. 2   BS 6281 and 6299

Pair No. 3   BS 6854 and 5859

The data was field reduced and punched on IBM cards. The computer results are shown in figure 13. The process and results of this test demonstrated satisfactory performance capabilities.

Scale factors (TI GN351-18-12). - The purpose of this test was to determine the scale factors of this photometric system. When supplemented with the results of the preceding and following tests (secondary and primary extinction coefficients, respectively), this will permit utilization of the photometric satellite data, or other data taken by this system, in reduction and derivation of absolute measurement values.

The test consisted of selecting suitable stars and taking photometric calibration data for determining the scale factors of this equipment for use in transforming U-B-V system data to standard reference values. For this a number of standard stars were selected as calibration stars. These calibration stars ranged widely in color spectral type, but were observed through substantially the same air mass near the zenith.

The selected overhead standard stars for use as scale factor calibration stars on 30 June 1966 were Yale Bright Stars, catalogue No. BS 6095, 6148, 6324, 6410, 6556, and 6703. These stars all had a low zenith distance between 7 hours, 14 minutes and 7 hours, 47 minutes U.T. on the date when the observations were taken. The data recorded was reduced according to the standard process developed (ref. 1), and processed by calibration program E1970. The results are shown in figure 14. The processes carried out and the results obtained demonstrated satisfactory performance capabilities.

Primary extinction coefficient and zero point terms (TI GN351-18-13). - The purpose of this test was to demonstrate and obtain representative values of the remaining calibration parameters needed to perform photometric measurement tasks on satellites or astronomic bodies. Since these parameters are time-dependent, in satellite photometry they must be determined specifically for each satellite pass.

The PAGEOS satellite pass starting shortly after 0900 hours U.T. on 1 July 1966 over the Palomar Mountain site was utilized for this test. Several non-variant stars of bracketing magnitudes with respect to that of the satellite and distributed along its path were selected as calibration stars for this pass. The raw analogue intensity data taken was then scaled (digitized) from the oscillograph record and tabulated against the corresponding WWV radio time signal values for the data points used in accordance with prescribed procedures in the U, B, and V bands. The tabulated data was then punched on IBM cards and transmitted (via dataphone) to GAC's computer center at Akron, where the U-B-V extinction coefficients and zeropoint terms required to define the adjacent sky conditions for that time were derived, using calibration program III of E1980 (ref. 1). The results obtained are shown in Table 4. The processes carried out and results obtained demonstrated satisfactory performance capabilities of the system.

Acquisition and track of a 7th magnitude satellite (TI GN351-18-14). - The purpose of this test was to demonstrate the magnitude reach of the mobile observatory for satellite photometry. This is one critical measure of the system's basic capability. Since the light reach

		SECOND ORDER		CALIBRATION PROGRAM (I)				6-23-66		E1960
B.S. NO.	Z	X	DV	DU	DB	DV	DU	DB	DEL(B-V)	DEL(U-B)
1 5854/5859	55.9	1.770	2.72/10	0.76/10	2.06/10	1.59/12	1.25/12	3.47/12	-1.08655	-1.14792
1 5854/5859	66.4	2.093	2.12/10	1.72/12	1.84/10	0.40/11	2.50/13	0.88/11	-1.02180	-1.23675
6/30/1966										
2 6281/6299	23.7	1.092	0.57/10	0.84/10	1.35/10	1.63/10	2.04/12	1.27/10	1.20650	1.46879
2 6281/6299	60.6	2.033	1.40/11	1.45/11	1.10/10	1.32/10	1.21/12	1.08/10	1.14836	1.48254
7/ 1/1966										
3 5854/5859	30.5	1.161	1.03/ 9	1.26/11	0.91/ 9	0.79/11	2.76/12	1.65/11	-0.93526	-1.38376
3 5854/5859	77.3	4.469	1.84/10	0.77/10	1.22/10	0.32/11	1.08/13	0.51/11	-0.98661	-1.37251

NO. OF POINTS =   6

1 5854/5859	-0.07788	0.03402
2 6281/6299	-0.05715	0.00975
3 5854/5859	0.01617	-0.01335

NO. OF POINTS =   3

SECOND ORDER EXTINCTION COEFFICIENTS

K-2-PRIME B-V = -0.03762
K-2-PRIME U-B =   0.03014

Figure 13. - Computer printout of determination of second-order extinction coefficients.

STAR	Z	X	DV	DU	DB	V0	(B-V)0	(U-B)0	V-V0	B-V-(B-V)0	U-B-(U-B)0
						(II)		6-30-66			E1970
6095	26.0	1.11247	0.96/10	1.93/11	1.77/10	10.90544	-1.02578	0.55129	-7.14544	1.29578	-0.35129
6148	23.3	1.08877	0.72/9	1.73/11	0.71/9	9.92007	-0.31082	1.00049	-7.15007	1.25082	-0.31049
6324	16.2	1.04123	0.86/10	2.80/11	1.96/10	11.05337	-1.24178	0.29089	-7.13337	1.23178	-0.40089
6410	16.8	1.04461	0.51/9	1.54/10	0.98/9	10.31214	-1.05037	0.30021	-7.19214	1.12037	-0.22021
6556	24.3	1.09672	1.40/9	1.07/9	0.89/8	9.19491	-1.05888	0.45219	-7.12491	1.19888	-0.34219
6703	8.6	1.01123	1.05/10	2.50/12	0.98/10	10.84865	-0.22561	0.98825	-7.13865	1.16561	-0.28825

NO. OF POINTS = 6

CONST	SLOPES	SUM(X-XBAR)**2	STD ERROR OF RESIDUALS	DIFFERENCE IN DEP VAR
-7.14998	0.00653	0.94428	0.02623	0.00277
				-0.00623
				0.01668
				-0.04262
				0.02416
				0.00520
1.20619	0.01111	0.94428	0.06983	0.08659
				0.03419
				0.02570
				-0.08659
				-0.00887
				-0.05102
-0.33597	0.06139	0.57188	0.06501	-0.02759
				-0.01688
				-0.05816
				0.11085
				-0.01297
				0.00475

SYSTEM TRANSFORMATION SCALE FACTORS

EPS = 0.00653, ε
MU = 1.01123, μ
PSI = 1.06540, ψ

Figure 14. – Computer printout to derive scale factors.

TABLE 4. - OBSERVATIONS FOR DETERMINING
PRIMARY EXTINCTION COEFFICIENTS

Star	U. T.	Spectrum	V	B-V	U-B	Z	X	$\dfrac{du}{gain}$	$\dfrac{db}{gain}$	$\dfrac{dv}{gain}$
8115	08:34	G8 II	3.19	1.76	1.00	23.3	1.0556	$\dfrac{1.16}{11}$	$\dfrac{1.70}{10}$	$\dfrac{1.71}{10}$
21	08:37	F2 IV	2.28	0.45	0.34	52.0	1.6233	$\dfrac{2.18}{10}$	$\dfrac{1.81}{9}$	$\dfrac{1.10}{9}$
168	08:41	K0 II-III	2.22	2.30	1.17	56.0	1.7825	$\dfrac{1.20}{11}$	$\dfrac{0.93}{9}$	$\dfrac{1.11}{9}$
163	08:46	G8 IIIp	4.39	1.34	0.87	63.1	2.2037	$\dfrac{1.10}{12}$	$\dfrac{1.41}{11}$	$\dfrac{1.48}{11}$
8278	08:54	A3 V	1.16	0.14	0.08	77.9	4.6807	$\dfrac{0.90}{10}$	$\dfrac{1.02}{8}$	$\dfrac{0.70}{8}$
8115	09:44	G8 II	3.19	1.76	1.00	8.7	1.0117	$\dfrac{1.10}{11}$	$\dfrac{1.59}{10}$	$\dfrac{1.63}{10}$
21	09:46	F2 IV	2.28	0.45	0.34	43.1	1.3683	$\dfrac{2.39}{10}$	$\dfrac{1.79}{9}$	$\dfrac{1.10}{9}$
168	09:49	K0 II-III	2.22	2.30	1.17	46.5	1.4511	$\dfrac{0.47}{10}$	$\dfrac{0.94}{9}$	$\dfrac{1.13}{9}$
15	09:52	B8p	2.06	-0.58	-0.11	43.8	1.3843	$\dfrac{1.92}{9}$	$\dfrac{1.03}{8}$	$\dfrac{1.28}{9}$
163	09:54	G8 IIIp	4.39	1.34	0.87	49.4	1.5353	$\dfrac{1.46}{12}$	$\dfrac{1.58}{11}$	$\dfrac{1.56}{11}$
8728	10:00	A3 V	1.16	0.14	0.08	69.9	2.8924	$\dfrac{1.16}{9}$	$\dfrac{1.42}{8}$	$\dfrac{0.77}{8}$

Results

Primary extinction coefficients: Zero point terms:

k'_v = + 0.136 ζ_v = - 7.432

k'_{b-v} = + 0.108 ζ_{b-v} = + 1.086

k'_{u-b} = + 0.271 ζ_{u-b} = - 0.568

of the system for photometric measurement is better than tenth magnitude (as demonstrated in the system sensitivity and accuracy test, TI GN351-18-16), the capability must necessarily depend on how faint a satellite one can acquire and track with the system. Actually, since SAO "Moonwatch" satellite tracking has repeatedly demonstrated visual acquisition capability for equipment such as this of better than 10th magnitude, the practical reach of this system would be entirely dependent on the magnitude that could be picked up and tracked following acquisition with the guide scopes and servo systems incorporated in this observatory system. Indications are that it should be possible to operate down to at least 8th or 9th magnitude; 7th magnitude was a design requirement. The purpose of this test was to confirm the above by demonstrating acquisition and initial track of a 7th magnitude satellite under adverse, low-altitude conditions (below 15°).

For this purpose the test consisted of acquisition of Explorer XIX on a very low pass, starting the track at as low an altitude as possible (as early as possible), and tracking while recording the photometric signal for at least several minutes.

Actually, during the test (which was carried out on 14 August 1966 at 1036 hours U.T.) acquisition was made and tracking begun at approximately 7° elevation, when the apparent magnitude was +7 or fainter, and Explorer XIX was tracked and recorded all the way across the sky through culmination to proximity of the other horizon. Since culmination was at a 16° elevation, practically the whole pass was below 15°. A satisfactory oscillograph data record was obtained for the entire pass, and a sample from this record is shown in figure 15. The 2-minute field stop was employed for this recording. It can be seen from this record that drop-out to sky background is less than 10 percent; or, conversely, that tracking is more than 90 percent continuous. This test amply demonstrated the capability of the system to exceed the requirements.

Polarization measurement of Echo II satellite (TI GN351-18-15). - The purpose of this test is to demonstrate the capability of the system to perform photoelectric polarimetric measurements on the light reflected by orbiting satellites. Echo II, originally, at least, had an alodine coating known to have polarizing characteristics, so the test consisted of operating the photometric observatory in the normal manner for satellite photometry of Echo II, taking and recording polarimetric data with the rotating polaroid filter in place ahead of the field stop. The polaroid filter was operated in the normal manner (advancing in short steps), the recorded data measured and analyzed, and the measured percent polarization was then calculated.

The results of the test showed 17 to 23 percent polarization of the light from Echo II. The measurements were taken at U.T. 1105 hours on 14 August 1966, at the Palomar Mountain site. The oscillograph record obtained is shown in figure 16. The filter was advanced 10° each step, as indicated by the notches on the gain position level indicator trace on the record shown in figure 16. It can be noted that nine steps (or 90°) appear between the E_{max} and E_{min} levels, as would necessarily be the case for linear polarization. The percent polarization was calculated from the measured data using the following formula:

$$\text{Percent polarization} = \frac{E_{max} - E_{min}}{E_{max} + E_{min}} \ 100$$

and the values obtained are listed in table 5. These measurements demonstrated the capability of the system to accomplish polarimetric photometry of satellites. They also provided operational data that can be utilized in future design.
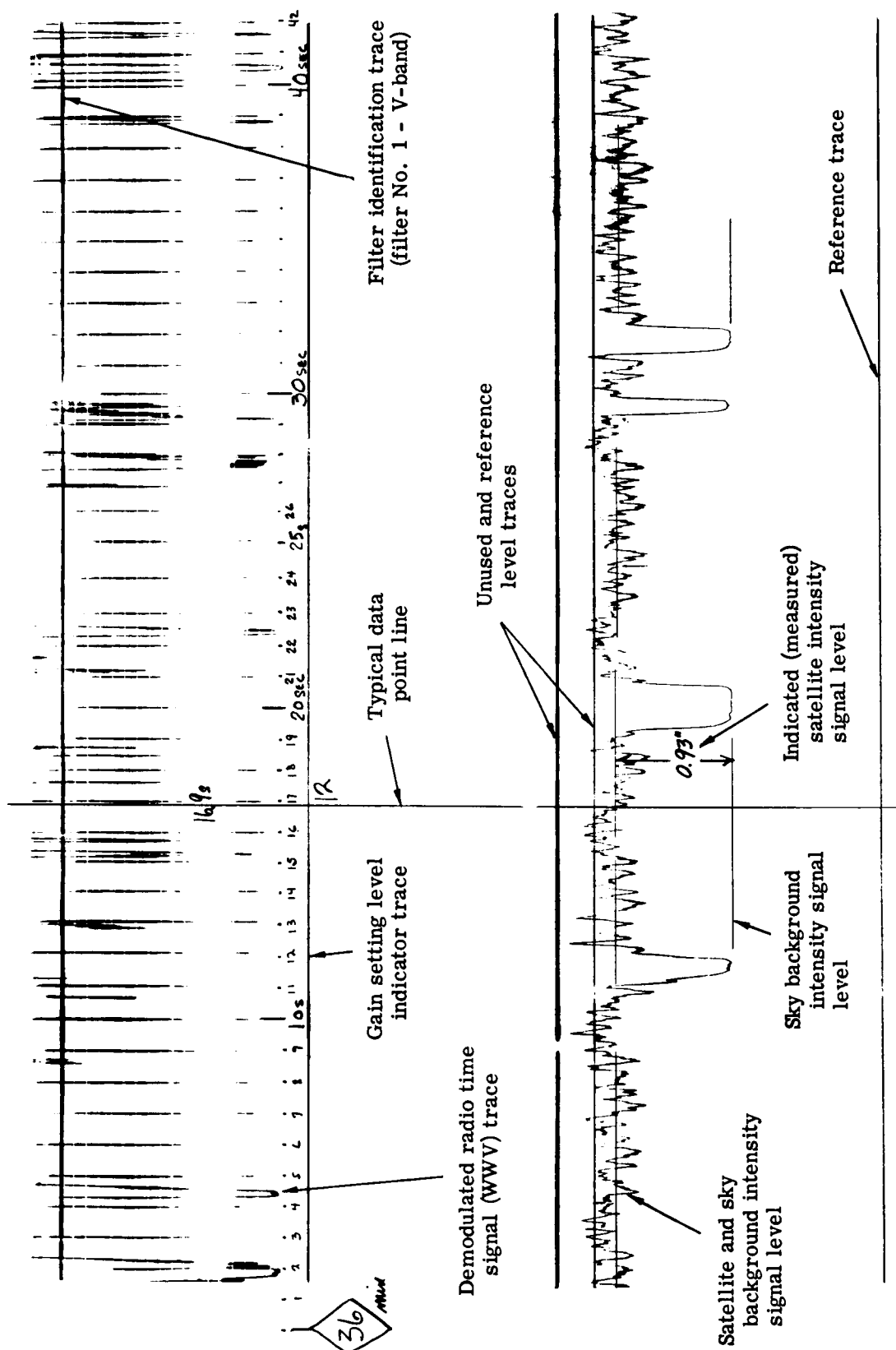
Figure 15. – Explorer XIX tracking at Palomar Mountain, 14 August 1966, 1036 hours U. T.

48

Figure 16. – Oscillograph record of polarimetric measurements of Echo II.

49

TABLE 5. - POLARIZATION MEASUREMENTS OF ECHO II

Observation	E_{max}	E_{min}	Polarization, percent
1	53	37	17.8
2	62	42	19.2
3	74	47	22.3

System sensitivity and accuracy for each data mode (TI GN351-18-16). - The purpose of this test was to determine the capability of the system to measure down to faint magnitudes and to determine the basic system accuracy in satellite photometric measurements. The test measurements, which were made on 21 August 1966 at the Palomar Mountain site, consisted of three main parts:

(1) Sensitivity demonstrated by measurement of one or more stars down to the 10th visual magnitude or more.

(2) Repeatability and accuracy of measurement in U, B, and V data modes.

(3) Accuracy and repeatability of polarimetric measurements, using standard stars from the Behr catalogue (ref. 3).

Repeatability tests were carried out by making two measurements of each star and comparing them. Accuracy was checked by comparing the measured value with the catalogue value in each color index. Results are discussed in the following paragraphs.

System sensitivity: The system sensitivity was demonstrated by tracking and measurement of the 10th magnitude field star of ϵ Lyrae along with the ϵ Lyrae component. These stars are shown in figure 17. The oscillograph record for each is shown in figures 18 and 19. This field star has a B. D. listing of 9.5 magnitude, which would represent a visual band photometric magnitude of 10.6 (ref. 2). These measurements were made at 0541 and 0539 hours U. T., respectively. Since a 2-minute field stop was being used, and a good signal was recorded, it can be seen that this was not anywhere near the limit of capability as far as sensitivity is concerned. In fact, use of the higher gain settings (less photomultiplier output attenuation) would give an order of magnitude sensitivity improvement, while use of the smaller field stops would give a still greater improvement in signal-to-noise ratio by reduction of sky background (noise) level.

U, B, and V repeatability and accuracy: The results of these measurements are given in table 6, which shows the following mean variations from the five repeated observations:

U-V	0.038
B-V	0.020
V	0.032

Mean accuracies of ten measurements, in terms of variation from catalogue value, was as follows:

U-V	0.029
B-V	0.014
V	0.050

Location		
R. A.	**Dec.**	**Characteristics and comments**
18hrs 41. 7min	N 39°35"	ε Epsilon Lyrae Two pair Distance 207. 1" Scale: (10" 20")
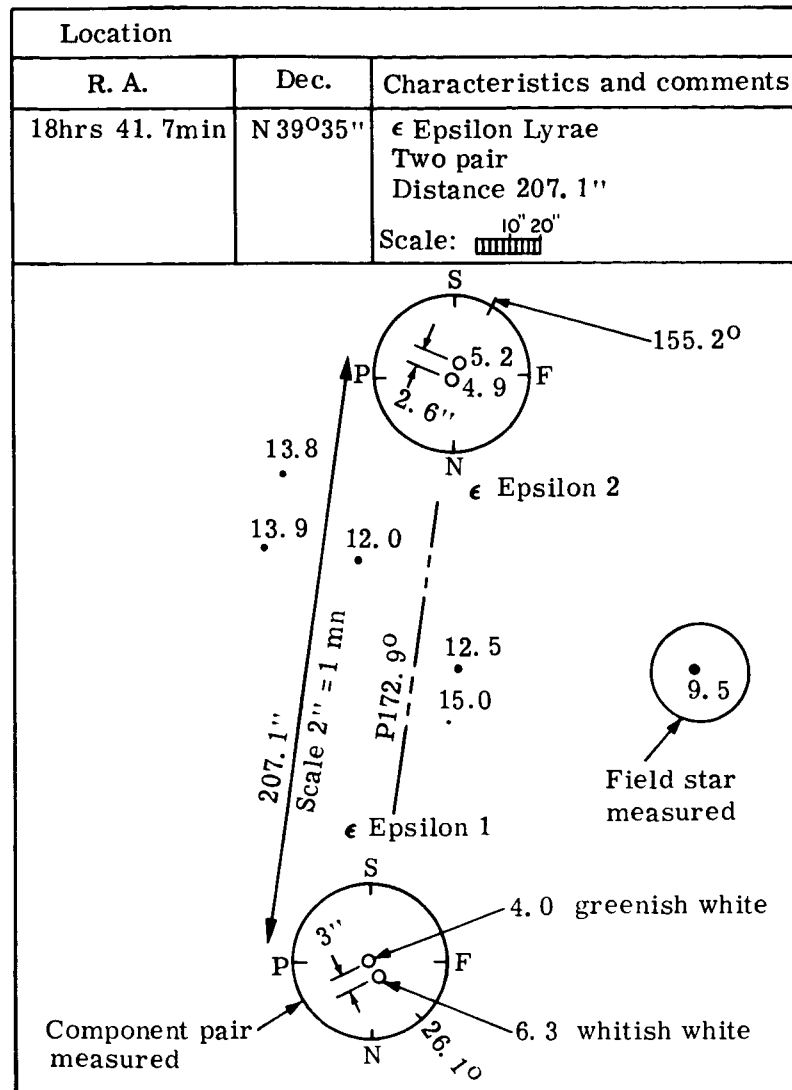
Figure 17. - Diagram showing characteristics of ε Lyrae components
(from Webb's Atlas of the Stars, 2nd ed, 1934-1944).

These measurements demonstrated clearly that both repeatability and accuracy were better than 0. 1 magnitude in all three color data modes.

Polarimetric accuracy and repeatability: The results of polarimetric and repeatability tests are given in table 7, which shows that instrumental and other polarization errors or bias apparently do not contribute more than 1 percent, and certainly no more than 2 percent. This is demonstrated by the fact that using several stars of low polarization (approximately 1 percent or less), no indicated polarization readings emerged above the 2-1/4 percent signal scintillation level. This, taken with the results obtained with the Echo II polarization measurement tests described above (TI GN351-18-15), which indicate the ability to pick up measurements of polarization above this level, seem to amply demonstrate a measurement accuracy and repeatability capability of at most a few percent error, and probably an accuracy in the order of 1 or 2 percent. This shows good compliance with original design objectives and requirements.
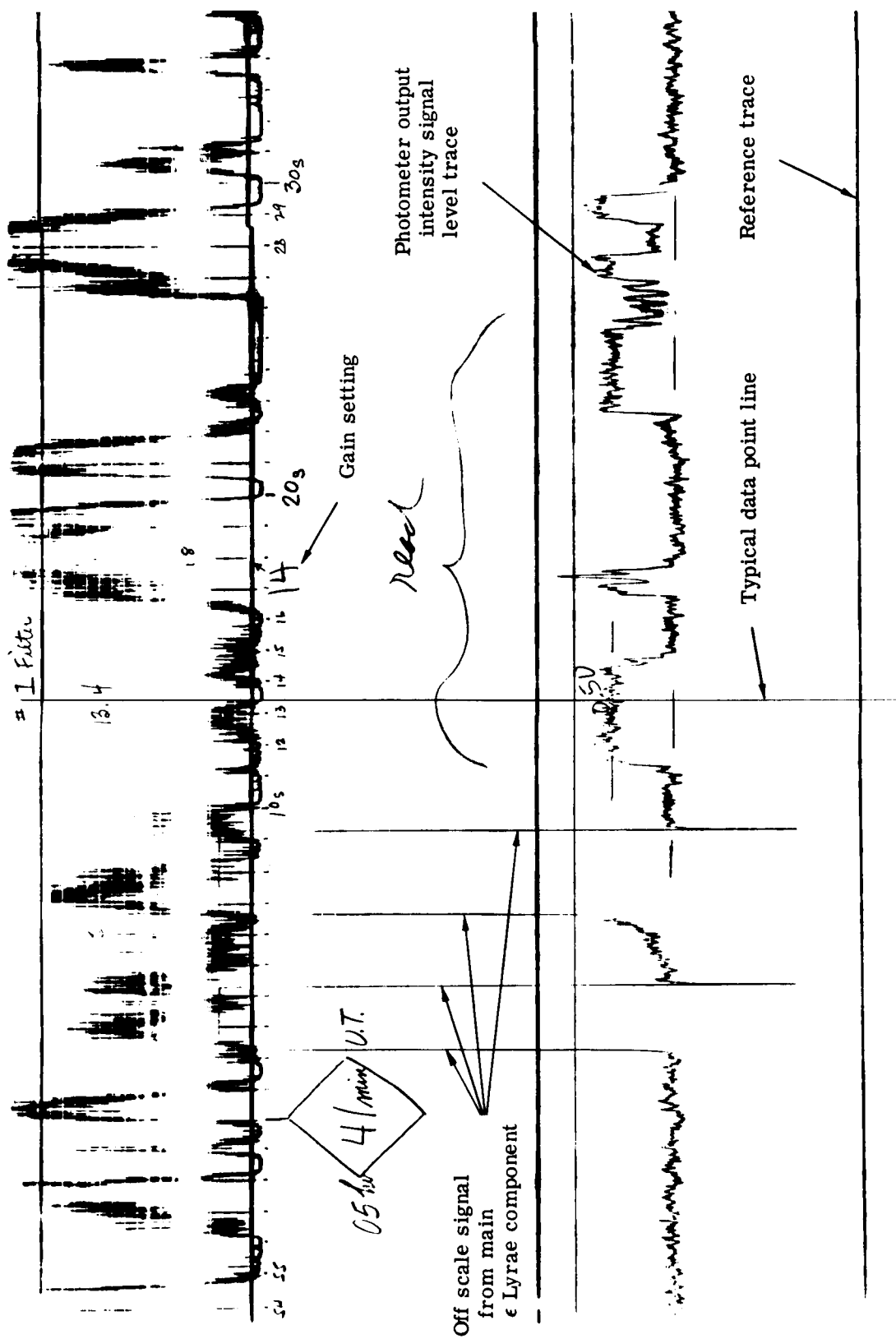
Figure 18. – Oscillograph record of photometric measurement of ε Lyrae field star.
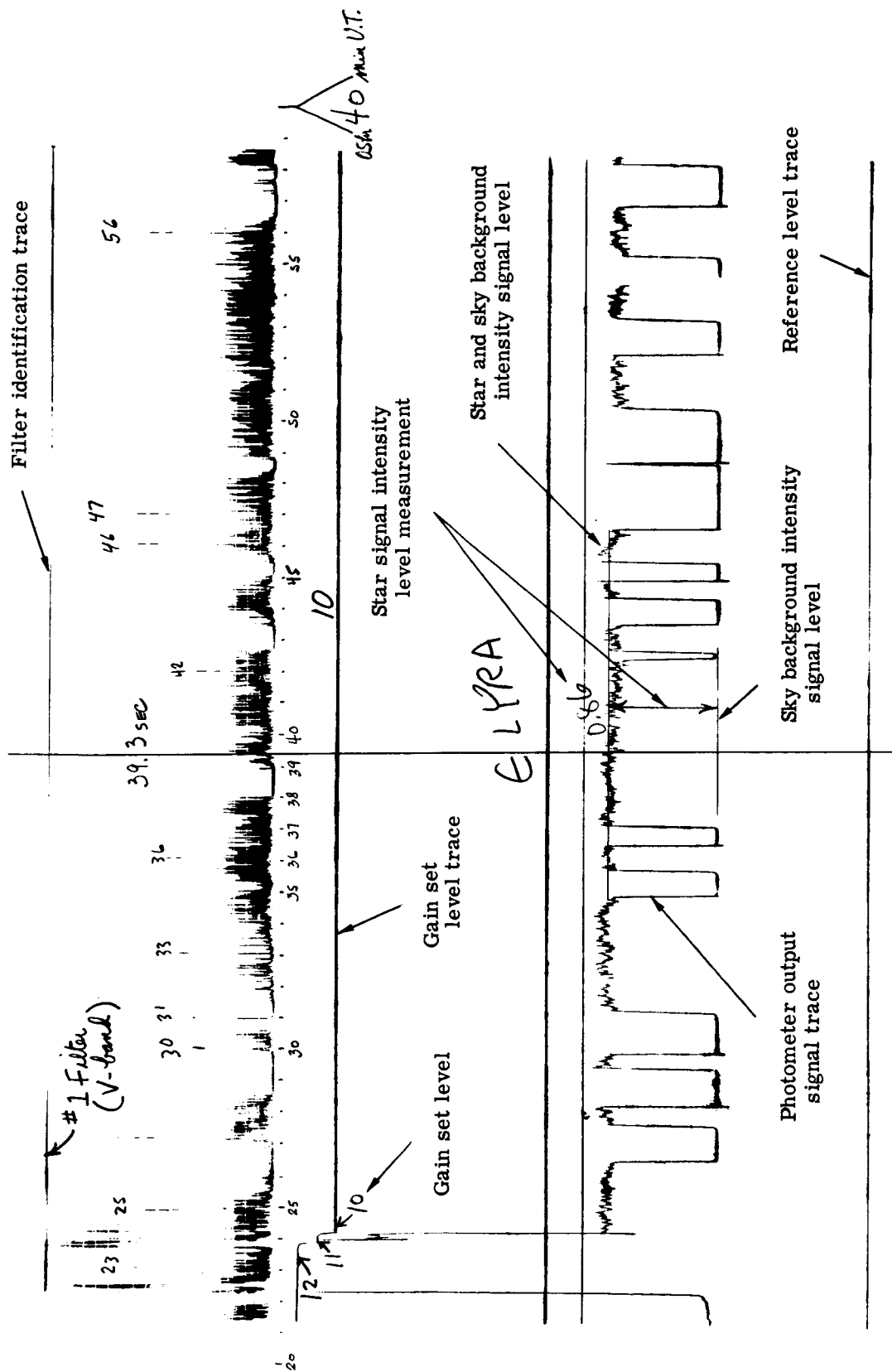
Figure 19. – Oscillograph record of photometric measurement of ε Lyrae components.

TABLE 6. - U-B-V REPEATABILITY AND ACCURACY DATA ON FIVE SELECTED STARS

Star	Catalogue values			Test 1			Test 2		
	U-V	B-V	V	Spectral regions	Reduced values	Change, magnitude	Spectral regions	Reduced values	Change, magnitude
1. 44 Cygni	1.74	1.00	6.31	U-V	1.76	0.02	U-V	1.71	0.05
				B-V	1.00	.00	B-V	0.99	.01
				V	6.24	.07	V	6.23	.01
2. 35 Cygni	1.13	0.65	5.16	U-V	1.16	.03	U-V	1.16	.00
				B-V	0.66	.01	B-V	0.68	.02
				V	5.15	.01	V	5.10	.05
3. 39 Cygni	2.87	1.34	4.45	U-V	2.84	.03	U-V	2.85	.01
				B-V	1.33	.01	B-V	1.31	.02
				V	4.46	.01	V	4.48	.02
4. γ Cygni	1.21	0.67	2.23	U-V	1.24	.03	U-V	1.21	.03
				B-V	0.67	.00	B-V	0.69	.02
				V	2.16	.01	V	2.19	.03
5. α Cygni	-0.12	0.09	1.25	U-V	0.06	.06	U-V	-0.16	.10
				B-V	0.11	.02	B-V	0.08	.03
				V	1.16	.09	V	1.21	.05

Notes: Sensitivity of faintest star measured to ±0.1 magnitude
Companion to star: ϵ Lyrae; B.D. - 9.5 magnitude, or
photometric magnitude of 10.6
Required accuracy of tests: ±0.1 magnitude
Required repeatability of tests: ±0.1 magnitude

TABLE 7. - POLARIMETRIC ACCURACY MEASUREMENTS

Star	Cat. value of % polarization	Test 1		Test 2	
		Reduced % polarization	Percent change	Reduced % polarization	Percent change
1. η Pegasi (B.S. 8650)	0.06	< 2.23	< 2.23	< 2.23	< 2.23
2. σ Cygni (B.S. 8143)	1.17	< 2.23	< 2.23	< 2.23	< 2.23
3. δ Cygni (B.S. 7528)	0.06	< 2.23	< 2.23	< 2.23	< 2.23
4. γ Aquili (B.S. 7525)	0.23	< 2.23	< 2.23	< 2.23	< 2.23
5. α Lyrae (B.S. 7001)	0.05	< 2.23	< 2.23	< 2.23	< 2.23
6. β Ophiuchi (B.S. 6603)	0.33	< 2.23	< 2.23	< 2.23	< 2.23

Notes: Required accuracy of tests: 1 percent
Required repeatability of tests: 5 percent
Scintillation noise was at a level of 3.23 percent (from peak to peak, or 3σ, measurement of 12.5 percent). This would give an MDS (minimum discernible signal) of 2.23 percent with the integration time available with the present equipment (galvonometers).

[a] Published values are from the Behr catalog (ref. 3).

The above tests indicate that the system precision and sensitivity in all its various data modes represents good to excellent performance, that it conforms to specified requirements, and represents a very satisfactory system capability. Since no suitable high polarization stars were available at the time, the extent of polarization performance capabilities was not fully determined.

Absolute intensity calibration in each data mode (TI GN351-18-17). - This is a companion test to the preceding one. It examines the accuracy of system calibration procedures and performance so that system precision can be fully utilized in obtaining accurate absolute measurement values. The tests considered the calibration function in the three operating data modes of the system:

(1) Visual band total intensity measurement

(2) Time-shared three-color (U-B-V) intensity measurements

(3) Visual band polarimetric measurements

The tests consisted of determining that the equipment and procedures were satisfactory for each mode. For the first two of the above categories, the calibration was an essential part of the preceding test (TI GN351-18-16). Using the values obtained in table 6, which were used to obtain repeatability and accuracy demonstration, these same star measurements represent calibration procedures used, and can be likewise considered as absolute intensity calibration for the system. By taking the sum of the deviations from the catalog values in each band from the measurements listed in table 6, averaging them, and normalizing the values to zenith conditions, we can obtain a measure of the system deviation based on this relatively small sample size (10 measurements each). For the V band this gives

$$\frac{0.07 + 0.08 + 0.01 + 0.06 + 0.01 + 0.03 + 0.07 + 0.04 + 0.09 + 0.04}{10 \times 1.4} = 0.036,$$

where 1.4 represents an approximate value of air masses involved in this typical group of star measurements. By similar means, we obtain values of 0.01 and 0.02 for the B-V and U-V spectral regions, respectively. It should be recognized that the total system accuracy will be significantly better than the above values, as demonstrated by a small sample size, and that continuous V band would also be better than that obtained for these time-shared measurements. Since these measurements involved a broad spread of star magnitudes rather than use of only brighter ones that would be advantageous for system calibration (thus reducing extra-system noise ratio), and since these measurements involve the entire operational error (including star calibration, data reduction, processing, etc), the accuracy of the system is judged to be at least 2 percent or better (as has since been demonstrated), indicating that the accuracy of the system calibration procedure and performance in these two modes is excellent.

Also, as in the preceding test, a determination had to be made as to the degree to which instrumental polarization could deviate the measurements or calibrations. Therefore, measurements were made of 10 stars from the Behr catalogue of standard polarization stars, 8 of which have a percent polarization equal to or less than 0.04 percent. The results are given in table 8. From the measurements presented in the table, we can determine that the average percent polarization for the stars used in this test was 0.036 percent.

The peak to peak scintillation was approximately 6.25 percent, and based on this, the rms scintillation is then estimated to be 2.23 percent. Basic theory indicates that an MDS signal occurs when the signal level is equal to rms noise. We can thus only measure polarization to an accuracy of 2.23 percent with the integration times used for this test.

TABLE 8. - INSTRUMENTAL POLARIZATION MEASUREMENTS

Star	BS	H. D.	U. T.	Catalog value of percent polarization[a]	Measured value of percent polarization
1	8694	216228	8-15	0.02	None discernible
2	8162	203280	8-15	.04	None discernible
3	8781	218095	8-15	.04	None discernible
4	8684	216131	8-15	.03	None discernible
5	7557	187642	8-15	.04	None discernible
6	6629	161868	8-15	.02	None discernible
7	6410	156164	8-15	.04	None discernible
8	6092	147394	8-15	.03	None discernible
9	8518	212061	8-15	.05	None discernible
10	7602	188512	8-15	.05	None discernible

[a]Catalog values are from the Behr catalog (ref. 3).

The fact that no polarization indication emerges in any direction (any angle of the polarization filter) shows that there was no instrumental polarization greater than this that would cause deviations to the calibration values being used in any measurement.

Therefore, it can be concluded that the absolute intensity calibration characteristics for this system and the associated procedures developed are satisfactory, except for polarization, where it was not possible to check this system against stars of other higher degrees of polarization. Maximum instrument polarization bias error, however, is shown not to be greater than about 2 percent.

Acceptance test summary and conclusions. - The acceptance test program, by the time it was completed, had demonstrated full compliance of the equipment with the requirements. A few problems and incidents that occurred during the testing program are worth noting.

By far the most significant of these had to do with the polar drive motor, which was found to be faulty during the acceptance testing. Although it checked out satisfactorily in most respects, in others it did not conform and caused recurrent trouble. Eventually, detailed measurements were made, which demonstrated that the motor had a shorted winding in the stator. Based on this determination, the supplier fabricated a replacement stator, which was installed before the test program was continued.

An improvement was required in the mountings for the 8-inch auxiliary scopes. To provide adequate adjustment capability and rigidity, several minor modifications and additions were made, which resulted in satisfactory performance characteristics.

One other trouble spot involved the rain seals, which required modification and improvement. These changes resulted in satisfactory performance.

The above items required action on the part of both GAC and the supplier involved. A few other minor elements were modified by GAC. Main bearing friction level on the tracking axes was a cause of some concern, but this steadily improved with use.

All these required modifications were handled prior to completion of the acceptance test involved. Hence the tests are applicable to the final delivered system. Specific conclusions of the test program, with the possible exception of polarization, can be listed as follows:

(1) The system meets all design and performance requirements.

(2) The design parameters analyzed and selected during development proved to be correct.

(3) The construction of the entire system was of such quality that design objectives were fully realized and performance objectives met.

In view of the results of this test program, it is concluded that the system meets all requirements and represents a quality product which can be expected to perform satisfactorily on all tasks within its intended and specified capabilities.

CONCLUSIONS

The detail design requirements for the transportable photometric observatory may be summarized in three broad performance categories. These are:

(1) Transportability

(2) Deployability

(3) Functional suitability for satellite observations

Transportability and deployability were satisfactorily demonstrated during the acceptance tests at GAC's Wingfoot Lake Knoll Site, and later confirmed in actual operation from the Palomar site for PAGEOS observations.

Functional suitability for satellite observations has been demonstrated, both during acceptance tests at Akron, and later by successful observations from Palomar of such satellites as PAGEOS, Echo I, Echo II, Explorer XIX, and AF/GAC's 30-foot diameter grid sphere. Communications and data links for transmission to GAC's IBM computer program at Akron were established and satisfactorily integrated with the photometric field observations.

Early concern with vibration isolation and stiffness of the telescope platform was alleviated during initial tracking observations. Despite movements of personnel and moderate winds, the deployed facility proved adequately rigid and the control system response was satisfactory for satellite tracking purposes. The motor-generator-set mounting on the van proved to be adequately isolated to avoid any discernible transmission of vibrations to the telescope.

The vidicon TV system works for up to first or second magnitude objects. This limits its usage to satellites of brightness such as that of Echo I. In order to utilize the full capability of the optical system, replacement of the vidicon TV with a higher resolution TV system,

such as image orthicon, would be necessary. Prior to incorporating any such improvement it would be of benefit to thoroughly exercise the current vidicon system in order to define and optimize the design parameters for an image-orthicon system.

In general, it is considered that the system has been shown to be capable of meeting the general objectives of satellite photometric observations. However, it should be pointed out that the reliability and accuracy of any observational results are directly related to the experience of the field operating crew, as well as the data reduction and computation personnel. The facility should not be operated by personnel who have not received adequate training in their specific tasks from experienced crew members. Even at the end of the two-month PAGEOS observations, daily improvement in crew proficiency and coordination was still apparent. Although the operating and maintenance instruction manuals furnished with the facility are comprehensive and complete, they are no substitute for individual instruction. Complete familiarization with the manuals should be the first step in any training program, followed by supervised practice with the equipment itself. It is also considered mandatory that at least one crew member be a fully qualified astronomer.

APPENDIX A

PRINCIPLES OF PHOTOMETRY

General

From careful observations of the intensity of sunlight reflected from a spherical artificial satellite, various inferences can be drawn concerning the present condition of its surface. For instance, the extent to which the initially specular reflecting surface is degraded can be determined, as well as the mean and local effective radii of curvature of the satellite. In general, the following parameters may be obtained through the use of a ground-based photometric system: (1) stellar magnitude (normalized); (2) specularity and diffusivity of surface of a satellite; (3) mean and local radii of curvature; and (4) solar reflectivity if radius of curvature is assumed.

Satellite Stellar Magnitude at Various Effective Wave Lengths

The satellite stellar magnitudes may be determined in the U or near-ultraviolet band (3600Å), B or blue band (4400 Å), and V or visual band (5500 Å). The specular illuminance (E_{sp}) of the radiation received in the U, B, or V spectral regions (depending on which spectral region is switched on at a given time) from a specular spherical satellite is given by

$$\frac{E_{sp}}{E_0} = \text{antilog}(-0.4m_{sp}) = \frac{1}{4} \frac{E_s}{E_0} \left(\frac{R}{D}\right)^2 \tag{A1}$$

Using this equation, the extra-atmospheric stellar magnitude, m_{sp}, for the specular component of a satellite can be determined. The stellar magnitudes for the diffuse spherical satellite are given by

$$\frac{E_d}{E_0} = \text{antilog} (-0.4m_d) = \frac{2}{3} \frac{E_s}{E_0} \left(\frac{R}{D}\right)^2 f(\psi) \tag{A2}$$

where

$$f(\psi) = \frac{1}{\pi} \left[\sin \psi + (\pi - \psi) \cos \psi \right]$$

m_{sp} is specular stellar magnitude

m_d is diffuse stellar magnitude

E_0 is illuminance value at zero stellar magnitude

E_s is solar illuminance on the satellite

R is satellite radius (ft)

D is satellite distance

E_{sp} is specular component of illuminance

E_d is diffuse component of illuminance

$f(\psi)$ is Russell phase function

Determination of Specular Component of Light Reflected from a Sphere's Surface

The specular spherical satellite has a convex mirror surface that provides a small image reflection of the sun, equal in brightness regardless of the viewing angle. Conversely, a diffuse sphere in sunlight exhibits phases like the moon or Venus. The integrated light from the diffuse sphere is a function of the phase angle ψ, which is the angle formed at the satellite between lines to the sun and the observer. As shown in figure A1, the phase angle is zero when the phase is full. The illuminance of the diffuse sphere increases as the phase angle decreases to the limit at the eclipse.

To determine the specularity of a satellite, photometric measurements are made over a wide range of phase angles. For moderate orbit inclinations these phase angles can be measured during single passes, when the satellite orbit has reached approximately the coplanar condition shown in figure A1. For a polar orbiting satellite, the range in phase angle during a single pass is limited, requiring combination of carefully calibrated data from various passes to achieve the desired span of phase range.
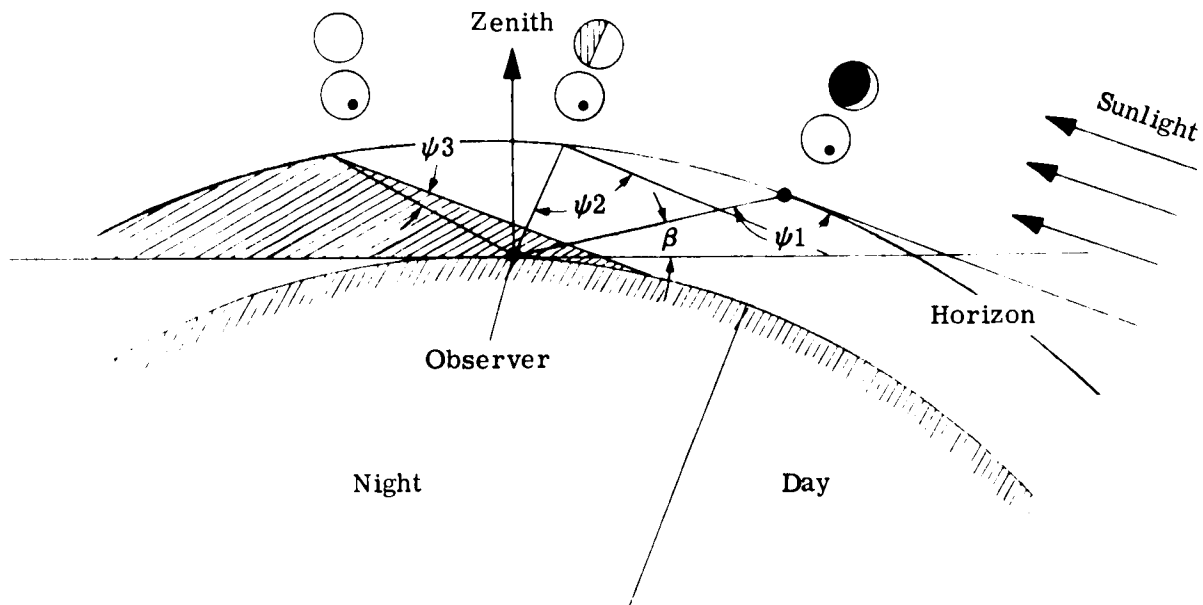
Figure A1. - Satellite phase angles.

APPENDIX A

The essential background and theory for the specularity determination is shown in equations (A1) and (A2) (refs. 4 and 5). They make possible the prediction of the extra-atmospheric stellar magnitudes, m, of specular and diffuse spherical satellites. The Russell phase function, $f(\psi)$ (ref. 6), gives the dependence of illuminance upon phase angle for a perfectly diffuse sphere that obeys Lambert's cosine law of reflection. (This law states that the reflection from a small area is proportional to the product of the cosine of the angle of incidence and the cosine of the angle between the normal and the direction to the observer.) These equations provide for photometric discrimination between specular and diffuse spherical reflecting surfaces. How closely the photometric data conforms to one or the other must be determined. The regression equation that permits this determination is (ref. 7)

$$\text{Antilog } (-0.4m) = 1/4A + 2/3B \, f(\psi) \tag{A3}$$

where A and B are the weighting factors for specularity and diffusivity, respectively. A and B are determined by a least-squares best fit to the normalized photometric data. Finally, equation (A4) provides the fractional specularity:

$$\text{Specularity} = \frac{A}{A + B} \tag{A4}$$

Before the analysis can proceed, the photometric data must be carefully calibrated and normalized. Observations of nonvariable stars of known illuminance are generally performed both before and after the satellite pass. The photometric data is then processed and the atmospheric extinction coefficients are determined. Simultaneously with the tracking of the satellite, the following information is time-correlated with the photometric data:

(1) Elevation (atmospheric thickness)

(2) Slant range

(3) Earth shine (effect of earth albedo)

(4) Phase angle

The calibrated photometric data is then processed for extra-atmospheric illuminance, normalized to zero earth shine and to a uniform slant range (1000 statute miles) by the inverse square law. A least-squares solution of the linear regression equation (A3) yields best fit values for the intercept A and the slope B, which are then employed in equation (A4) to determine specularity.

Mean and Local Radii of Curvature

Another consideration in the photometric study of satellites is the mean and local radii of curvature, R_c, and their extreme values. This is referred to as macrotexture measurement and analysis.

Having previously determined the diffuse-reflecting weighting coefficient, B, it is possible to remove from the normalized magnitudes the contribution of diffuse reflection in each, $-2.5 \log[2/3BF(\psi)]$, to obtain purely specular magnitudes, m_{sp}. If a good value for the specular reflectance, γ, is known, the radius of curvature can next be determined from the relation

$$R_c \text{ (ft)} = \text{antilog} \left[\frac{(m_\odot - m_{sp})}{5} - 0.5 \log \gamma + \log \text{ S.R. } + 0.30103 \right] \tag{A5}$$

where $m_\odot$ is the U, B, or V magnitude of the sun at that date, S.R. is the slant range, m_{sp} is the extra-atmospheric stellar magnitude contributed solely by the specular components of sunlight reflected from the satellite, and γ is specular reflectance. Since the observed illuminances depend on both γ and R_c in equation (A5), one may be obtained only if the other is known.

Using equation (A5), the mean radius of curvature may be obtained from a large number of observations of the local radii of curvature. The range and variability of the local radius of curvature may be examined, in relation to the original design and available material, for gross implications for a possible new mean radius of curvature.

Determination of Solar Reflectivity

The solar reflectivity for an assumed radius of curvature can be obtained by solving equation (A5) for γ (specular reflectance). The equation for this value is

$$\gamma = \text{antilog} \left[\frac{m_\odot - m_{sp}}{2.5} - 2 \log R_c + 2 \log \text{S.R.} + 0.60206 \right] \tag{A6}$$

As before, this refers to all three colors (U-B-V), when the values of m_{sp} are known. The specular reflectance is $\gamma = sr$ where s is specularity and r is solar reflectivity.

Calibration Theory

Before the satellite's solar reflectivity and specular and diffuse components of reflectivity can be determined, the raw satellite photometric analog data must be digitized and then processed to accomplish the following:

(1) Allow for atmospheric extinctions and transformations to standard U-B-V systems.

(2) Normalize to a uniform satellite distance, e.g., 1000 statute miles.

(3) Allow for present solar distance.

(4) Allow for contribution of earth albedo.

In practice, nearly all of the data processing is performed by a digital computer; computer programs for this processing have been developed.

Atmospheric extinctions. - The reduction of data for U-B-V photometry consists primarily of two steps: correction for atmospheric extinction effects, and transformation to a standard system of magnitudes and colors.

The magnitude (m_0) of a celestial body outside the atmosphere is

$$m_O = m - kX \tag{A7}$$

where m is the measured magnitude, k is the extinction coefficient, and X is the path length in units of air mass at the zenith of the observer. It is thus possible to deduce the extra-atmosphere magnitude of a celestial body from the observed magnitude, provided that both k and X are determined.

APPENDIX A

The air mass, X, is given to a high degree of accuracy by the secant of the zenith distance, Z. The error at a zenith distance of 60° is 0.005, so that it is convenient to use sec Z except for zenith distances in excess of 60°. The value of sec Z may be found by

$$\sec Z = (\sin \theta \sin \delta + \cos \theta \cos \delta \cos HA)^{-1} \tag{A8}$$

where θ is the observer's latitude, δ is the declination of the star, and HA is the local hour angle of the star.

To calculate X, one uses the formula

$$X = \sec Z - 0.0018167 (\sec Z - 1) - 0.002875 (\sec Z - 1)^2$$

$$- 0.0008083 (\sec Z - 1)^3 \tag{A9}$$

This equation is accurate to better than 1 percent up to X = 10, which corresponds to a zenith angle of about 85° as shown in table A1. Note that the divergence of Z when Z > 80° is rapid; however, this is really not important, since observations at these zenith angles will not be used. To calculate the various extinction coefficients, etc, required in this calibration, an extensive series of calculations is required to transform the natural system to the standard system of H.L. Johnson through the use of standard stars. Goodyear Aerospace Corporation is using the photoelectric reduction method of R.H. Hardie (ref. 8) to calculate atmospheric extinction and transform to the standard U-B-V system. The U-B-V values used for the standard stars during the transformation procedure are given in the Arizona-Tonantzintla catalog (ref. 9, and also reproduced as appendix H of ref. 1).

TABLE A1. - OPTICAL AIR-MASS CORRECTION TERMS

Z, deg	Sec Z	X	Correction	Z, deg	sec Z	X	Correction
0	1.000	1.000	0.000	73	3.420	3.388	0.032
30	1.155	1.154	.001	74	3.628	3.588	.040
60	2.000	1.995	.005	75	3.864	3.816	.048
61	2.063	2.057	.006	76	4.134	4.075	.059
62	2.130	2.123	.007	77	4.445	4.372	.073
63	2.203	2.196	.007	78	4.810	4.716	.094
64	2.281	2.273	.008	79	5.241	5.120	.121
65	2.366	2.356	.010	80	5.759	5.598	.161
66	2.459	2.448	.011	81	6.392	6.171	.221
67	2.559	2.546	.013	82	7.185	6.873	.312
68	2.670	2.655	.015	83	8.206	7.742	.464
69	2.790	2.773	.017	84	9.567	8.832	.735
70	2.924	2.904	.020	85	11.474	10.211	1.263
71	3.072	3.049	.023	86	14.336	11.884	2.452
72	3.236	3.209	.027	87	19.107	13.332	5.775
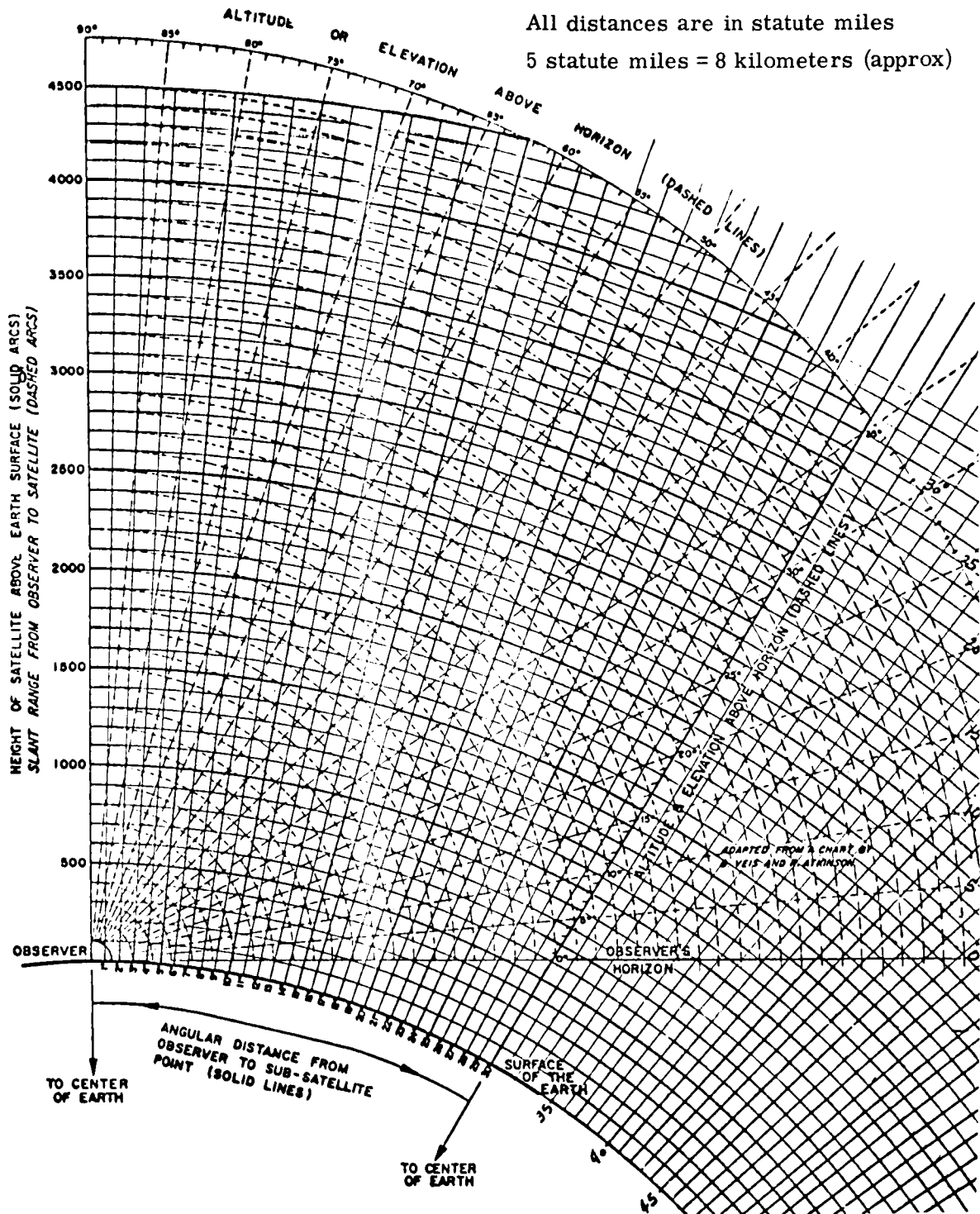
Figure A2. - Chart for determining elevation and slant range of a satellite.

APPENDIX A

Normalized slant range. - Normalization of the photometric data to a uniform range is accomplished by applying the inverse square law of illumination to the illuminances, first having determined the satellite's slant range at the observation time. Figure A2 gives slant range and elevation angles as functions of height and subsatellite distance. Satellite photometric data must be normalized for the instantaneous slant range from the observer before a meaningful analysis can be made. The instantaneous slant range may be computed for the times at which photometric data was taken from an accurate ephemeris of the satellite, or by triangulation from real-time simultaneous positional observations. Note that a one-percent error in slant range will propagate an error in the normalized stellar magnitude of 0.02.

Correction of solar distances. - The sun's visible radiation is constant in output to within one percent, but owing to the eccentricity of the earth's orbit, the sun's illuminance upon an earth satellite varies. For example, the sun's visual magnitude varies from -26.70 in early July to -26.78 in January. The corresponding distances are approximately 94.5×10^6 miles in July and 91.5×10^6 in January. These minor variations in magnitudes with distance of the sun will be reflected in corresponding variations in magnitudes for sunlit satellites. For subsequent determinations of the satellite's effective radius of curvature and U, B, or V reflectivity, the instantaneous U, B, or V solar magnitude is required.

Contribution of earth albedo. - The correction for the contribution of the earth's albedo (earthshine) for a specular spherical satellite is a function of the satellite's orbital height and geocentric angle (elongation) from the sun. Figure A3 presents the stellar magnitude increments
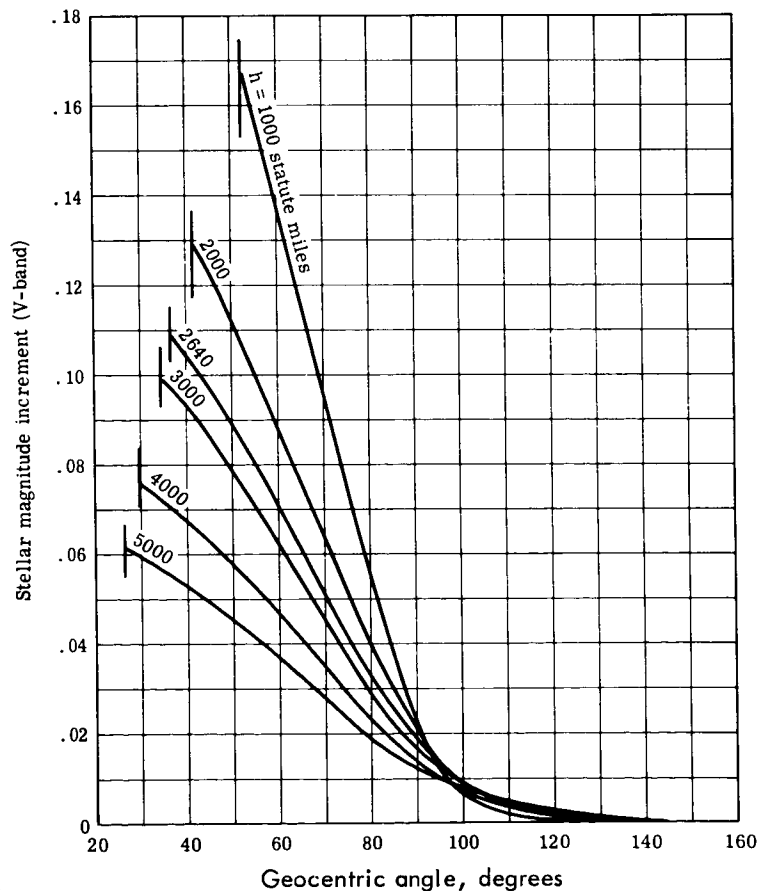
Figure A3. - Earth-reflected stellar magnitude increments.

APPENDIX A

based on a 0.36 earth-atmosphere albedo and a specular spherical satellite. The appropriate increment must then be applied as a correction to the reduced stellar magnitude of a near-specular spherical satellite before proceeding to the determination of effective radius of curvature or specular reflectivity, or to the degree of specularity of the surface (ref. 10).

Polarization Theory

A polarization observation of an astronomical object is usually that of measuring I_{max}, the intensity maximum for partially plane polarized light in the plane of vibration, and I_{min}, the intensity minimum at right angles. The classical definition of the amount of polarization is

$$\text{Percent polarization (P\%)} = 100 \ \frac{(I_{max} - I_{min})}{I_{max} + I_{min}} \tag{A10}$$

with the plane of polarization referred to the magnetic vector. Another property which is frequently used in the field of stellar astronomy is the polarization magnitude, P_{mag},

$$P_{mag} = 2.5 \log \frac{I_{max}}{I_{min}} \tag{A11}$$

and the plane as the plane of vibration of the electric vector. Degree of polarization and polarization magnitude are related by the equations

$$P_{mag} = 2.1717 \left[P + \frac{P^3}{3} + \frac{P^5}{5} + \ldots \right] \tag{A12}$$

$$= 2.1717 \ (\tan h)^{-1} \left[\frac{I_{max} - I_{min}}{I_{max} + I_{min}} \right] \ ; \text{ where } P = \frac{P\%}{100}, \text{ degree of polarization.}$$

Since the parameter to be determined by the measurements is the percent polarization, this term will be used exclusively. Behr's catalog (ref. 3) will be used as a standard in all polarization measurements. Although the values in this catalog are in terms of polarization magnitude, the transformation to percent polarization is achieved with a high degree of accuracy by multiplying the first term in the series by 2.1717.

There are several sources of error that must be examined before acceptable polarization values are obtained. The errors are of two types: accidental and systematic. Accidental errors arise from the small variations in the transparency during the observing time required for a complete measurement and from the noise level of the photomultiplier. To minimize the former source of error, only nights of good photometric quality should be used. The elimination or reduction of noise level is accomplished by refrigeration, which lowers the noise level of the signal to that by the shot noise of the photomultipliers at low light levels.

Systematic errors are of several types: instrumental polarization, alignment errors, imperfections in the depolarizer, and atmospheric effects. Instrumental polarization is produced predominantly by variations in the reflection coefficients in, and perpendicular to, the planes of incidence of the rays on the telescope mirrors. Errors caused by alignment are usually due to the axis of rotation of the analyzer not being in coincidence with the optical axis of the telescope. When a fair alignment is achieved, the errors arising from misalignment are small and tend to be eliminated by the procedure of measuring through 360°. Depolarization

66

APPENDIX A

errors refer to errors in determination of the thickness measurement of compensator plates (this error is negligible in a well-made depolarizer) and a residual error of 1 to 1-1/2 percent due to using quartz depolarizers. This can be avoided by using calcite depolarizers.

The procedure for performing an instrumental polarization analysis uses up to 10 stars. Stars with percent polarizations of less than 0.04 percent are selected from the Alfred Behr catalog. Even if the observed polarizations are real, the average observed polarization should be zero because of the nearly uniform distribution of position angles of the stars. A newly aluminized set of mirrors should have an essentially null measurement for all of the stars selected for determination of instrumental polarization.

The instrumentation to be used for the determination of percent polarization of the standard stars and the satellite surface is shown in figure A4. This instrumentation is essentially a Polaroid plane wave analyzer followed by the V-filter and a depolarizer. The intensity of the radiation is observed by discrete settings of the analyzer at 10° increments. For calibration of stars and for satellite polarization measurements, plane wave analyzer steps are taken in 10° increments from 0 to 360°. The time intervals for the step periods are from 0.6 to 2.0 seconds. Dark current and adjacent sky readings are performed several times during each 0 to 360° cycle.

It is believed at this time that the following limits may be given to the percent polarization measurements:

Accuracy   1 percent

Sensitivity   1 percent

Reproducibility   5 percent
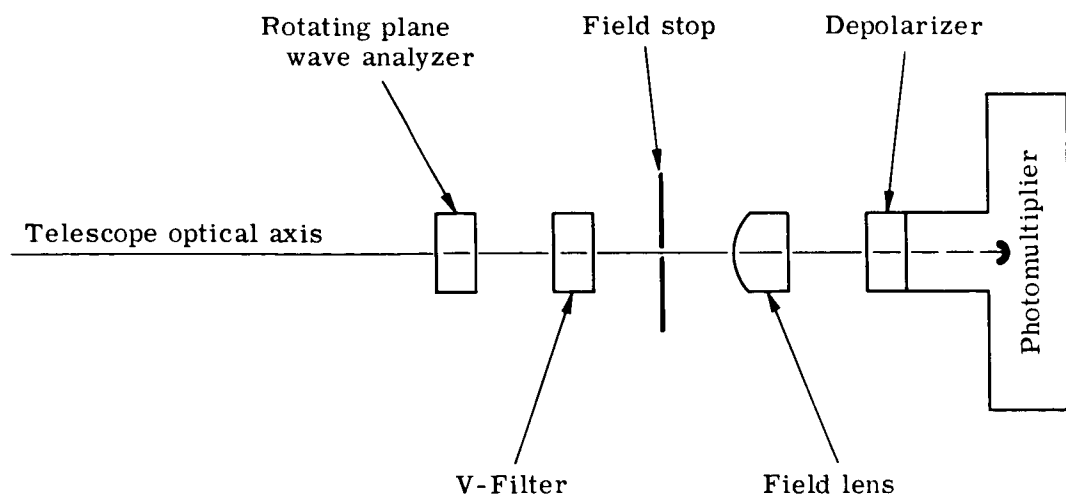
Figure A4. - Polarization instrumentation.

The reduction of data is performed by measurement of maximum and minimum intensity values taken from the oscilloscope strip chart. The following information should be plotted out on the oscillograph strip chart for polarization:

(1) Polaroid analyzer position (in 36 steps) at 10° increments

(2) Photometer gain

(3) Intensity readings

(4) Track angle

(5) Cross-track angle

(6) WWV time signal

The various correction factors (if significant) such as instrumental polarization, dark current, sky background, etc, should be provided for before the percent polarization is calculated by equation (A10). It is somewhat difficult to determine the significance of the satellite polarization values, since this type of measurement has not been performed previously. However, the literature on the polarization of metals and dielectrics (refs. 11 and 12) shows that such parameters as index of refraction, size and shape of the object being researched, type of material, etc, may be obtained from polarization measurements.

APPENDIX B

DESIGN ANALYSIS

Major determinations that had to be made at the start of the program were requirements for the van and truck, necessary characteristics of the control system for the telescope, the requirements for the telescope and mount, and requirements for the instrumentation.

Van Design Analysis

The functions of the van and truck are to provide mobility, a stable base for the telescope when deployed, and housing for the electronic equipment and instrumentation. The most difficult requirement to meet is the requirement for a stable base or platform.

The specification requirement to furnish a stable platform, in which transient excursions would not exceed a few seconds of arc under normal operating conditions and disturbances such as those caused by movement of personnel and wind variations up to 20 mph, necessitates a very stiff structure when the vehicle is located on an unimproved site.

It was considered inadvisable to attempt to construct a rigid platform incorporating the truck chassis, since normal design of a truck chassis allows for "working" of the structure as the vehicle travels over irregular terrain. The structural integrity therefore had to be built into the floor of the van. A box structure down the center of the floor with box sections out to the jacks was determined to be adequate for the job.

Another contributor to deflection is the compliance of the ground area under the jack pads. This is a function of the pad area and the type of soil.

Also of importance in the design of the floor structure, and related to the stiffness, is the lowest structural resonant frequency. This is important to the design of the control system, since it is undesirable to actuate the structure at its resonance. Since the position of the telescope is manually controlled, it can be considered that the control system has positive feedback with a man in the loop. If we consider the transfer function of a man in its simplest form as a one-cycle, low-pass filter, and if we desire to use his maximum potential, it would be desirable to have the structural natural frequency no lower than 4 cps, and preferably higher.

Appendix C contains an analysis of the deflection errors caused by movement of personnel and a 20 mph wind and the calculation of the natural frequency of the structure, jacks and pads, and soil. The deflection of the axis of the telescope due to movement of a man is calculated under the worst conditions as 8.8 seconds of arc for loamy soil and 6.8 seconds of arc for dry, soft, silty clay. The deflection of the axis of the telescope due to winds of 20 mph is 14 seconds of arc for loamy soil and 9.1 seconds of arc for dry, soft, silty clay. The lowest natural frequency is 6.9 cps, which is the coupled mode in the horizontal and azimuth direction, calculated for the soft soil condition.

The purchase order for the truck and the specification control drawing for the van incorporated the results of the deflection analysis and the other operational requirements.

APPENDIX B

Control Design Analysis

General. - Before the parameters of the control system could be specified, the mount rates had to be determined. The previous study program had determined that the mount should have four axes where the azimuth and elevation are set prior to tracking. The polar axis is established perpendicular to the track of the satellite and the declination axis, or cross track, is required only to make occasional corrections. From the orbital parameters of several satellites it was determined that the tracking acceleration was very small, about 60 sec/sec^2 for the polar axis and 6 sec/sec^2 in declination. The acquisition or slewing acceleration was much higher, in the neighborhood of 2 deg/sec^2 for the polar axis and 0.8 deg/sec^2 in declination. The track velocities could range from 2 deg/sec down to a sidereal rate of 15 sec/sec. A mount capacity of 3 deg/sec seemed advisable.

The two major problems on the control system were to get a drive system to cover the wide speed range and to choose a rate feedback element that would have sufficient sensitivity at sidereal rate, be able to cover the speed range, and have sufficiently low ripple voltage.

Motor selection. - The wide speed range ruled out the choice of a conventional motor - gear box drive system. The backlash in the high gear ratio box would have resulted in large tracking errors and the motor would probably "cog" at the low speed needed to reach sidereal rate. The construction of the mount lent itself to the application of d-c direct-drive motors and tachometers.

The total torque required of the motor is the sum of the torque necessary to overcome wind disturbances, to accelerate the telescope, and to overcome friction. The friction must be kept to a minimum for smooth tracking at low velocities. Since special bearings and non-contacting seals are to be used on the telescope axes, it is estimated that the friction will be very low - less than 4 ft-lb.

To determine the torque required for acceleration, the inertia of the polar and declination axes was estimated (refer to appendix D) as 199 lb-ft-sec^2 for the polar axis and 168 lb-ft-sec^2 for the declination axis. The acceleration torque is equal to the inertia times the rotary acceleration. Considering first the polar axis, the tracking acceleration of 60 seconds of arc per second would require only 0.058 ft-lb of torque. The acquisition and slew acceleration of 2 deg/sec^2 requires a torque of 7.4 ft-lb. The acceleration torque for the declination axis is 0.0049 ft-lb for tracking and 2.33 ft-lb for acquisition. The torque required to overcome wind disturbance, calculated in appendix E, is 10.33 ft-lb. The total tracking torque for the polar axis is 4 + 0.058 + 10.33 = 14.338 ft-lb. The total acquisition torque is 4 + 7.4 + 10.33 = 21.73 ft-lb. Note that this peak torque assumes the maximum wind velocity, the worst aspect angle, and maximum acceleration occurring simultaneously.

For the declination axis, the peak torque for acquisition is 16.66 ft-lb and 14.33 ft-lb for tracking.

Based on the above torque requirements, a commercially available motor that has a peak torque of 22 ft-lb was used. Since the motor-tachometer had to be mechanically designed for the application, it was deemed desirable to use the same unit on both axes to reduce design costs.

Tachometer selection. - The parameters to be designated in the choice of a tachometer are the voltage sensitivity, the ripple frequency, and the percent ripple voltage. The sensitivity must be sufficient to provide a signal that can be distinguished from the background

noise at the lowest operating frequency. The normal maximum sensitivity of tachometers for this use is about 50 volts/radian/sec. At sidereal rate, this would provide slightly less than 4 mV of tachometer signal. This is a rather small signal to route through the mount to the control console. A special winding is available for the tachometers which raises the sensitivity to 105 volts/radian/sec. This provides approximately 7.5 mV at sidereal rate.

Since the control system is essentially a manually controlled rate loop in which the man establishes the reference voltage, any variation in the feedback voltage due to tachometer ripple will result in positional errors. The most obvious way to get rid of the ripple would be to place a filter on the output of the tachometer. Two commercially available tachometers were considered and their performances compared. One has a ripple frequency of 97 cycles per revolution and the other has 279 cycles per revolution. Table B1 shows the relationship between telescope angular velocity and the ripple frequency in cycles per second for the two tachometers.

TABLE B1. - TELESCOPE ANGULAR VELOCITY VERSUS RIPPLE FREQUENCY

Telescope rate, deg/sec	Ripple frequency, c/s	
	Type I	Type II
0.0008	0.000215	0.00062
.004	.00108	.0031
.1	.027	.078
.5	.135	.388
1.0	.27	.78
2.0	.54	1.55

Since the ripple frequencies fall within the bandpass of a normal control system, the ripple cannot be removed by filtering. The magnitude of the excursion caused by the tachometer ripple voltage can be calculated using the following equation (from ref. 13):

$$\Delta\theta = DB/2\pi$$

where

$\Delta\theta$ is the peak ripple amplitude, degrees

D is the ripple voltage ratio - $\dfrac{\text{percent of ripple}}{100}$

B is the number of degrees for one cycle of ripple - deg/c

Table B2 is a comparison of various available tachometers.

TABLE B2. - COMPARISON OF TACHOMETERS

Tachometer type	Ripple freq, c/rev	B, deg/c	D	$\Delta\theta$, deg	$\Delta\theta$, sec
I	97	3.7	0.01	0.0059	21.2
Ia	97	3.7	.0025	.00147	5.3
II	279	1.3	.0025	.00052	1.87
III	386	0.935	.002	.0003	1.07

A tachometer with the characteristics of Type II results in a peak error of 1.87 seconds of arc. This is an acceptable error, and is a good compromise considering accuracy, cost, and size of the unit for the telescope mount.

Motor and load transfer function. - The transfer function block diagram of the motor and load is shown in fig. B1. The output position θ_O as a function of the input voltage E_M and the torque disturbance T_D can be expressed as

$$\theta_O = \frac{\dfrac{E_M}{K_B} - \dfrac{T_D\, R_T}{K_B\, K_T}\,(\tau_E\, S + 1)}{S\,(\tau_E\, \tau_M\, S^2 + \tau_M\, S + 1)}$$

where $\tau_E = \dfrac{L_M}{R_T}$ and $\tau_M = \dfrac{R_T\, J_T}{K_B\, K_T}$.
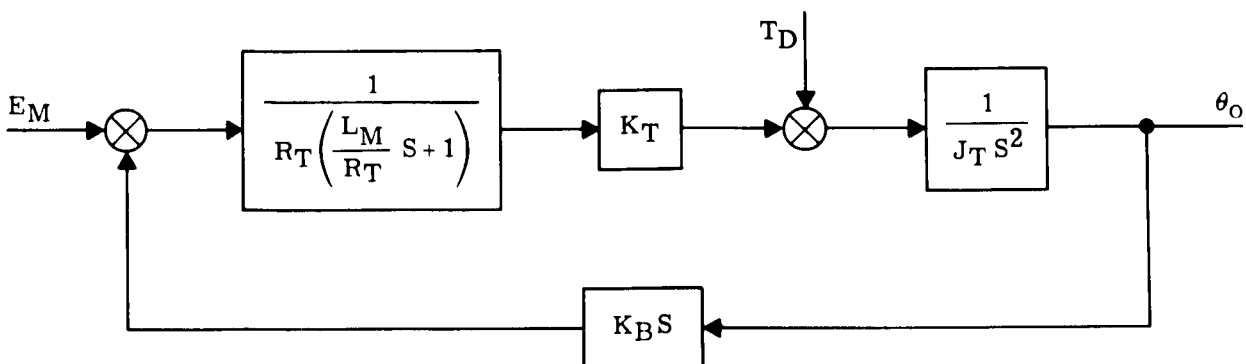
Figure B1. - Transfer function of the motor and load.

If

$\tau_M \gg \tau_E$, the expression can be changed to

$$\theta_O = \frac{E_M/K_B}{S(\tau_M S + 1)(\tau_E S + 1)} - \frac{T_D R_T/K_B K_T}{S(\tau_M S + 1)}$$

The transfer function block diagram for the motor can then be arranged as shown in figure B2.
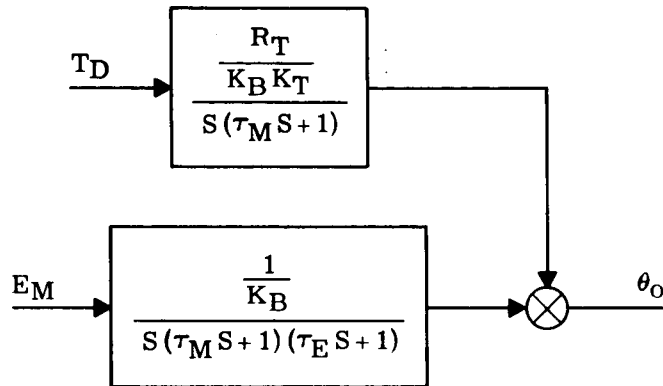
Figure B2. - Transfer function of the motor.

The following values were used:

K_T = 2.58 ft-lb/A

K_F = 105 volts/radian/sec

K_A = amplifier gain

K_B = 3.5 volt/radian/sec

$R_T = R_M + R_A + R_W$

    = 5.9 + 0.1 + 0.3 = 6.3

J_T = 199 lb-ft/sec^2

L_M = 0.04 henry

The motor transfer function is

$$\frac{\theta_O}{E_M} = \frac{0.286}{S\left(\dfrac{S}{0.007} + 1\right)\left(\dfrac{S}{158} + 1\right)}$$

As was stated previously, the system consists of a velocity or rate inner loop, with an outer position loop consisting of an operator manually adjusting the reference voltage.

Velocity loop. - The velocity loop consists of a direct-drive torque motor, a high-gain, direct-drive tachometer, a solid-state operational amplifier, and a combination amplifier comprising a solid-state preamplifier and power amplifier. A transfer function block diagram of the velocity loop is shown in figure B3.

Assuming the torque disturbance to be zero, the block diagram can be rearranged as shown in figure B4.
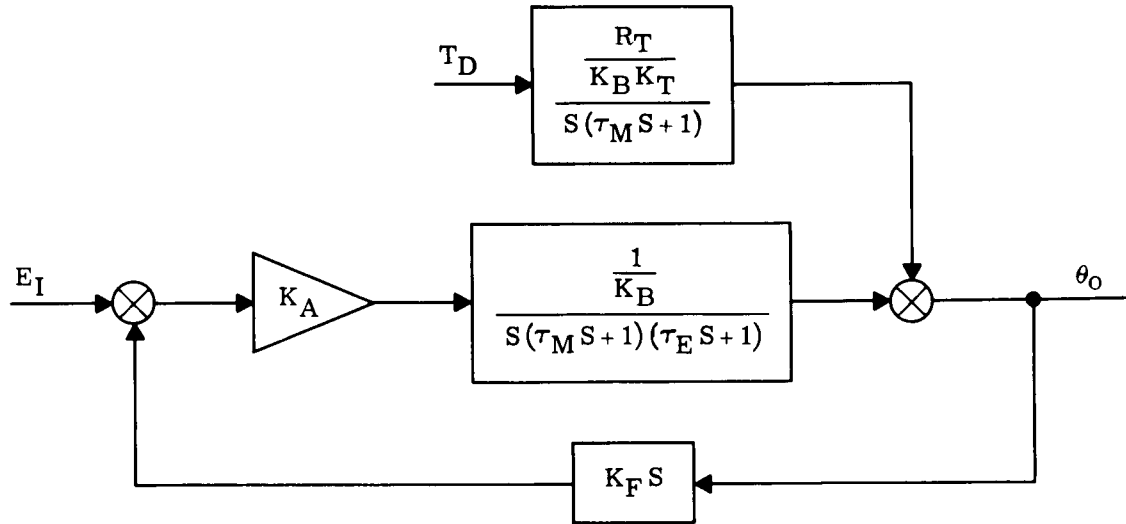
Figure B3. - Transfer function of the velocity loop.
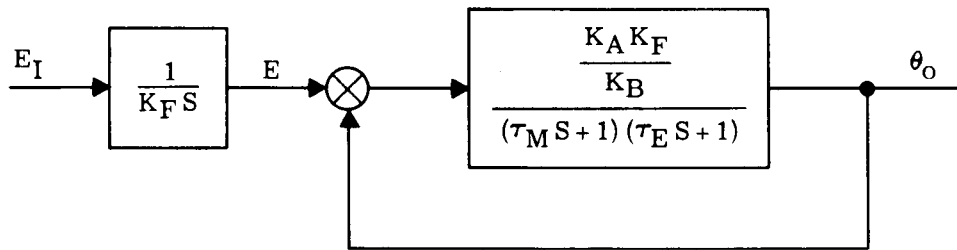
Figure B4. - Transfer function of velocity loop with
zero torque disturbance.

The open-loop transfer function of the unity feedback loop is:

$$KG = \frac{K_A\,105\,(0.286)}{\left(\frac{S}{0.007} + 1\right)\left(\frac{S}{158} + 1\right)}$$

A Bode plot of the open loop is shown in figure B5.

The open loop gain has been established as 70 dB or a gain ratio of slightly greater than 3000. The amplifier gain K_A for this overall loop gain is 100. Closing the unity feedback loop results in

$$\frac{KG}{1+KG} = \frac{\dfrac{3000}{\left(\frac{S}{0.007} + 1\right)\left(\frac{S}{158} + 1\right)}}{1 + \dfrac{3000}{\left(\frac{S}{0.007} + 1\right)\left(\frac{S}{158} + 1\right)}}$$
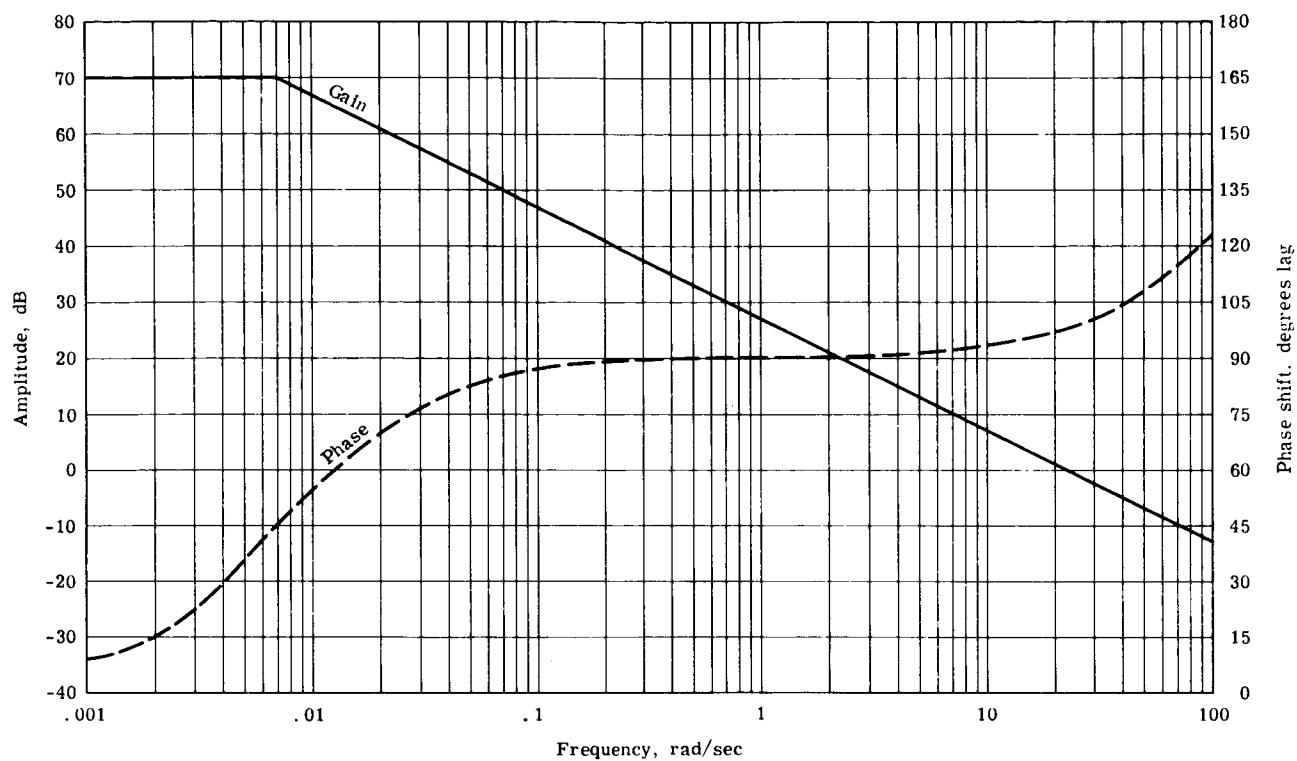
Figure B5. - Open velocity loop.

$$\frac{KG}{1+KG} = \frac{1}{3 \times 10^{-4} S^2 + 4.77 \times 10^{-2} S + 1}$$

and factoring gives

$$\frac{KG}{1+KG} = \frac{1}{\left(\frac{S}{25} + 1\right)\left(\frac{S}{134} + 1\right)}$$

Multiplying by $1/K_F S$ gives the closed velocity loop transfer function:

$$\frac{\theta_O}{E_I} = \frac{0.0095}{S\left(\frac{S}{25} + 1\right)\left(\frac{S}{134} + 1\right)}$$

Position loop. - The position loop is composed of the closed velocity loop, compensation circuits, the telescope, a force transducer, and the operator. The compensation circuits provide electrical integration, dual lead networks for stabilization, and high-frequency noise limiting. These circuits are sometimes referred to as an aided track network. The output of the force transducer is 1-volt rms for 10 pounds of force. The force transducer is a two-axis device that will allow the operator to control both the polar and declination axes simply by the direction and magnitude of the applied force. The field of vision of the guide scope, or particular scope being used to trace the object, will determine the operator's gain in the loop. The operator, or man, is an adaptive portion of the tracking loop. In general, man resembles a transport lag of about 0.4 second per step input. In following a repeatable signal such as sine wave, the simplest simulation of a man is an RC lag network with a bandpass of about 1 c/s. The main adaptability of man in this tracking situation will occur as a gain change. The error, as observed in the field of view of the telescope, will be converted to a force and direction on the force transducer. The combined units of the man's response to the angular error and of the transducer is in volts per radian. Man will learn to adjust this combined gain in order to maintain an optimum tracking loop.

A block diagram of the position loop is shown in figure B6. The structure included in the loop is that which determines the lowest natural resonant frequency presented to the drive system; in this case, it will be strongly influenced by the floor structure, jacks and pads, and the soil compliance. The natural frequency used for analysis was 6 cycles per second (37 rad/sec) and the damping factor for the combination was estimated at 0.06. The selection of 6 cycles per second was made so as to be less than the calculated frequency of any of the involved elements (see Appendix C, fig. C10); and the damping factor of 0.06 was based on that which is characteristic for structures of this type.
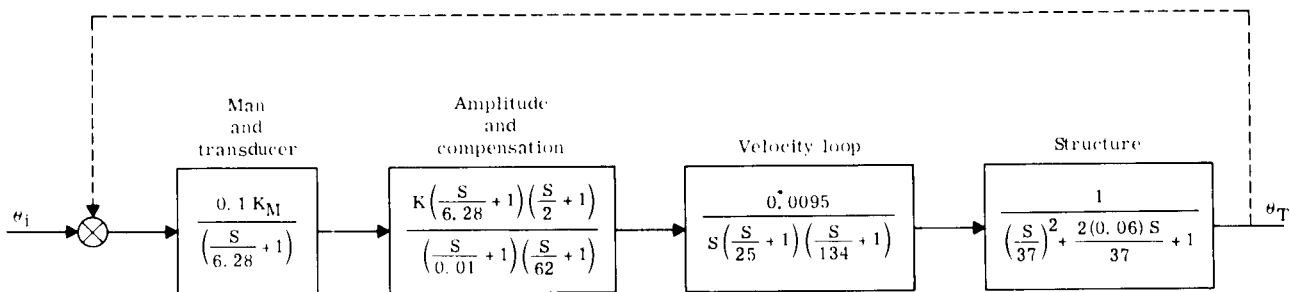
Figure B6. - Position loop transfer function.

One of the lead compensation networks was set to a break frequency of 6.28 rad/sec to cancel the lag caused by the operator. The lag network at 62 rad/sec is a noise filter. The other lead and lag terms are used to stabilize the loop and give the desired response.

A Bode plot of the open position loop is shown in figure B7. A loop gain of 16 has been established. Since the maximum desired mount velocity is 3 deg/sec (0.0523 rad/sec), the maximum voltage reference required by the velocity loop is 5.5 volts (0.0523/0.0095). With a loop gain of 16 and a transducer gain of 0.1 V/lb, the gain required of a man is

$$K_M = \frac{16}{(0.1)(5.)(0.0095)} = 3050 \text{ lb/radian, or } 0.015 \text{ lb/second of arc error.}$$

This requirement seems well within the capability of the operator.

76
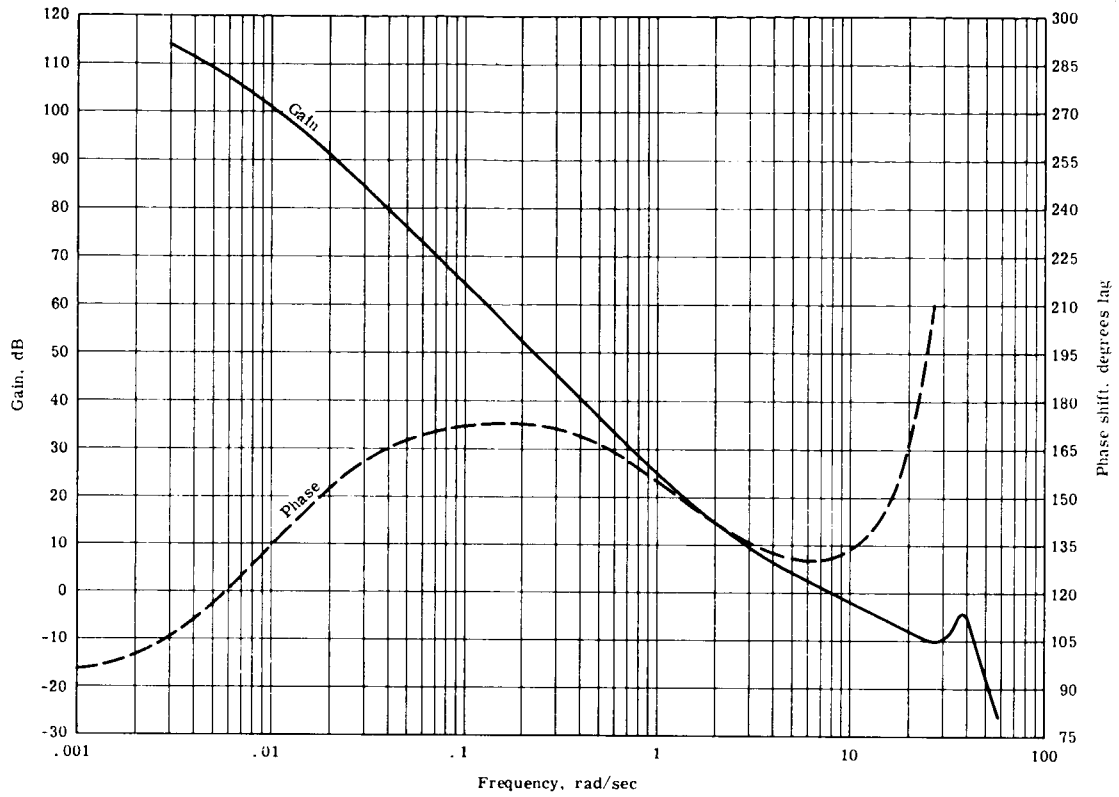
Figure B7. - Open position loop response.
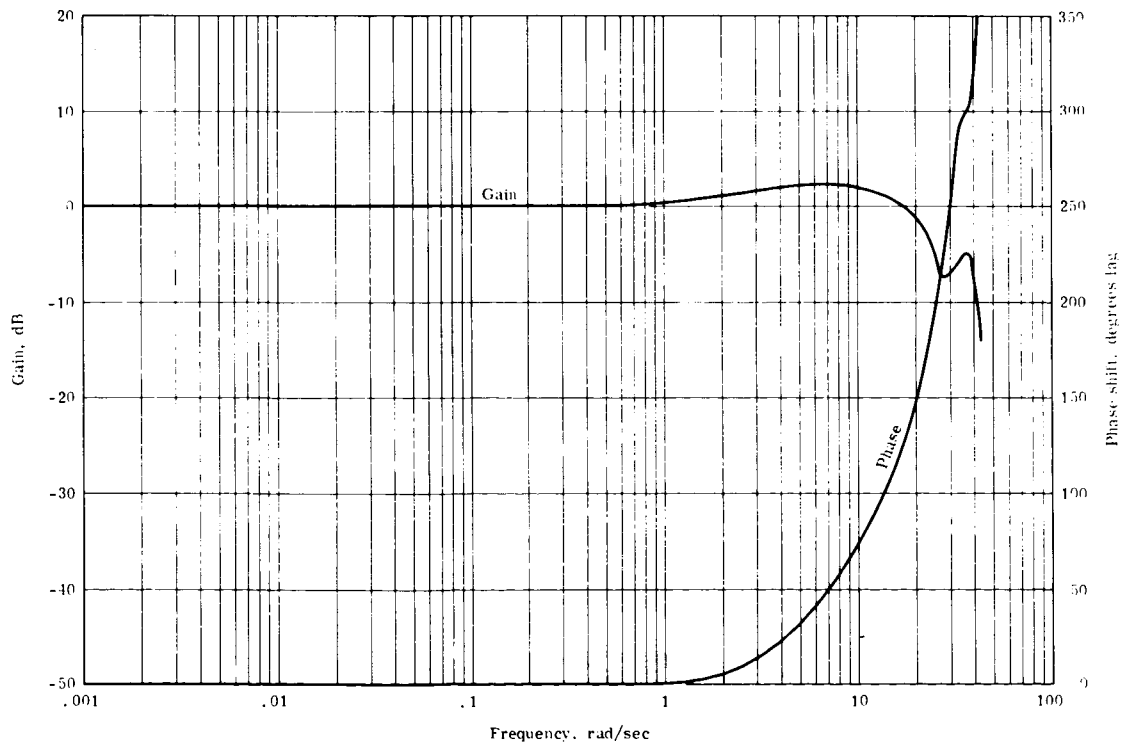
Figure B8. - Closed position loop response.

The open loop data was closed by the use of a Nickols chart analysis, and the closed position loop response is shown in figure B8.

Compensation networks. - As discussed previously, the compensation networks consist of provisions for two lead and two lag terms generated by operational amplifiers. The circuits and equations are as follows:
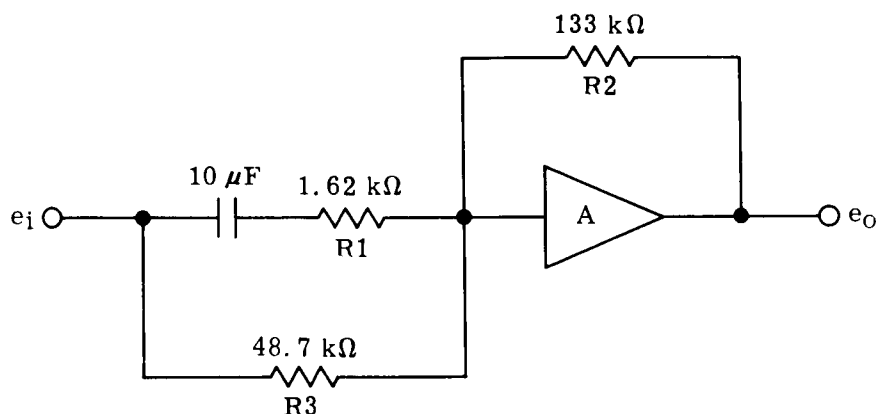
$$\frac{e_0}{e_i} = \frac{R2}{R3}\left[\frac{(R1 + R3)CS + 1}{R1(CS + 1)}\right]$$

Substituting the values and reducing gives:

$$\frac{e_0}{e_i} = \frac{2.7\left(\frac{S}{2} + 1\right)}{\left(\frac{S}{62} + 1\right)}$$
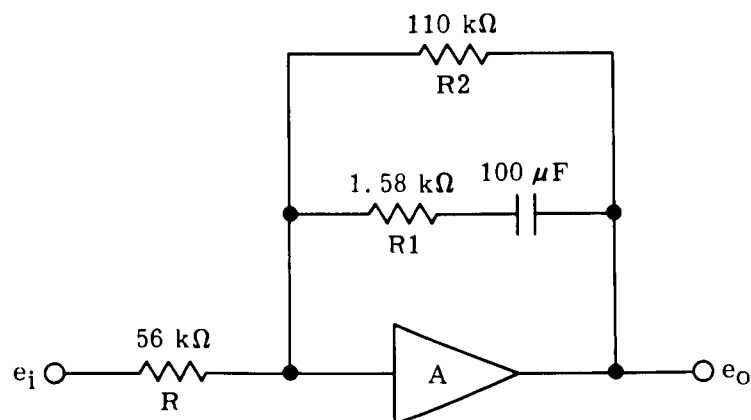
$$\frac{e_o}{e_i} = \frac{R2}{R}\left[\frac{R1\ (CS + 1)}{(R1 + R2)\ CS + 1}\right]$$

Substituting the value and reducing gives:

$$\frac{e_o}{e_i} = 1.96\ \frac{\left(\dfrac{S}{6.28} + 1\right)}{\left(\dfrac{S}{0.09} + 1\right)}$$

The total compensation, including the RC filter at 147 radians, is:

$$\frac{e_o}{e_i} = \frac{5.4\left(\dfrac{S}{2} + 1\right)\left(\dfrac{S}{6.28} + 1\right)}{\left(\dfrac{S}{62} + 1\right)\left(\dfrac{S}{0.09} + 1\right)\left(\dfrac{S}{147} + 1\right)}$$

The measured response of the polar axis operational amplifiers is shown in figure B9.
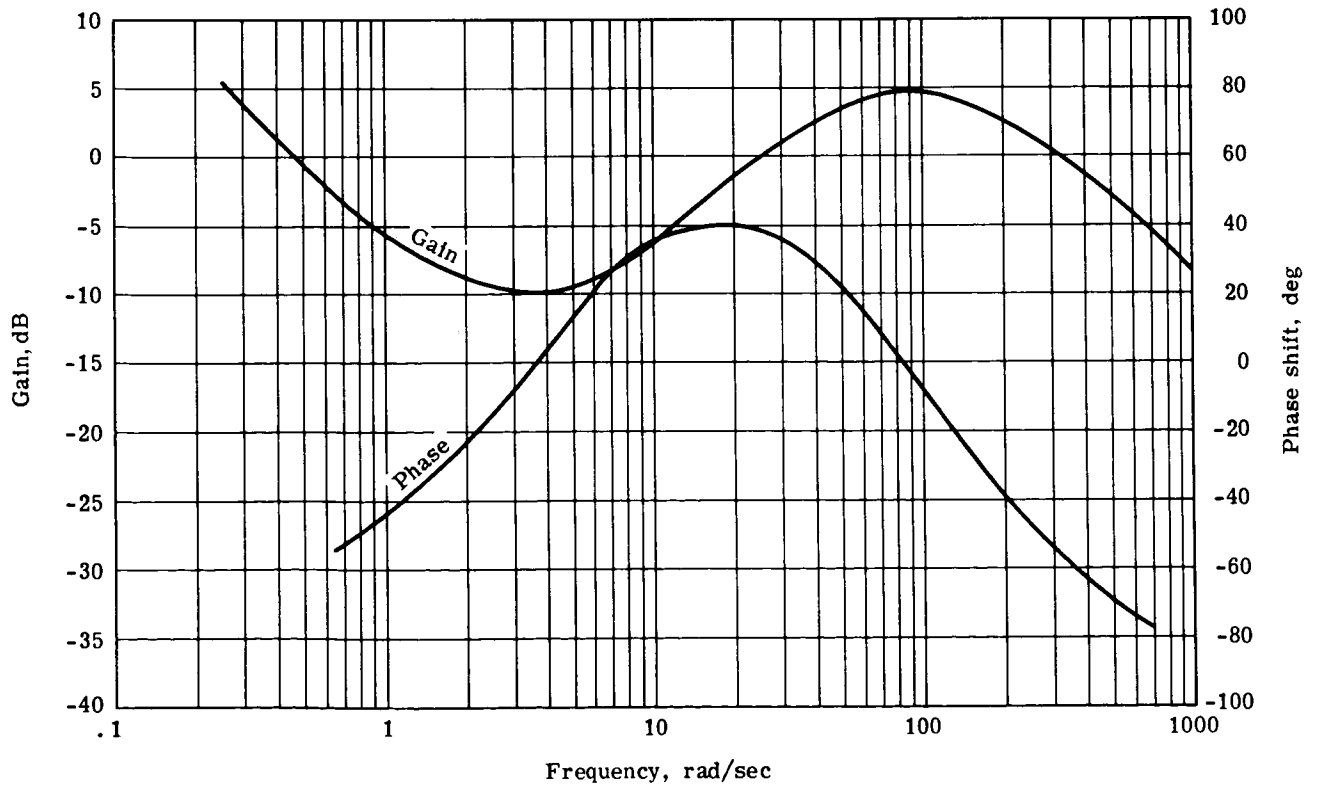
Figure B9. - Polar axis operational amplifier response.

APPENDIX B

Final Parameters. - Test data on the motors as delivered indicates that several of the parameters vary slightly from the originally indicated values. The new values are as follows:

$$R_M = 5.3 \text{ ohms}$$

$$L_M = 0.03 \text{ henry}$$

The final inertia of the two axes as furnished by the telescope manufacturer was 240 lb-ft/sec^2 for the polar axis and 200 lb-ft/sec^2 for the declination axis. This changed the motor transfer function to

$$\frac{\theta}{E_M} = \frac{0.323}{S\left(\frac{S}{0.0067} + 1\right)\left(\frac{S}{190} + 1\right)}$$

The gain of the velocity loop was increased to 6000 (75.7 dB) to minimize the error due to wind disturbances.

The closed unity feedback loop gives:

$$\frac{KG}{1+KG} = \frac{1}{\left(\frac{S}{71} + 1\right)\left(\frac{S}{118} + 1\right)}$$

The measured closed-velocity loop response is shown in figures B10 and B11 for the polar and declination axes. The measurements were made with the rate potentiometer disconnected and the input into the rate summing resistor. The output was the measured tachometer voltage. These curves show an anti-resonance and resonance due to the reflection of the structure on the loop. However, they occur well beyond the position loop cross-over and do not present any difficulty. Figure B12 shows tachometer outputs at sidereal rate.

The final position loop was modified from the original design. During tests of the system the operator indicated a need for faster response from the hand control for satellite tracking. This was accomplished by changing the lowest dynamic lag from 0.01 rad/sec to 0.09 rad/sec. Testing also revealed that a small amount of the 800 c/s ripple appeared at the output of the hand control demodulator. Additional filtering to remove this ripple was added by changing the demodulator filter break frequency from 333 to 40 rad/sec and adding an additional 147 rad/sec filter prior to the input of the rate loop.

The open loop transfer function of the position loop, based on the above characteristics, is

$$KGH = \frac{K_A\left(\frac{S}{2} + 1\right)}{S\left(\frac{S}{0.09} + 1\right)\left(\frac{S}{62} + 1\right)\left(\frac{S}{40} + 1\right)\left(\frac{S}{147} + 1\right)\left(\frac{S}{71} + 1\right)\left(\frac{S}{118} + 1\right)\left[\left(\frac{S}{37}\right)^2 + \frac{0.125}{37} + 1\right]}$$

The closed loop transfer function will therefore be

$$\frac{KGH}{1 + KGH},$$

which will have essentially the form as shown by the plot in figure B8.
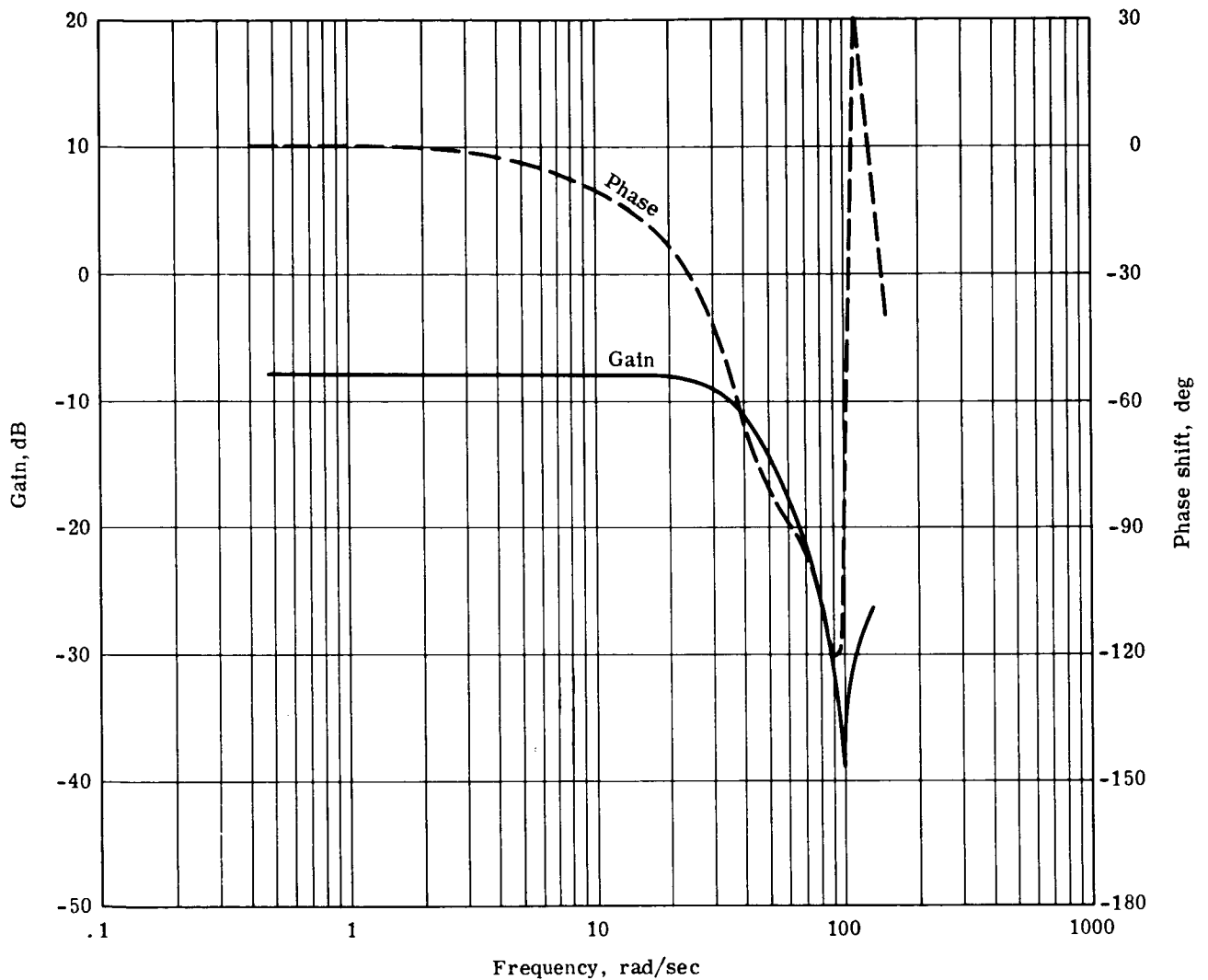
Figure B10. - Polar axis closed velocity loop tests.

During test of the system the control loops performed satisfactorily and had a response which was quite adaptable to the operator. The major problem experienced was the bearing friction load reflected to the motor. When the axes of the telescope were set so that the bearings experienced a large overhanging load, the bearing friction torque increased rapidly and peaks of approximately 14 ft-lb were measured. This was considerably higher than the estimated friction torque of less than 4 ft-lb.
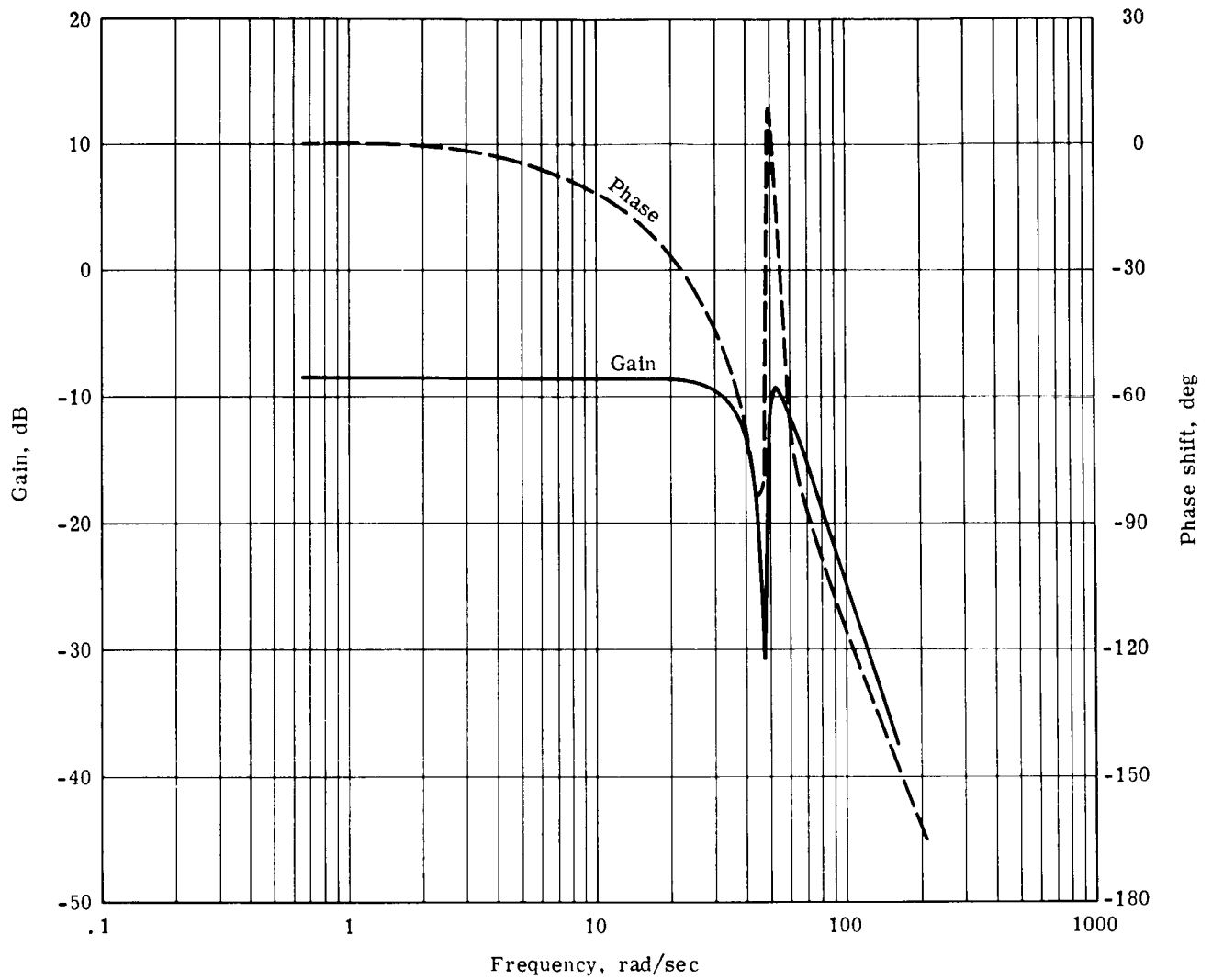
Figure B11. - Declination axis closed velocity loop tests.
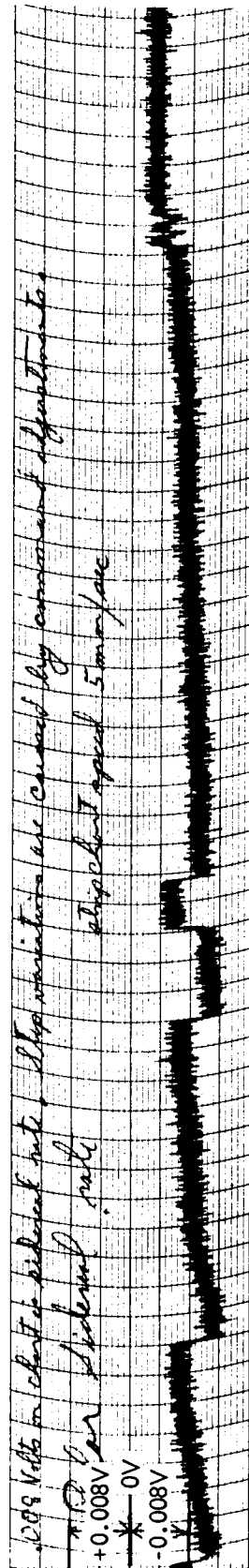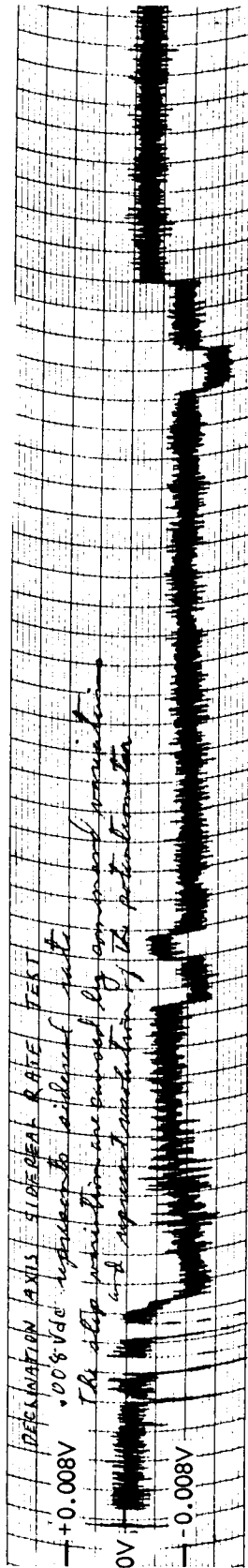
Figure B12. – Tachometer output recordings at sidereal rate.

APPENDIX B

Instrumentation Design Analysis

System Sensitivity. - The final photomultiplier output current is a function of the illuminance of the star or satellite, the diameter of the primary mirror of the telescope, the telescope efficiency, the sensitivity of the cathode of the light-sensitive photomultiplier, and the amplification of the photomultiplier. This output current must be measurable within the sensitivity of the photometer.

The illumination from a satellite or star of magnitude $m_v = 0$ is 2.74×10^{-10} lumens/ cm^2 at the top of the atmosphere. A 10th magnitude source would provide an illumination of 2.74×10^{-14} lumens/cm^2. Typical atmospheric transmission in the visual band varies from 0.25 to 0.75 as a function of zenith angles from 0° to 70°.

The 24-inch telescope aperture gathers a light flux in the visual spectrum from a 10th magnitude source of

$$F = E_v A_T T_{a1}$$
$$= 2.74 (10)^{-14} \pi (12)^2 (2.54)^2 (0.25 \rightarrow 0.75)$$
$$= (2.01 \rightarrow 6.03) (10)^{-11} \text{ lumens.}$$

The telescope and instrumentation system efficiency in handling light incident on the aperture is estimated from the following considerations:

(1) The primary and secondary mirrors are aluminized glass, with reflectivity, $R_{s1} \cong R_{s2}$, greater than 0.92 over the range of 0.25 to 0.75 micron.

(2) The field lens of fused silica has a transmittance, T_f, of 0.93 for a thickness of 0.39 inch. The interface reflection losses are calculated from the index of refraction of 1.46. The calculated reflection at each surface is

$$R_{s3} = \left(\frac{1.46 - 1.00}{1.46 + 1.00}\right)^2$$
$$= 0.035.$$

The apparent transmissivity of the field lens, T_{a2}, is calculated as

$$T_{a2} = (T_f) (1 - R_{s3})^2$$
$$= (0.93) (0.965)^2$$
$$= 0.865.$$

(3) The filters used were measured to have an apparent transmissivity, T_{a3}, of 0.78 at the V and the U band effective wave lengths. The B filter comprised two unbonded elements and had an apparent transmissivity of 0.73.

(4) A focus compensating plate of fused silica is inserted in the V and U band optical paths and has an apparent transmissivity, T_{a4}, of 0.93.

(5) The Lyot depolarizer has an apparent transmissivity, T_{a5}, of 0.8.

84

The S4 cathode of the 1P21 photomultiplier has a sensitivity, G_1, from 40 to 70 microamperes per lumen. The cathode current, I_c, corresponding to a 10th magnitude visual band illumination is calculated as

$$I_c = F (R_{s1}) (R_{s2}) (T_{a2}) (T_{a3}) (T_{a4}) (T_{a5}) (G_1)$$

$$= (2.01 \rightarrow 6.03) (10)^{-11} (0.92)^2 (0.865) (0.78) (0.93) (0.8) (4 \rightarrow 7) (10)^{-5}$$

$$= (3.42 \rightarrow 17.9) (10)^{-16} \text{ amperes.}$$

The 1P21 photomultiplier gain for an applied voltage of 1000 volts equally between cathode and dynode No. 1, between each of the 8 dynodes, and between dynode No. 8 and the anode is, typically, $G_2 = 2(10)^6$.

The photomultiplier anode current is directly coupled to the photometer input and is treated as a current source. The maximum sensitivity, S_1, of the photometer is 10^{-10} amperes for full-scale deflection. The sensitivity margin of the system for measuring a 10th magnitude star is then calculated as

$$M = \frac{I_c G_2}{S_1}$$

$$= \frac{(3.42 \rightarrow 17.9) (10)^{-16} (2) (10)^6}{10^{-10}}$$

$$= 6.84 \rightarrow 35.8$$

and is therefore considered to be approximately 10, representing the photometer sensitivity margin when measuring 10th magnitude stars (calculated value for 2/3 scale deflection at 70° zenith angle).

The photometer is so constructed that two sequential gain steps yield a gain change of 10. Therefore, gain setting No. 14 on the photometer should give approximately a midscale deflection for a 10th magnitude light input. The measurement of a 5th magnitude satellite is available with a gain margin of 1000, or 6 gain steps. A minimum level measurement of PAGEOS (the first satellite to be tracked) thus would be available using gain range 10 or 11, where gain range 17 is the most sensitive. Actually, gain ranges of 8 and 9 were used, indicating PAGEOS to be brighter than 4th magnitude.

Accuracy. - The accuracy of the instrumentation system as a whole is described by the photometer specifications as "within 3 percent of full scale on all ranges from 10 milliamperes to 10 millimicroamperes, and within 4 percent of full scale from 3 millimicroamperes to 0.1 millimicroamperes." The photometer supplies both high voltage to the photomultiplier and all amplification required. The contributing factors to accuracies stated above are as follows:

(1) The effect of the high voltage variation of 0.05 percent as a function of 100 to 130 volt a-c input change and 0 to 5 milliampere load change is estimated from the tube manufacturer's published data, indicating a 1 percent change in output per volt change. The variation to be expected as a function of high voltage change is

$$\Delta G_V = 5(10)^{-4} (1000) (1)$$

$$= 0.5 \text{ percent}$$

(2) Ripple and noise, ΔG_N, are less than 0.05 percent.

(3) Zero drift, ΔG_D, is less than 2 percent in a 24-hour period.

(4) The operational amplifier gain stability, ΔG_G, is established by the feedback component tolerances and is less than 0.2 percent, except on the two high-gain scales, where this error may approach 1 percent.

Overall measurement system tolerance is the rms sum of these effects and is calculated as

$$\Delta G_T = \sqrt{(\Delta G_V)^2 + (\Delta G_N)^2 + (\Delta G_D)^2 + (\Delta G_G)^2}$$
$$= \sqrt{(0.5)^2 + (0.05)^2 + (2)^2 + (0.2)^2}$$
$$= \sqrt{4.3}$$
$$\cong 2.14 \text{ percent}$$

Other error-contributing factors may be made negligible with proper use of the system. These include:

(1) Scintillation, which can be minimized with integration time.

(2) Chart reading error, which can be minimized with expanded scales.

(3) Galvanometer non-linearity of 1 percent.

For a 2-inch record deflection, the accuracy in reading is better than 1 percent and is typically used in data acquisition.

Overall data system accuracy is estimated at

$$\Delta G_S = \sqrt{(2.14)^2 + (1)^2 + (1)^2}$$
$$= 2.56 \text{ percent.}$$

The photometer errors discussed are all long term, particularly the d-c drift term, which is the most significant error incurred. Short-term photometer accuracy, as incurred by the stellar comparison technique, with a total time lapse of two hours should approach 1 percent.

Design implementation. -

Fabry lens: Initially the field lens was constructed of borosilicate glass. Using this lens, transmission in the ultraviolet spectrum was measured to be down 3 percent of 3400 Å. This lens was replaced with a fused silica lens, which provided uniform transmission to a wave length of 2500 Å.

Compensating plates: The color filters are positioned between the field stop (prime focus) and the secondary mirror. Since the filters are of different thicknesses, prime focus appeared at different positions along the optical axis. Correction plates of fused silica were designed and placed in series with each of the thin filters, permitting prime focus to be the same for each color filter.

Field stops: Fabrication and matching of the complementary field-stop knife edges were precision machining operations. Nine measurements of the diameter of each hole were made at 20° increments to determine the match of the on-axis and off-axis field stops. The mean diameters of each stop were calculated as follows:

For the 30-second field: $\bar{d}_1$ = 0.06932 inch

$\bar{d}_2$ = 0.06888 inch

For the one-minute field: $\bar{d}_1$ = 0.14081 inch

$\bar{d}_2$ = 0.14116 inch

For the two-minute field: $\bar{d}_1$ = 0.27843 inch

$\bar{d}_2$ = 0.28026 inch

The areas of the two stops are thus expected to match to better than 1.5 percent.

Factors affecting signal determination. - To measure the illumination from a satellite reflecting the sun's energy, a differencing technique is used. Energy is received from the sky background as well as from the satellite. The energy from the background is proportionate to the solid angle subtended by the field. This is shown graphically in figure B13.

(1) In field ϕ_1^2 energy received is proportionate to $W_{SAT} + W_{\phi_1}^2$.

(2) In field ϕ_2^2, energy is proportionate to $W_{\phi_2}^2$.

(3) It is required that $\phi_1^2 = \phi_2^2$ to some degree of accuracy.

(4) It is further required that the sky be uniformly bright over the small angle, ϕ_3.

(5) Then $W_{SAT} = W_{SAT} + W_{\phi_1}^2 - W_{\phi_2}^2$.
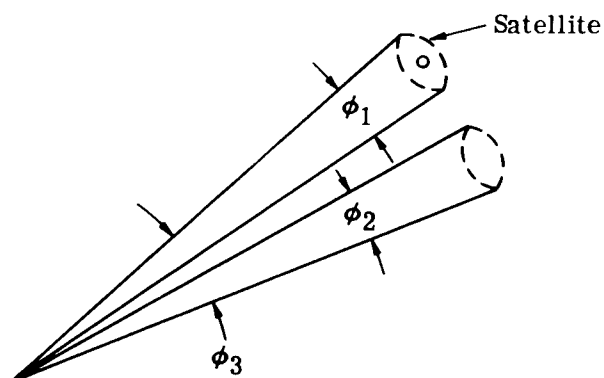
Figure B13. - Satellite energy determination.

Calculations of background: In order that the significance of background variation be understood, the ratio of signal, W_{SAT}, to background, W_{ϕ_2}, must be investigated. The signal level that will be received from the specular PAGEOS satellite varies from 0 to +2.5 visual magnitudes for altitudes of 90° and 15°, respectively. Table B3 indicates that the background is expected to be no more than 23 percent of the signal level when the 240-second field is used.

Field stop measurements: Field stop measurements were made to compare the on-axis stop with the off-axis stop and thus estimate the error contribution of the mismatch of field stop holes. The mean diameter of the on-axis field stop is $\bar{d}_1$, and the mean diameter of the off-axis field stop is $\bar{d}_2$. The difference of these mean diameters is $\Delta \bar{d}$. The mean of these two mean diameters is $(\bar{d}_1 + \bar{d}_2)/2$, and the coefficient of variation between the two field stop diameters can be approximated by $(2\,\Delta\bar{d})/(\bar{d}_1 + \bar{d}_2)$. The solid angle ϕ_1^2 is matched to the

TABLE B3. - SIGNAL-TO-BACKGROUND RATIO FOR PAGEOS OBSERVATIONS

Field, arc seconds	PAGEOS signal, visual magnitude		Dark sky zenith, visual magnitude	Conservative sky, visual magnitude	Satellite-to-background ratio			
					Visual magnitude		Ratio	
	Max	Min			Best case	Conservative	Best case	Conservative
1	2.0	5.0	21.5	18.5	19.5	14	$6.35(10)^7$	$3.97(10)^5$
30[a]	2.0	5.0	14.12	11.12	12.12	6.62	$7(10)^4$	$4.28(10)^2$
60[a]	2.0	5.0	12.61	9.61	10.61	5.61	$1.75(10)^4$	$1.01(10)^2$
120	2.0	5.0	11.12	8.12	9.12	3.62	$4.33(10)^3$	$2.79(10)^1$
240[a]	2.0	5.0	9.59	6.59	7.59	1.59	$1.06(10)^3$	4.33
360[a]	2.0	5.0	8.71	5.71	6.71	1.21	$4.76(10)^2$	2.85

[a]Available on instrumentation head

solid angle ϕ_2^2 as a function of the square of the diameter match. The first-order approxima-
tion of the coefficient of variation between the solid angles ϕ_1^2 and ϕ_2^2 is $(4\,\Delta\bar{d})/(\bar{d}_1 + \bar{d}_2)$.
The percentage error in the match of the two solid angles is 100 times the coefficient of varia-
tion. The following is a tabulation indicating the calculation of percentage error:

$\bar{d}_1$	$\bar{d}_2$	$\Delta\bar{d}$	$\bar{d}_1 + \bar{d}_2$	$\dfrac{400\,\Delta\bar{d}}{\bar{d}_1 + \bar{d}_2}$
0.06932	0.06888	0.00044	0.13820	1.27
0.14081	0.14116	0.00035	0.28197	0.50
0.27843	0.28026	0.00183	0.55869	1.31

From table B3, the conservative satellite-to-background ratio of approximately 4.33 might
be encountered when using the 4-minute field stop. The background error contribution is 1.3
percent of the background, or stated another way, the coefficient of variation of the background
signal is 0.013. Performing the subtraction on a normalized signal level of 1, appearing in
the on-axis field along with a background of 0.23, the contribution to erroneous signal measure-
ment can be estimated:

$$W_{SAT} = W_{SAT} + W\phi_1^2 - W\phi_2^2$$

$$= 1 + 0.23 - 0.23 \pm (0.013)(0.23)$$

$$= 1 \pm 0.003$$

The normalized rms error on a unity signal is thus 0.003. A percentage error of 0.3
percent would be incurred under conservative sky estimates of errors incurred by the field
stop mismatch.

Observational procedure: The considerations involved point to the possibility of a data
error that will have to be checked in every observation. A procedure is required to check for
field bias of the types discussed above. The procedure recommended is to position the tele-
scope over the fields anticipated to be traversed and observe the difference between back-
ground and signal level. This difference, if discernible, represents a positive bias on the
information taken.

APPENDIX B

In observing the PAGEOS satellite, the possibility of this error could be removed where necessary by making both sky and satellite observations through the same field stop.

Noise limitation: All observations to the 10th magnitude are scintillation-limited. Galvanometer response determines the integration time of approximately 0.005 second. Changing the galvanometer frequency response from 100 to 10 c/s reduces the noise power by the square root of the ratio of bandwidths, since the scintillation has a constant power spectral density over the bands considered.

Television monitoring. - A vidicon camera can be mounted on each of the 8-inch auxiliary telescopes so that remote control tracking may be accomplished through the use of television. The TV monitor screen is located at the control station in the instrumentation room.

The two 8-inch telescopes are two different types of telescope. Figure B14 is a schematic diagram of the wide-field, Newtonian tracking telescope. The vidicon camera has an image size of one inch. The telescope field desired is approximately 1 degree. Considering the image size for the f/4.5 Newtonian telescope with an objective of 8 inches,

$$f_1 = 8(4.5) = 36 \text{ inches}$$

$$\frac{I}{36} = \frac{\pi(1^O)}{180^O}$$

$$I = 0.63 \text{ inch}$$

The field of the vidicon 1-inch tube is:

$$\phi = \frac{1}{0.63} (1^O)$$

$$= 1.58^O$$

and is deemed acceptable.
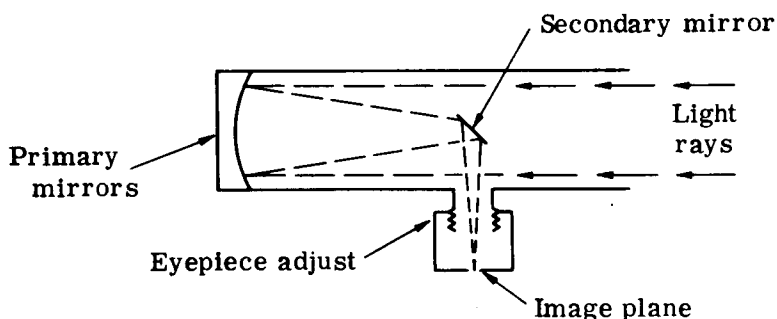
Figure B14. - Newtonian telescope schematic.

Figure B15 is a schematic of the Cassegrain, small-field type guide telescope. The 8-inch Cassegrain telescope has a focal ratio of f/20 and a true field of view of 8.5 minutes. The image size of the true field of view at prime focus is

$$I = \frac{(8.5)\ (8)\ (20)}{(60)\ (57.3)}$$

$$= 0.40 \text{ inch.}$$

The vidicon camera has a one-inch diameter image acceptance size and provides adequate coverage of the true field of the telescope.

The minimum size on the vidicon image plane that can be resolved by the camera is

$$\frac{60}{15\ 750} \times \frac{2}{700}$$

or $1.08\ (10)^{-5}$ square inches. Seeing is typically such that image shifts are less than 2
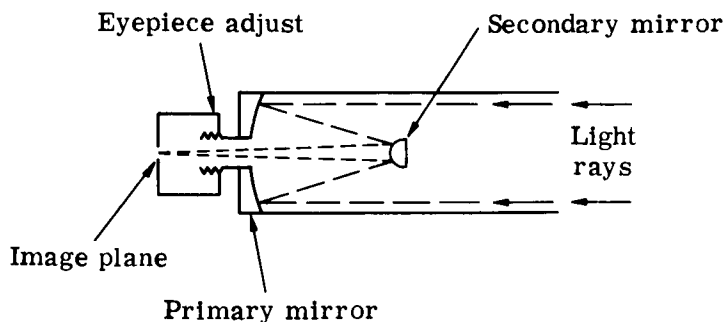
Figure B15. - Cassegrain telescope schematic.

seconds of arc in the image plane. This corresponds to less than $2 (10)^{-4}$ inches. It is seen that the image of a point source would appear within a single resolution element.

The area on the TV screen corresponding to a resolution element is $(8)^2 (1.05) (10)^{-5}$ or $6.74 (10)^{-4}$ square inches. The field of view on the Cassegrain telescope which corresponds to a resolution element is approximately

$$\frac{\left(\frac{1}{380} \text{ by } \frac{1}{350}\right) (8.5) (60)}{0.4}$$

or 3.4 seconds x 3.7 seconds.

The vidicon threshold response is stated by manufacturer's specification as 0.2 ft candela. This may be converted to lumens by multiplication of the area of the tube. The threshold of the vidicon is thus

$$\frac{(0.2)\pi}{(4) (144)}$$

or 0.011 lumen.

A single resolution element can be viewed at the monitor, and thus the point source threshold approximately has an improvement over wide scene threshold by the ratio of the area of the tube to the area of the resolution element. The point source threshold is thus

$$\frac{(1.1) (10)^{-2} 4 (1.08) (10)^{-5}}{\pi}$$

or $1.4 (10)^{-7}$ lumens. This corresponds to the energy received from a first to second magnitude star or satellite with an 8-inch telescope.

Sky Camera. - In estimating the ability of the sky camera to take pictures of a moving satellite, an exposure was made of a star field close to the celestial equator. The photographic figure of merit,

$$\text{pfm} = \frac{D^2 E}{f\Omega},$$

is applied in the sense that resolution of a moving point source across a field is inversely proportional to the angular rate, Ω. Since stars could be photographed to approximately 10th magnitude, a point is established on the slope $1/\Omega$ and figure B16 is generated to provide an estimate of the ability of the camera to record satellite trails.
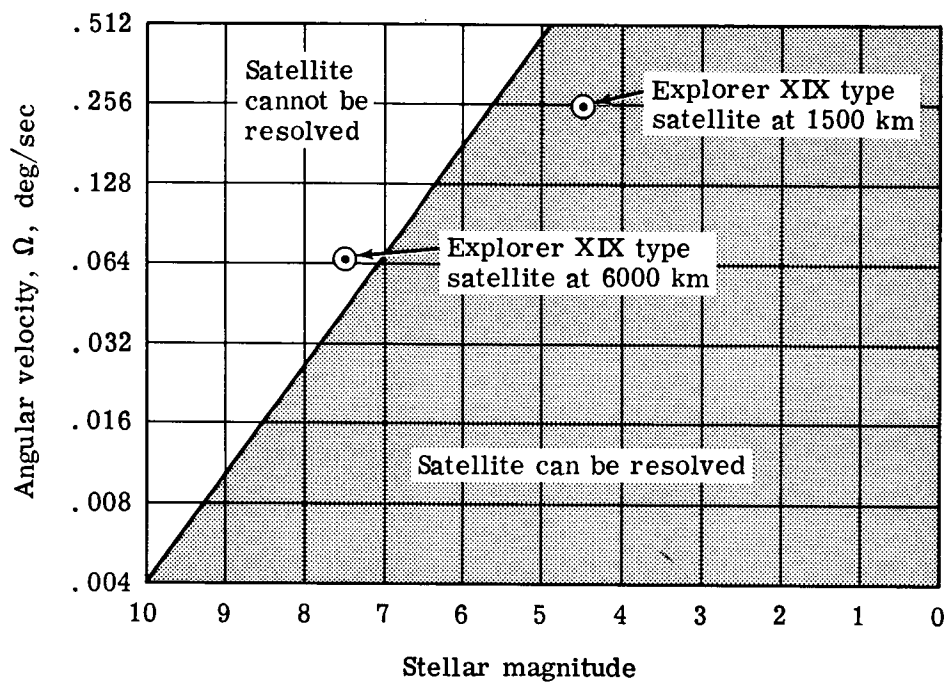
Figure B16. - Sky camera evaluation.

APPENDIX C

POINTING ERROR AND NATURAL FREQUENCY OF THE 24-INCH

NEWTONIAN/CASSEGRAIN TRANSPORTABLE

SATELLITE TRACKING TELESCOPE

Summary

Design requirements for the 24-inch Newtonian/Cassegrain Transportable Satellite Tracking Telescope System state that transient excursions of less than one second time constant not exceed a few seconds of arc under normal operating conditions and disturbances, such as those caused by movements of personnel and wind variations up to 20 mph.

The calculations shown in this appendix indicate that a 20 mph wind will cause a pointing error of 14.0 seconds. A 200-pound man changing position on the van frame will cause a pointing error of 8.8 seconds. Pointing errors for various conditions are calculated. The lowest natural frequency is 6.9 cps, which is the coupled mode in the horizontal (side to side) and the azimuth (yawing) direction. Frequencies for other modes are also shown. The structural pointing error is well within the minimum field of view of 30 seconds for the 24-inch telescope.

General Description

The satellite-tracking telescope system consists of a commercial 39 000-pound gross weight truck, a van, and a 24-inch telescope (see fig. C1). The van provides an enclosure and support for the telescope.

The van frame (see fig. C2) consists of two 8-inch longitudinal channels, with a 1/2-inch bottom cover plate and a 1/4-inch top cover plate. The channels and cover plates form a box beam capable of carrying torsional and bending loads. This van frame is tied to the truck frame at two places at the rear bogie; thus the truck and van frames act independently of each other. This method of attachment allows the truck frame to twist without racking the telescope support as the vehicle is driven over uneven roads. Two transverse beams, one aft and one forward, each made of two 8-inch channels and cover plates, pick up four leveling and supporting jacks to support the van frame.

During operation of the telescope, the four jacks are lowered to the ground to level and stabilize the telescope.

All loads are carried by the longitudinal box beams to the transverse beams, to the jacks, and to ground. In the following analysis these structural components are treated as elastic members and the change of slope of the telescope is found for various load conditions.

The weight of the van, telescope, and equipment is 22 000 pounds. Therefore, the truck is satisfactory. The section modulus of the truck frame is 14.72 in^3 and the moment of
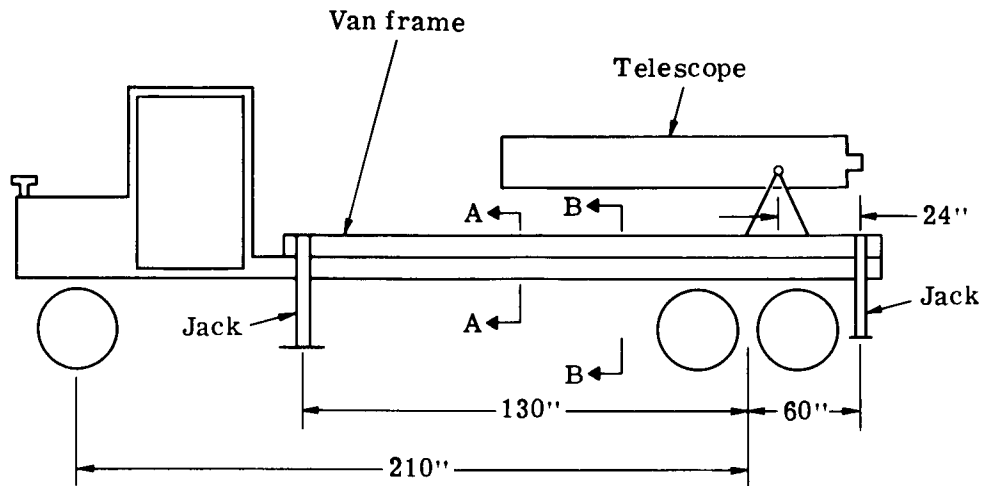
Figure C1. - Side view of truck and van.
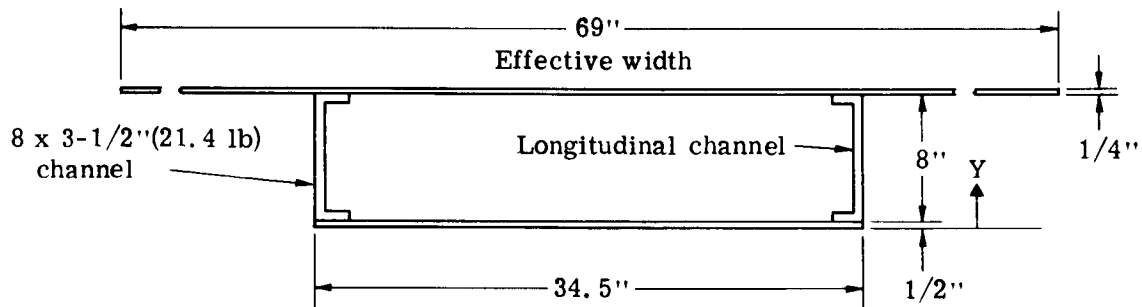
Figure C2. - Cross section of van frame (section AA, figure C1).

inertia is 75 in^4. The section modulus of the van frame is 166 in^3 and the moment of inertia is 736 in^4. Comparing these values with the truck frame, the van frame is satisfactory.

The telescope is controlled by a servo system in which a person is required to close the loop of the servo. In order for the servo to operate correctly, the natural frequency of the structure is required to be 4 cps or higher. The natural frequency was found by a matrix method employing influence coefficients. The pointing errors calculated herein are for the soil, jacks, beams, and van frames only, and do not include any errors due to the servo system, the telescope tube, or the telescope mounting yoke and bearings.

APPENDIX C

Pointing Error Analysis

Analysis of error in the pitching direction. - The bending stiffness of the van frame (see figure C2) is as follows:

A, in^2	Y, inches	AY, in^3	AY^2, in^4	I_0, in^4
17.25	0.25	4	1	-
12.46	4.50	56	252	122
17.25	8.62	148	1281	-
46.96		208	1534	122

$\overline{Y}$ = 208/46.96 = 4.42 inches.

I = 122 + 1534 - 208 x 4.42 = 736 in^4.

Torsional rigidity, $J = 4A^2/(\Sigma dP/t)$

$$J = 4 (8.37 \times 34.2)^2 \Big/ \left(\frac{34.5}{0.5} + \frac{34.5}{0.25} + \frac{8 \times 2}{0.3}\right) = 1258 \text{ in}^4.$$
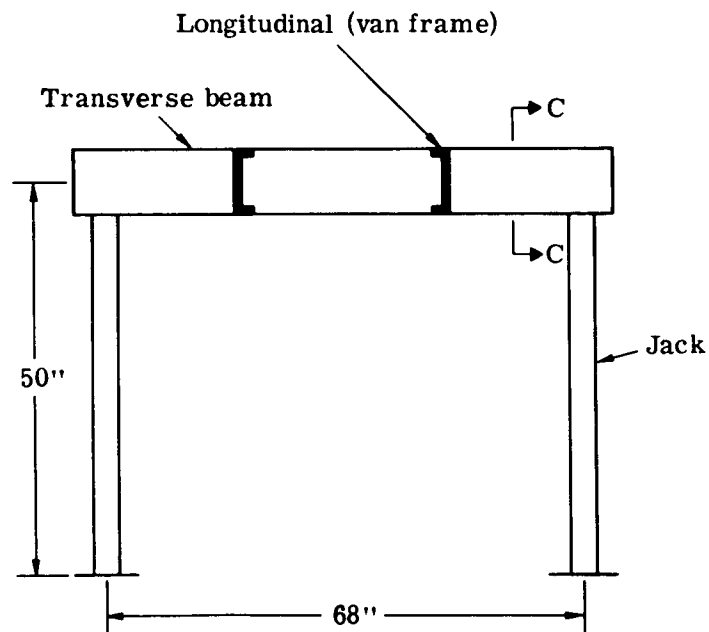
Figure C3. - Cross section of jack frame
(section BB, fig. C1).

8 x 3-1/2"(21.4 1b) channel
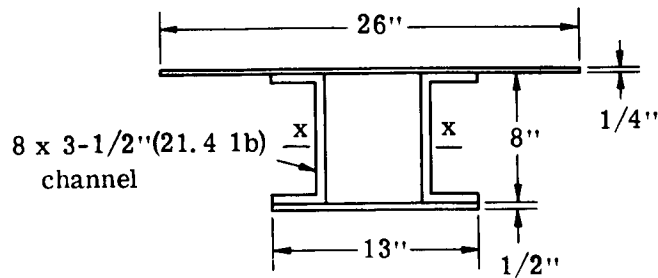
Figure C4. – Cross section of transverse beam (section CC, fig. C3).

$$I_{xx} = 122 + 6.5 \times 2 \times 4.12^2 = 342 \text{ in.}^4$$

The vertical stiffness of the jack frame is

$$\Delta = \frac{PL}{AE} + \frac{Pa}{6EI} \ (3\ell a - 4a^2)$$

$$\Delta = \frac{0.5 \times 50}{4.5 \times 30 \times 10^6} + \frac{0.5 \times 17}{6 \times 30 \times 10^6 \times 342} \ (3 \times 68 \times 17 - 4 \times 17^2)$$

$$\Delta = 0.5 \times 10^{-6} \text{ in/lb}$$

$$K = 1/\Delta = 2\,000\,000 \text{ lb/in.}$$
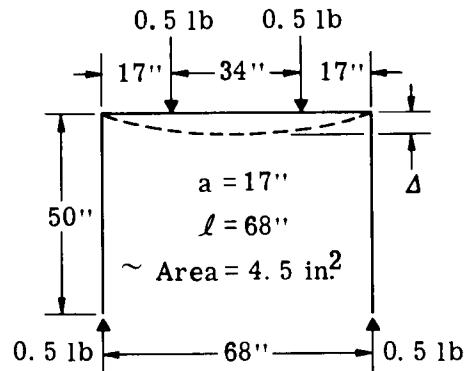
The vertical deflection of the soil (for loamy sand) is:

$$K = 11\,500 \ R_0 \text{ lb/in (refs. 14, 15, and 16)}$$

where R_0 = 9 in. (jack pad size)

$$K = 11\,500 \times 9 = 103\,000 \text{ lb/inch}$$

$$\Delta = 1/K = 9.7 \times 10^{-6} \text{ in/lb per pad.}$$

The total vertical deflection of the jack frame and soil is:

$$\Delta = 9.7 \times 10^{-6} \times 0.5 + 0.50 \times 10^{-6} = 10.2 \times 10^{-6} \text{ in/lb}$$

$$K = 98\,000 \text{ lb/inch}$$

The van frame can be treated as a beam supported on two springs, as shown in this sketch:
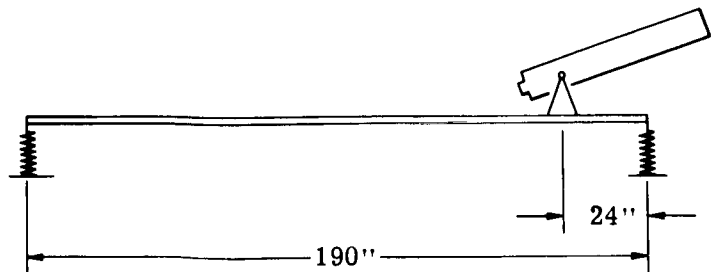
Figure C5, a summary of the calculations of pointing errors due to movement, shows the various positions of a 200-pound man on which the calculations are based. The change of slope of the telescope due to the deflection of the jack frame when a 200-pound man is standing over the forward jack frame (position 1) is:

Δ = 200 x 10.2 x 10^{-6} = 0.00204 inch

ϕ = 0.00204/190 = 0.000010 rad = 2.2 seconds

As the man moves to the rear, the slope would go to zero in the center and would be 2.2 sec in the opposite direction for a person standing over the rear jack frame (position 5).
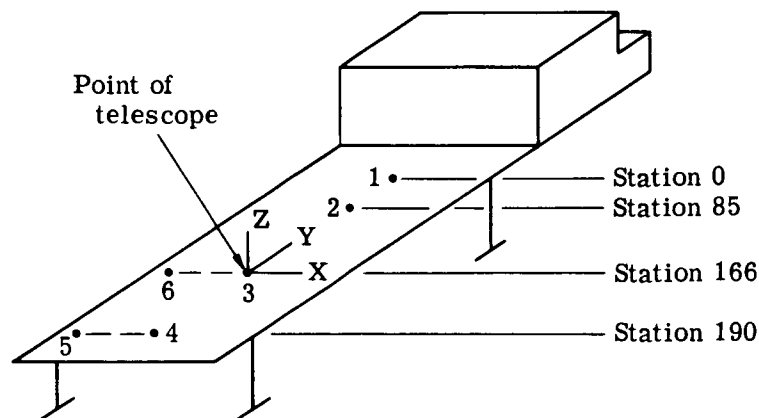
Position of man	YZ error, seconds		XZ error, seconds	
	(a)	(b)	(a)	(b)
1	2.2	1.2	0	
2	4.1		0	
3	.3		0	
4	2.1	1.2	0	
5	2.2		6.5	4.1
6	.3		8.8	6.8

[a]Vehicle on loamy soil

[b]Vehicle on dry, soft, silty clay

Figure C5. - Summary of pointing errors due to movement of a 200-pound man.

The change of slope of the telescope due to the deflection of the van frame for a 200-pound man standing on the van frame (position 2 or 3) is:
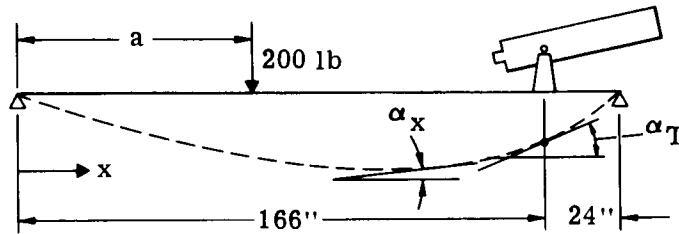
The slope at point x is:

$$\alpha_x = \frac{Wa}{6EIL}\left(2L^2 - 6Lx + 3x^2 + a^2\right) \quad \text{(ref. 17)} \quad x > a$$

The slope at the telescope is: (x = 166)

$$\alpha_T = \frac{Wa}{6EIL}\left(2L^2 - 996L + 82668 + a^2\right) \quad a < 166$$

The position of the 200-pound man to produce a maximum slope at the telescope occurs when $d\alpha/da = 0$

$$\frac{d\alpha_T}{da} = \frac{W}{6EIL}\left(2L^2 - 996L + 82668 + 3a^2\right) = 0$$

$$2 \times 190^2 - 996 \times 190 + 82668 + 3a^2 = 0$$

$$a = 107 \text{ inches}$$

The slope at the telescope due to a 200-pound man standing at station 107 is

$$\alpha_T = \frac{200 \times 107}{6 \times 30 \times 10^6 \times 736 \times 190}\left(2 \times 190^2 - 996 \times 190 + 82668 + 107^2\right)$$

$$\alpha_T = \frac{19.5}{10^6} \text{ rad} = 4.02 \text{ sec}$$

Figure C6 summarizes the above analysis.

The preceding calculations are for the vehicle on loamy sand. Since loamy sand is the softest soil, the pointing errors listed are high. Pointing errors are recalculated for a harder soil, such as dry, soft, silty clay. Figure C5 includes the results of these calculations.

The vertical deflection of the soil is

$$K = 20\ 800\ R_0 \text{ lb/in} \quad \text{(refs. 14, 15, and 16)}$$

$$K = 20\ 800 \times 9 = 187\ 000 \text{ lb/inch}$$

$$\Delta = 1/K = 5.3 \times 10^{-6} \text{ in/lb per pad}$$
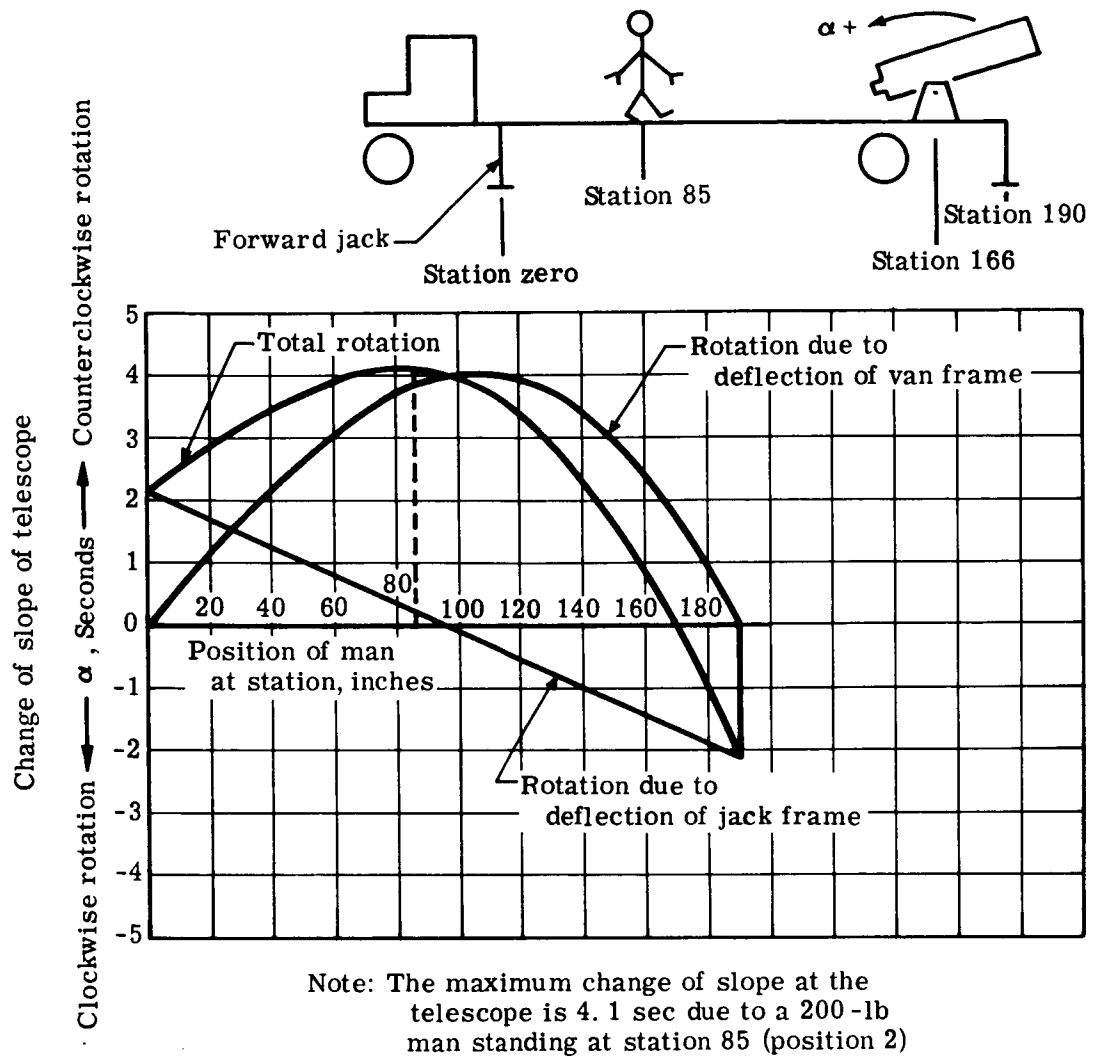
Figure C6. - Summary of pitching direction errors, calculated for loamy sand.

The total vertical deflection of the jack frame and soil is:

$$\Delta = 5.3 \times 10^{-6} \times 0.5 \times 10^{-6} = 5.5 \times 10^{-6} \text{ in/lb}$$

$$K = 180\ 000 \text{ lb/inch}$$

The change of slope of the telescope due to the deflection of the jack frame for a 200-pound man standing over the jack frame (position 1, fig. C5) is:

$$\phi = (200 \times 5.5 \times 10^{-6})/190 = 0.0000058 \text{ rad} = 1.2 \text{ sec}$$

Figure C7 summarizes the above analysis.
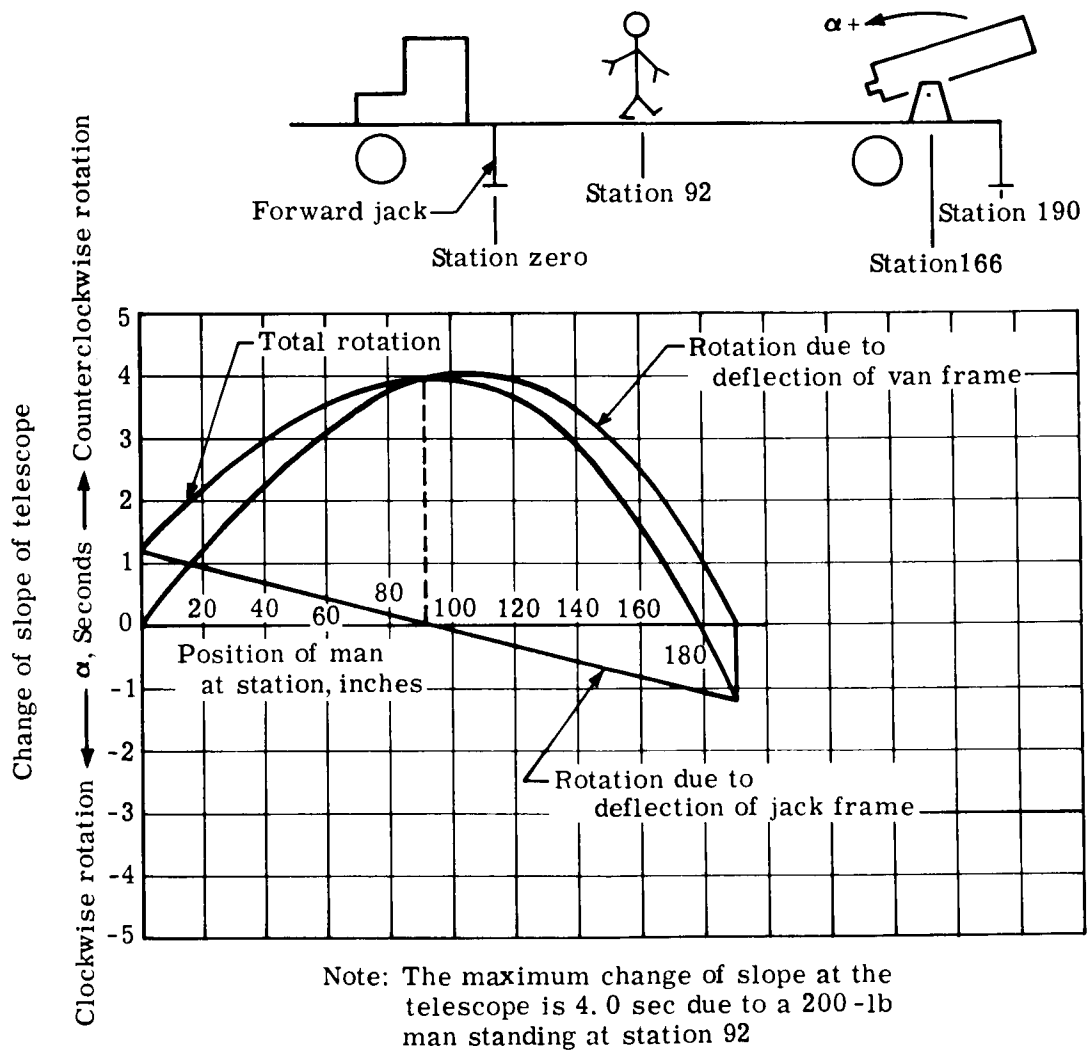
Figure C7. - Summary of pitching direction errors, calculated for dry clay.

Analysis of error in the overturning direction. - The spring rate of the jack frame in the overturning direction is,
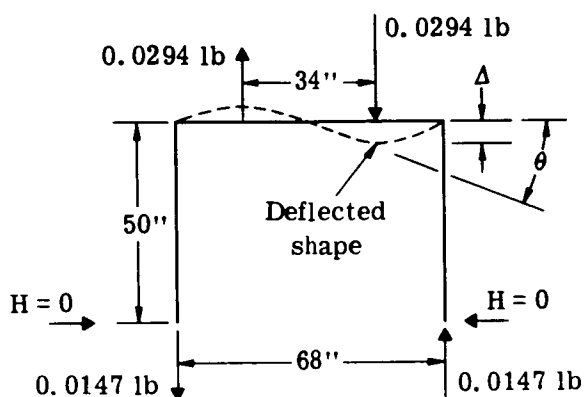
$$\theta = \Delta 2/34$$

$$E\theta = \int \frac{Mmds}{I} + \int \frac{Ppds}{A}$$

$$M_{0 \text{ to } 17} = 0.0147x \qquad\qquad m_{0 \text{ to } 17} = 0.0147x$$

$$M_{0 \text{ to } 17} = 0.249 - 0.0147x \qquad\qquad m_{0 \text{ to } 17} = 0.249 - 0.0147x$$

$$P_{0 \text{ to } 50} = 0.0147 \qquad\qquad p_{0 \text{ to } 50} = 0.0147$$

$$E\theta = 2 \int_0^{17} \frac{0.0147^2 x^2 dx}{342} + 2 \int_0^{17} \frac{(0.249 - 0.0147)^2 dx}{342} + 2 \int_0^{50} \frac{0.0147^2 dx}{4.5}$$

$$E\theta = 0.00206 + 0.00206 + 0.00476 = 0.0088$$

$$\theta = 0.0088/30 \times 10^6 = 0.00029 \times 10^{-6} \text{ rad/in.-lb}$$

$$= 0.0000605 \text{ sec/in-lb}$$

The spring rate of the soil in the overturning direction, calculated for loamy sand, is

$$\Delta = 0.0147 \times 9.7 \times 10^{-6} = \frac{0.142}{10^6} \text{ in/in.-lb}$$

$$\theta = \frac{0.142 x 2}{10^6 x 68} = \frac{0.00417}{10^6} \text{ rad} = 0.00086 \text{ sec/in-lb}$$

$$\text{Total } \theta = 0.00086 + .0000605 = 0.00092 \text{ sec/in-lb}$$
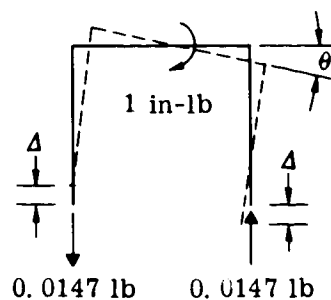
APPENDIX C

The van frame can be treated as a torsion bar supported by two torsion springs, which represent the jack frames, jack, and soil.

Overturning

Fore and aft

$J = 1258 \text{ in}^4$

Spring rate $= 0.00092 \text{ sec/in-lb} = 0.00445 \times 10^{-6} \text{ rad/in-lb}$
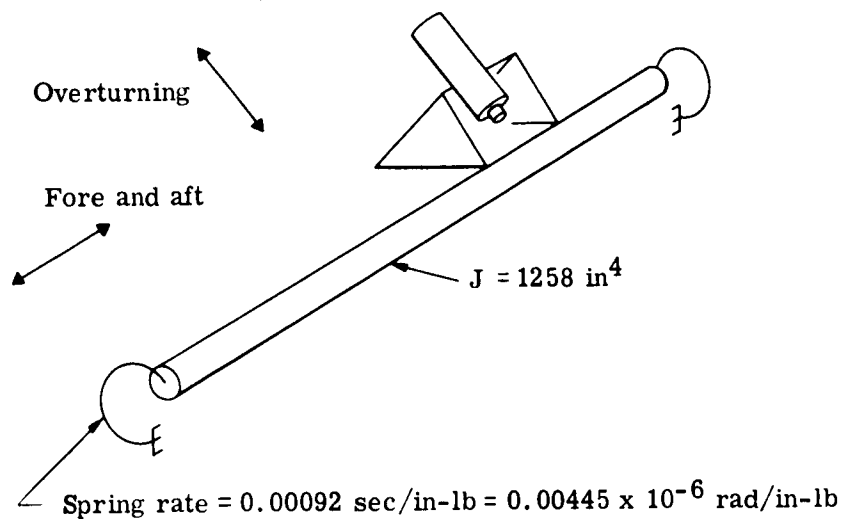
The change of slope of the telescope for a 200-pound man standing on the edge of the van is

$T = T_1 + T_2$
$T = 9600 \text{ in-lb}$
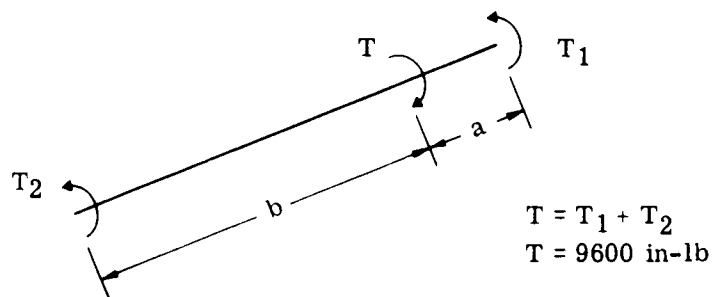
Overturning moment $= 200 \times 48 = 9600 \text{ in-lb}$

The twist of portion b is

$$\gamma_b = T_2 \times 0.00445 \times 10^{-6} + \frac{T_2 b}{GJ}$$

The twist of portion a is

$$\gamma_a = T_1 \times 0.00445 \times 10^{-6} + \frac{T_1 a}{GJ}$$

$$\gamma_b = \gamma_a$$

$$T_2 \times \frac{0.00445}{10^6} + \frac{T_2 b}{11 \times 10^6 \times 1258} = \frac{T_1 a}{11 \times 10^6 \times 1258} + \frac{T_1 \times 0.00445}{10^6}$$

$$T_1 = T(0.00445 + b \; 0.000072)/(0.00890 + a \; 0.000072 + b \; 0.000072)$$

APPENDIX C

Consider the man standing on the rear jack frame. Then a = 0, b = 190.

$$T_1 = 9600 \, (0.00445 + 190 \times 0.000072)/(0.0089 + 190 \times 0.000072)$$

$$T_1 = 7700 \text{ in-lb}$$

$$T_2 = 9600 - 7700 = 1900$$

The slope of the telescope is

$$\theta = \frac{1900 \times 0.00445}{10^6} + \frac{1900 \times 166}{11 \times 10^6 \times 1258} = \frac{31.2 \text{ rad}}{10^6} = 6.4 \text{ sec}$$

Consider the man standing next to the telescope. Then a = 24, b = 166.

$$T_1 = 9600 \, (0.00445 + 166 \times 0.000072)/(0.0089 + 24 \times 0.000072 + 166 \times 0.000072)$$

$$T_1 = 6988 \text{ in-lb}$$

$$T_2 = 2612 \text{ in-lb}$$

The slope of the telescope is

$$\theta = 6.4 \times \frac{2612}{1900} = 8.8 \text{ sec}$$

Consider the man standing on the forward jack frame. Then a = 190, b = 0.

$$T_1 = 9600 \, (0.00445)/(0.00890 + 190 \times 0.000072)$$

$$T_1 = 1900 \text{ in-lb}$$

$$T_2 = 7700 \text{ in-lb}$$

The slope of the telescope is

$$\theta = \frac{1900 \times 0.00445}{10^6} \times \frac{1900 \times 24}{11 \times 10^6 \times 1258} = \frac{11.7 \text{ rad}}{10^6} = 2.4 \text{ sec}$$

Figure C8 summarizes the above analysis.

Van stabilized on loamy sand
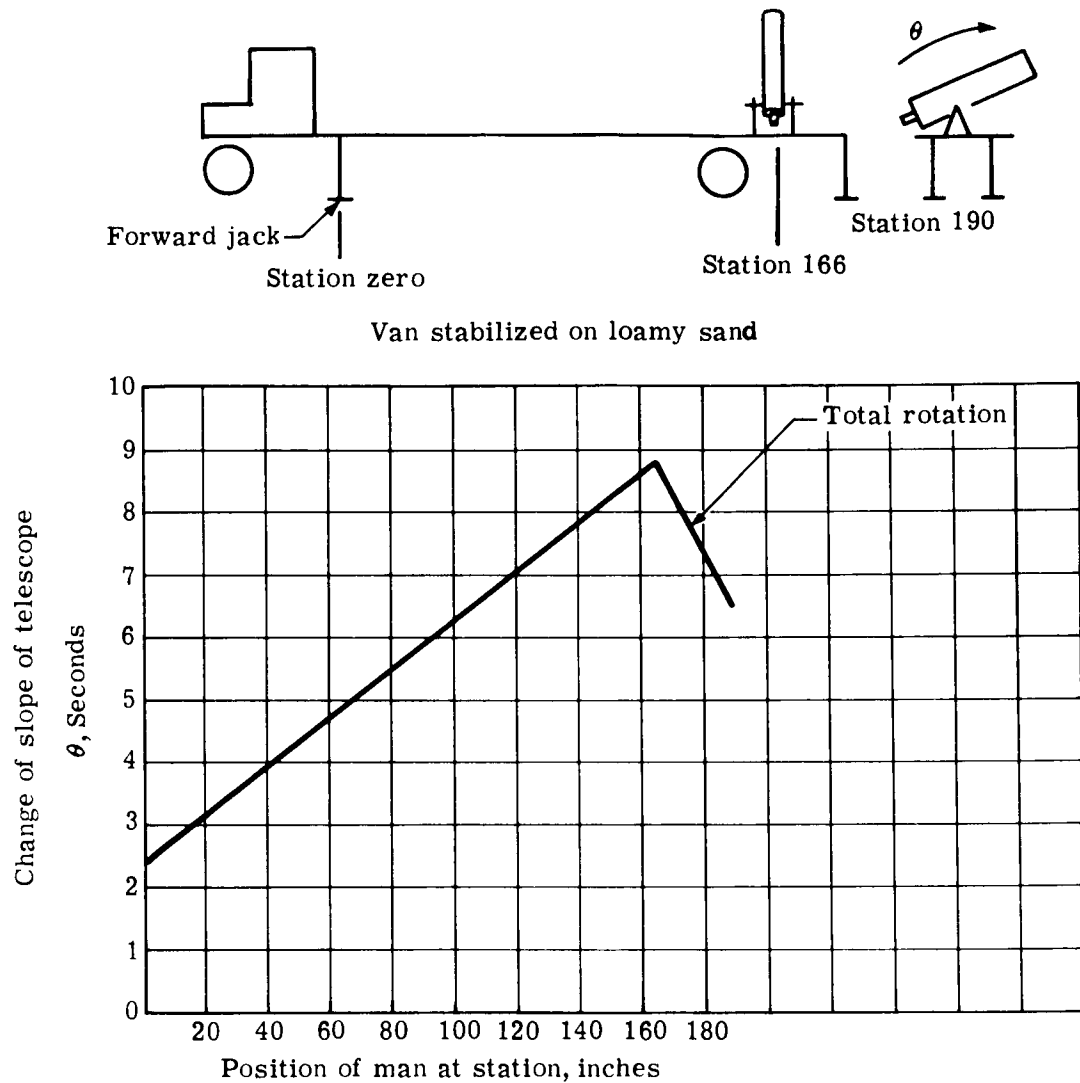
Note: The maximum change of slope at the telescope is 8.8 sec
due to a 200-lb man standing at station 166

Figure C8. - Summary of overturning direction errors, calculated for loamy sand.

The preceding calculations are for the vehicle on loamy sand. The spring rate of the soil in the overturning direction for better soil condition is

$$\Delta = 0.0147 \times 5.3 \times 10^{-6} = 0.0779 \times 10^{-6} \text{ in/in-lb}$$

$$\theta = \frac{0.0779 \times 2}{10^6 \times 68} = 0.00229 \times 10^{-6} \text{ rad/in-lb} = 0.00047 \text{ sec}$$

Total $\theta = 0.0000605 + 0.00047 = 0.00053$ sec/in-lb
or $\theta = 0.00257 \times 10^{-6}$ rad/in-lb

0.0147 lb   0.0147 lb
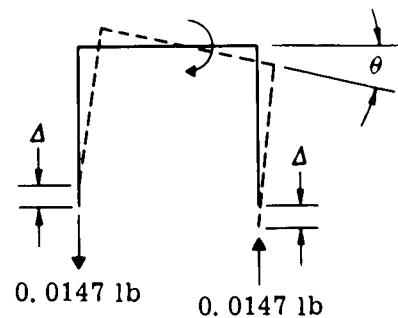
APPENDIX C

Refer to the calculations for loamy sand conditions for an explanation of terms. For the better soil conditions, the equation becomes:

$$\frac{T_2 \times 0.00257}{10^6} + \frac{T_2 b}{11 \times 10^6 \times 1258} = \frac{T_1 a}{11 \times 10^6 \times 1258} + \frac{0.00257\, T_1}{10^6}$$

$$T_1 = T(0.00257 + b\, 0.000072)/(0.00514 + a\, 0.000072 + b\, 0.000072)$$

Consider the man standing on the rear jack frame. Then $a = 0$, $b = 190$.

$$T_1 = 9600\, (0.00257 + 190 \times 0.000072)/(0.00514 + 190 \times 0.000072)$$

$$T_1 = 8280 \text{ in-lb}$$

$$T_2 = 9600 - 8280 = 1320 \text{ in-lb}$$

The slope of the telescope is: (better soil condition)

$$\theta = \frac{1320 \times 166}{11 \times 10^6 \times 1258} + \frac{1320 \times 0.00257}{10^6}$$

$$\theta = 15.8 \times 10^{-6} + 3.4 \times 10^{-6} = 19.2 \times 10^{-6} \text{ rad} = 4.0 \text{ sec}$$

Consider the man standing next to the telescope. Then $a = 24$, $b = 166$.

$$T_1 = 9600\, (0.00257 + 166 \times 0.000072)/(0.00514 + 24 \times 0.000072 + 166 \times 0.000072)$$

$$T_1 = 7400 \text{ in-lb}$$

$$T_2 = 2200 \text{ in-lb}$$

$$\theta = 4.0 \times \frac{2200}{1320} = 6.7 \text{ sec}$$

Consider the man standing on the forward jack frame. Then $a = 190$, $b = 0$.

$$T_1 = 9600\, (0.00257)/(0.00514 + 190 \times 0.000072)$$

$$T_1 = 1300 \text{ in-lb}$$

$$T_2 = 8300 \text{ in-lb}$$
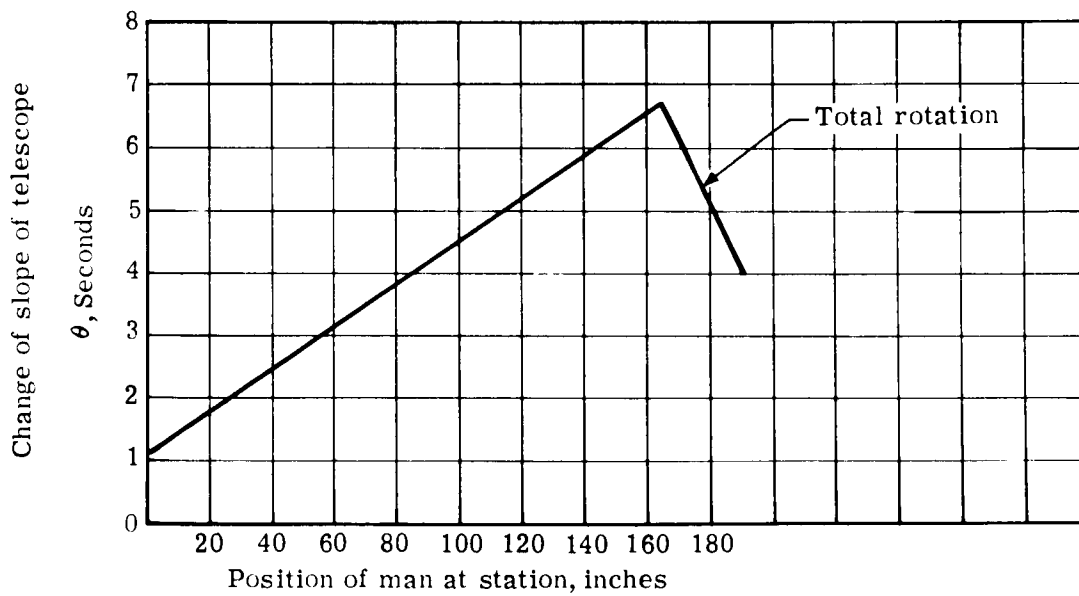
The slope of the telescope is

$$\theta = 1300 \times 0.00257 \times 10^{-6} + \frac{1300 \times 24}{11 \times 10^6 \times 1258} = \frac{5.59 \text{ rad}}{10^6} = 1.15 \text{ sec}$$

Figure C9 summarizes the above analysis.
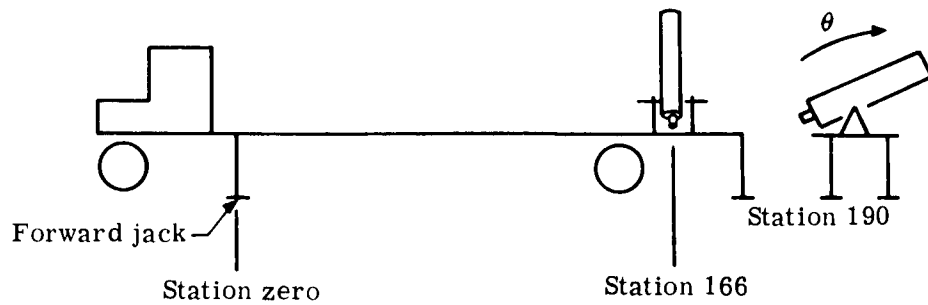
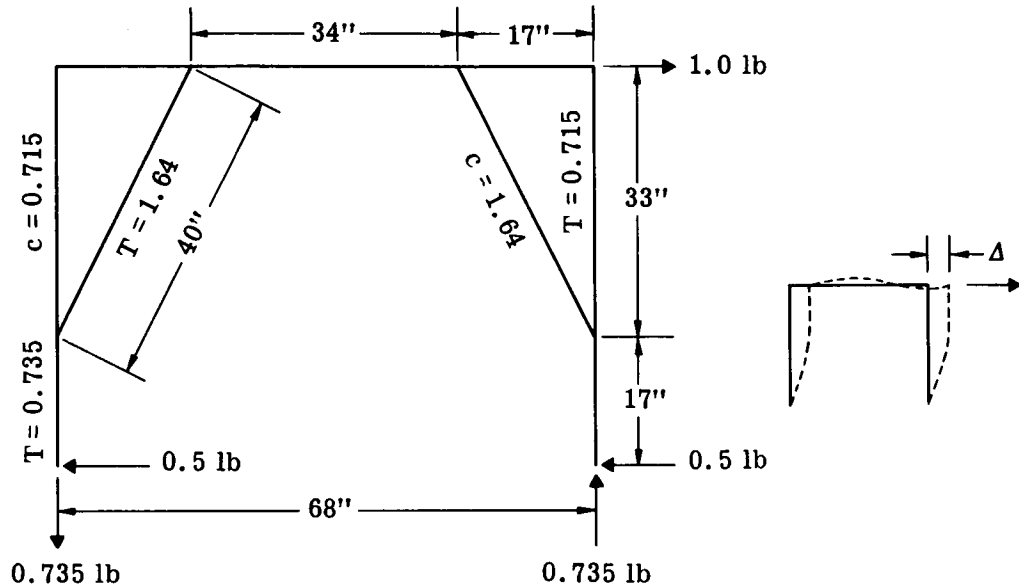Van stabilized on dry, soft, silty clay

Note: The maximum change of slope at the telescope is 6.8 sec
due to a 200-lb man standing at station 166

Figure C9. - Summary of overturning direction errors, calculated for dry clay.

Natural Frequency Analysis

<u>Horizontal natural frequency.</u> - The spring rate of the jack frame in the horizontal direction is as follows:

$$\Delta = \int \frac{MmdS}{EI} + \int \frac{PpdS}{AE}$$

$M_{0\ to\ 17} = 0.5x$		$m = 0.5x$
$M_{0\ to\ 33} = 8.5 - 0.257x$		$m = 8.5 - 0.257x$
$M_{0\ to\ 17} = 0.715x$		$m = 0.715x$
$M_{0\ to\ 17} = 12.15 - 0.735x$		$m = 12.15 - 0.735x$
$P_{0\ to\ 17} = 0.735$		$p = 0.735$
$P_{0\ to\ 33} = 0.715$		$p = 0.715$
$P_{0\ to\ 22} = 0.257$		$p = 0.257$
$P_{0\ to\ 17} = 0.5$		$p = 0.5$
$P_{0\ to\ 40} = 1.64$		$p = 1.64$

$$\frac{E\Delta}{2} = \int_0^{17} \frac{0.5^2 x^2 dx}{18} + \int_0^{33} \frac{(8.5 - 0.257x)^2 dx}{18} + \int_0^{17} \frac{0.715^2 x^2 dx}{167}$$

$$+ \int_0^{17} \frac{(12.15 - 0.735x)^2 dx}{167} + \int_0^{17} \frac{0.735^2 dx}{4.5} + \int_0^{33} \frac{0.715^2 dx}{4.5}$$

$$+ \int_0^{17} \frac{0.257^2 dx}{12.4} + \int_0^{17} \frac{0.5^2 dx}{12.4} + \int_0^{40} \frac{1.64^2 dx}{4.5}$$

$$E\Delta = 45.4 + 88.8 + 10.1 + 25.2 + 3.9 + 4.9 + 0.23 + 0.6 + 23.8 = 202.3$$

$$\Delta = 202.3/30 \times 10^6 = 6.7 \times 10^{-6} \text{ in/lb}$$

The horizontal spring constant of the soil is

$$K = 6300 R_0 = 6300 \times 9 = 56\,700 \text{ lb/in (refs. 14, 15, and 16)}$$

The horizontal deflection of the soil is

$$\Delta = 0.5/56\,700 = 8.8 \times 10^{-6} \text{ in/lb}$$

Total horizontal deflection is

$$\Delta = 8.8 \times 10^{-6} + 6.7 \times 10^{-6} = 15.5 \times 10^{-6} \text{ in/lb}$$

$$K = 10^6/15.5 = 64\,500 \text{ lb/inch}$$

The rotation of the jack frame due to a horizontal load is

$$\theta = \int \frac{Mmdx}{EI} + \int \frac{Ppdx}{EA}$$

$M_{0 \text{ to } 17} = 0.715x$ $m = 0.0147x$

$M_{0 \text{ to } 17} = 12.15 - 0.735x$ $m = 0.249 - 0.0147x$

$P_{0 \text{ to } 17} = -0.735$ $p = -0.0147$

$P_{0 \text{ to } 33} = 0.715$ $p = -0.0147$
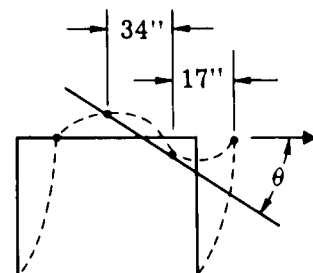
$$\frac{E\theta}{2} = \int_0^{17} \frac{0.715x^2(0.0147)dx}{167} + \int_0^{17} \frac{(12.15-0.735x)(0.249-0.0147x)dx}{167}$$

$$+ \int_0^{17} \frac{0.735(0.0147)dx}{4.5} - \int_0^{33} \frac{0.715(0.0147)dx}{4.5}$$

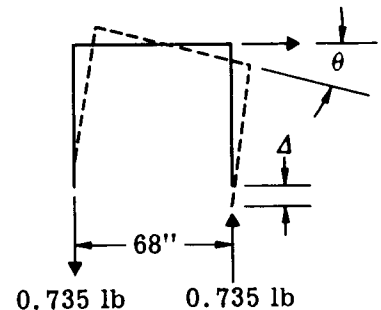$$\frac{E\theta}{2} = 0.103 + 1.04 + 0.0406 - 0.076 = 1.25$$

$$\theta = \frac{1.25 \times 2}{30 \times 10^6} = 0.0833 \times 10^{-6} \text{ rad/lb}$$

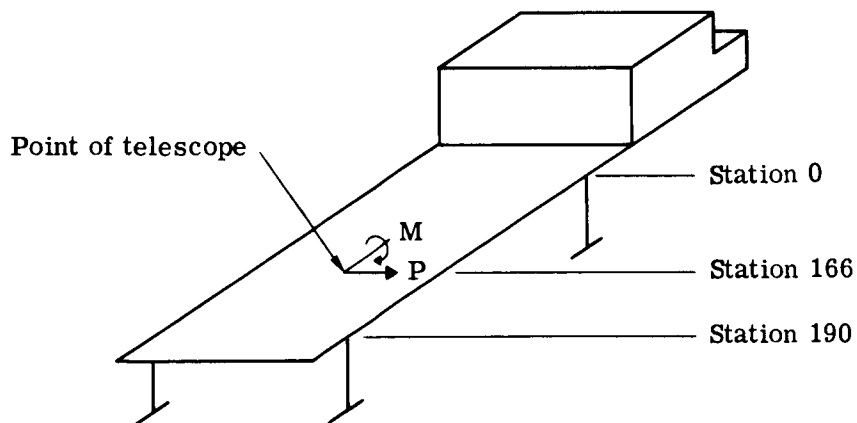Rotation due to soil deflection is calculated as follows:

$$\Delta = 0.735 \times 9.7 \times 10^{-6} = 7.12 \text{ inch} \times 10^{-6}$$

$$\theta = \frac{7.12 \times 2}{10^6 \times 68} = 0.209 \times 10^{-6} \text{ rad/lb}$$

Total $\theta = 0.209 \times 10^{-6} + 0.0833 \times 10^{-6}$

$$= 0.292 \times 10^{-6} \text{ rad/lb.}$$

0.735 lb   0.735 lb

In the horizontal mode the van frame and telescope are treated as a single mass and spring system. Deflections and rotations at the telescope will be found for unit load and moment.

The rotation at the telescope due to a unit moment is

$$\theta = 8.8 \text{ sec}/9600 \text{ in-lb}$$
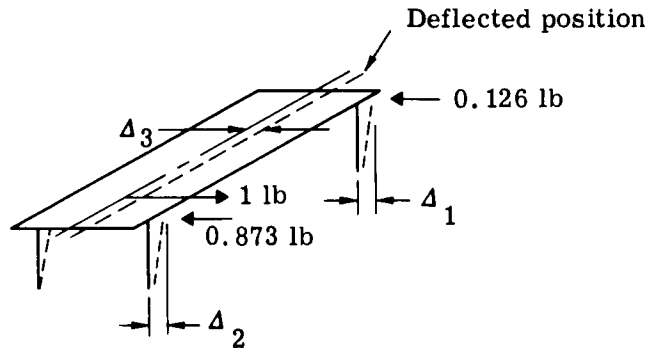
or

$$\theta = 42.6 \times 10^{-6} \text{ rad}/9600 \text{ in-lb}$$

$$\theta = 0.00445 \times 10^{-6} \text{ rad/in-lb}$$

The horizontal deflection of a jack frame, as calculated previously, is $15.5/10^6$ in/lb
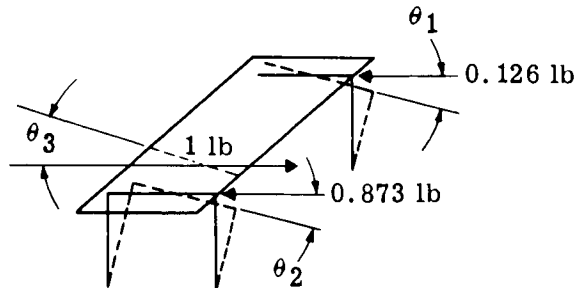

Deflected position

$$\Delta_1 = 0.126 \times 15.5 \times 10^{-6} = 1.95 \times 10^{-6} \text{ in/lb}$$

$$\Delta_2 = 0.873 \times 15.5 \times 10^{-6} = 13.53 \times 10^{-6} \text{ in/lb}$$

$$\Delta_3 = 1.95 \times 10^{-6} + \left(\frac{13.53 - 1.95}{190 \times 10^6} \right) 166 = 12.05 \times 10^{-6} \text{ in/lb}$$

The rotation of a jack frame due to a unit load is 0.292×10^{-6} rad/lb

$$\theta_1 = 0.126 \times 0.292 \times 10^{-6} = 0.036 \times 10^{-6} \text{ rad/lb}$$

$$\theta_2 = 0.873 \times 0.292 \times 10^{-6} = 0.254 \times 10^{-6} \text{ rad/lb}$$

$$\theta_3 = 0.036 \times 10^{-6} + \frac{(0.254 \times 10^{-6} - 0.036 \times 10^{-6})}{190} \times 166 = \frac{0.226}{10^6} \text{ rad/lb}$$

The influence coefficient matrix is

$$K = \begin{bmatrix} 0.00445 & 0.266 \\ 0.266 & 12.05 \end{bmatrix} \times 10^{-6}$$

The mass matrix is

$$M = \begin{bmatrix} 14\,200\,000 & 0 \\ 0 & 10\,700 \end{bmatrix} \times \frac{1}{386}$$

$$U = KM$$

The dynamic matrix "U" is

$$\frac{386 \times 10^6}{\omega^2} \begin{bmatrix} \theta_4 \\ x_4 \end{bmatrix} = \begin{bmatrix} 63\,400 \\ 3\,209\,000 \end{bmatrix} \begin{bmatrix} 2400 \\ 129\,000 \end{bmatrix} \begin{bmatrix} \theta_4 \\ x_4 \end{bmatrix}$$
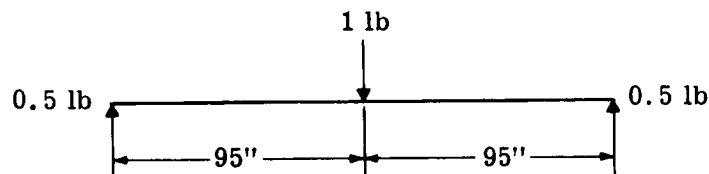
The above is normalized and the results are
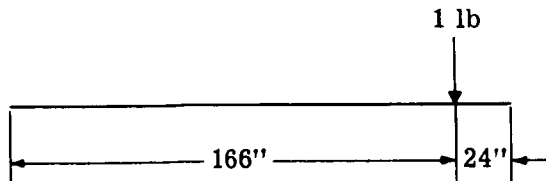
$$\theta_4 = 0.018 \quad x_4 = 1.0$$

$$\frac{10^6\,386}{\omega^2} x_4 = 186\,000 \;; \quad \omega = 45 \text{ rad/sec}$$

$$f = 7.1 \text{ c/s}$$

<u>Vertical natural frequency.</u> - The vertical stiffness of the van frame is

$$\Delta = \frac{PL^3}{48EI} = \frac{1 \times 190^3}{48 \times 30 \times 10^6 \times 736} = 6.49 \times 10^{-6} \text{ in/lb}$$

Deflection under the one-pound load is

$$\Delta = \frac{Pa^2b^2}{3EIL} = \frac{1 \times 166^2 \times 24^2}{3 \times 30 \times 10^6 \times 736 \times 190} = 1.26 \times 10^{-6} \text{ in/lb}$$

Deflection at center of span due to load at 166 inches from left is

$$\Delta = \frac{Pbx}{6EIL} \; (L^2 - b^2 - x^2) = \frac{1 \times 24 \times 95}{6 \times 30 \times 10^6 \times 736 \times 190} \; (190^2 - 24^2 - 95^2) = \frac{2.39}{10^6}$$

The vertical natural frequency of the system is found by the influence coefficient method. The van frame is divided into four parts - the jack frames, the center part, and the telescope area.
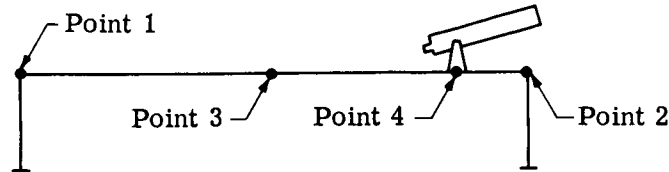
The influence coefficient matrix is

$$K = \begin{bmatrix} 10.2 & 0 & 5.1 & 1.3 \\ 0 & 10.2 & 5.1 & 8.9 \\ 5.1 & 5.1 & 11.6 & 7.5 \\ 1.3 & 8.9 & 7.5 & 9.2 \end{bmatrix} \times 10^{-6}$$

The mass matrix is

$$M = \begin{bmatrix} 1600 & & & \\ & 1600 & & \\ & & 1500 & \\ & & & 6000 \end{bmatrix} \times \frac{1}{386}$$

$$U = KM$$

The dynamic matrix U is

$$\frac{10^6 \; 386}{\omega^2} \begin{bmatrix} z_1 \\ z_2 \\ z_3 \\ z_4 \end{bmatrix} = \begin{bmatrix} 16\,320 & 0 & 7650 & 7800 \\ 0 & 16\,320 & 7650 & 53\,400 \\ 8160 & 8160 & 17\,400 & 45\,000 \\ 2080 & 14\,240 & 11\,250 & 55\,200 \end{bmatrix} \begin{bmatrix} z_1 \\ z_2 \\ z_3 \\ z_4 \end{bmatrix}$$

The above is normalized and the results are
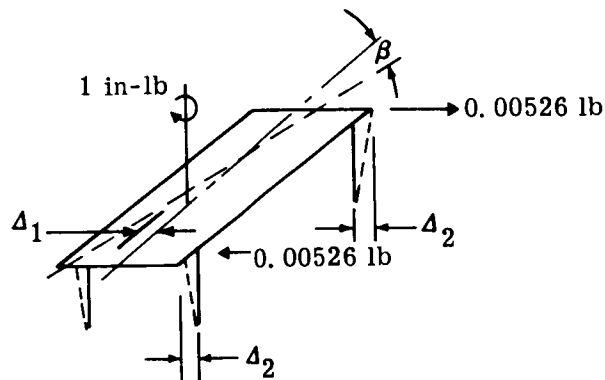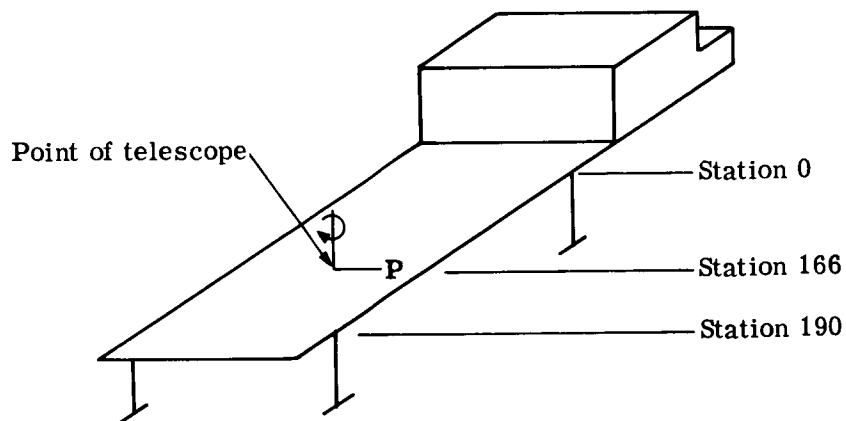
$$z_1 = 0.228, \; z_2 = 0.956, \; z_3 = 0.884, \; z_4 = 1.0$$

$$\frac{10^6 \; 386z_4}{\omega^2} = 79\,200$$

$$\omega^2 = 4800$$

$$\omega = 69 \text{ rad/sec} = 11 \text{ c/s}$$

Azimuth natural frequency. - In the azimuth mode, the van frame and telescope are treated as a single mass and spring system. Rotations and deflections at the telescope will be found for a unit load and moment.

$$\Delta_2 = 0.00526 \times 15.5 \times 10^{-6} = 0.0815 \times 10^{-6} \text{ in/in-lb}$$

$$\beta = \frac{0.0815 \times 10^{-6} \times 2}{190} = 0.000857 \times 10^{-6} \text{ rad/in-lb}$$

$$\Delta_1 = 0.0815 \times 10^{-6} - 0.000857 \times 24 \times 10^{-6} = 0.0609 \times 10^{-6} \text{ in}$$

The influence coefficient matrix is

$$K = \begin{bmatrix} 0.000857 & 0.0609 \\ 0.0609 & 12.05 \end{bmatrix} \times 10^{-6}$$

The mass matrix is

$$M = \begin{bmatrix} 27\ 700\ 000 & 0 \\ 0 & 10\ 700 \end{bmatrix} \times \frac{1}{386}$$

$$U = KM$$

The dynamic matrix "U" is

$$\frac{386 \times 10^6}{\omega^2} \begin{bmatrix} \beta_4 \\ x_4 \end{bmatrix} = \begin{bmatrix} 23\ 738 & 651 \\ 1\ 686\ 930 & 128\ 935 \end{bmatrix} \begin{bmatrix} \beta_4 \\ x_4 \end{bmatrix}$$

The above is normalized and the results are
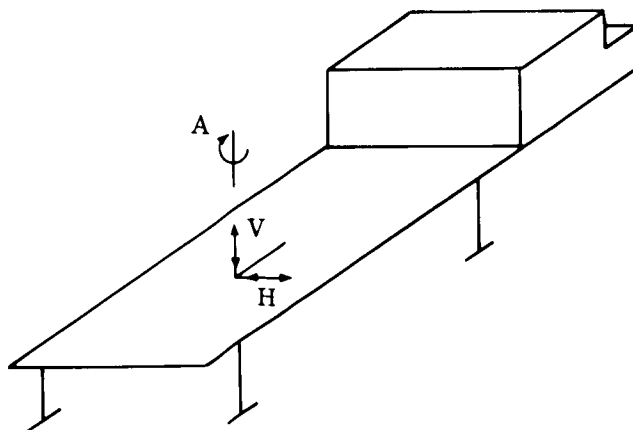
$$\beta_4 = 0.005,\ x_4 = 1.0$$

$$\frac{10^6\ 386}{\omega^2} x_4 = 137\ 300$$

$$\omega = 53\ \text{rad/sec}$$

$$f = 8.5\ \text{c/s}$$

There is coupling between the azimuth and horizontal modes, and the coupled frequency is 6.9 c/s.

Figure C10 summarizes the natural frequency analysis.

Direction	Frequency, c/s
H (uncoupled with A)	7.1
V	11.0
A (uncoupled with H)	8.5
AH	6.9

Figure C10. – Summary of natural frequency analysis.

APPENDIX C

Pointing Error Due to Wind

The drag load on the telescope and frame is 160 pounds due to a 20-mph wind. The overturning moment of the telescope about the center line of the van frame is 7200 in-lb. The pointing error for an overturning moment of 9600 in-lb is 8.8 seconds (2.09). Therefore, the overturn pointing error is 8.8 x 7200/9600 = 6.6 seconds.

The pointing error due to the 160-pound drag load is $160 \times 0.226 \times 10^{-6} = 36.1 \times 10^{-6}$ rad (2.18) = 7.4 seconds. The total pointing error is 6.6 + 7.4 = 14.0 seconds.

The pointing error with the unit on better soil is 9.1 seconds.

APPENDIX D

## ESTIMATED INERTIAS FOR SATELLITE PHOTOMETRIC OBSERVATORY
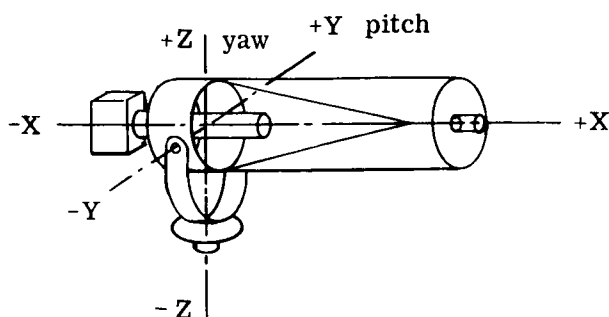
Item	W, lb	X, in	Y, in	Z, in	WX, in-lb	WY, in-lb	WZ, in-lb	WX², lb-in²	WY², lb-in²	WZ², lb-in²	Roll, I_{ox},[a] lb-in²	Pitch, I_{oy},[a] lb-in²	Yaw, I_{oz},[a] lb-in²
Black box	25	-38.0	0	0	- 950	0	0	36 100	0	0	1 068	1 068	1 068
Cell and miscellaneous	250	-16.6	0	0	-4 150	0	0	68 890	0	0		27 700	27 700
Mirror - primary	200	-15.1	0	0	- 302	0	0	4 560	0	0			
Center section	220	- 4.8	0	0	-1 056	0	0	5 069	0	0		24 400	24 400
Struts	55	37.6	0	0	2 068	0	0	77 757	0	0		26 100	26 100
Mirror - secondary	40	65.0	0	0	2 600	0	0	169 000	0	0		5 160	5 160
Outer ring	65	72.0	0	0	4 680	0	0	336 960	0	0		3 660	3 660
Total - pitch axis	855	3.4	0	0	2 890	0	0	698 336				88 088	88 088
Axis transfer												698 336	698 336
Total inertia about ref axes												786 424[b]	786 424[b]
Yoke	400	0	0	-16.0	0	0	-6 400	0	0	102 400			143 000
Total - yaw axis	1 255	2.3	0	- 5.1	2 890	0	-6 400	698 336	0	102 400			231 088
Axis transfer													698 336
Total inertia about ref axes													929 424[c]

[a] Inertia about own axis.

[b] 786 424 lb-in² = 168 slug-ft²

[c] 929 424 lb-in² = 199 slug-ft²

APPENDIX E

WIND LOAD ON TELESCOPE
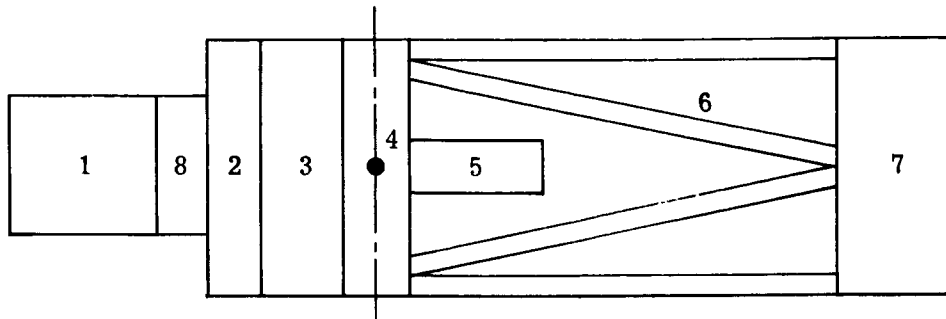
$$q = 0.76 \text{ lb/ft}^2$$

Item	S, ft^2	C_D	$C_D S(q)$, lb	Moment Arm, ft	Torque, ft-lb
1	1.78	1.25	1.69	- 2.70	- 4.56
2	1.67	.6	.76	- 1.22	- .93
3	1.88	1.00	1.43	- .50	- .72
4	.63	1.25	.60	0.00	
5	.47	1.20	.43	.75	+ .32
6	4.88	1.20	4.44	2.33	+10.40
7	3.33	.60	1.52	5.20	+ 7.90
8	1.11	1.25	1.06	- 1.96	- 2.08
					10.33 ft-lb

APPENDIX F

TELESCOPE OPTICS VERIFICATION

Since 1932   **DAVIDSON OPTRONICS, INC.** 2223 RAMONA BOULEVARD, WEST COVINA, CALIFORNIA 91792 Telephone: 962-5181

27 September 1966

Goodyear Aerospace Inc.
1210 Massillon Way
Akron, Ohio

Attention: Richard H. Emmons
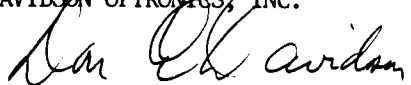   Dept. 454 Plant G

Gentlemen:

I personally inspected and approved the optics for the 24" Cassigrain telescope we furnished to Joseph Nunn Company for your telescope.

The system was tested in collimation against a 48" diameter optical flat using the Foucalt knife edge method. The cut-off was uniform and I judged the system to be of 1/20 wave accuracy. The pinhole image was round and sharp as seen with a high power eyepiece.

Sincerely yours,

DAVIDSON OPTRONICS, INC.

Don E. Davidson
President

DED/d

REFERENCES

1. Anon.: Operation and Service Instructions for NASA Satellite Photometric Observatory. Goodyear Aerospace Corp. for NASA-Langley Research Center, Hampton, Va., 1966.

2. Stewart, Russell D.: Astronomy. Ginn and Company, New York, 1938, p 612.

3. Behr, Alfred: Die Interstellar Polarization des Sternliches in Sonnenumgebung. Nochrichten der Akedemic-Wissenchaften in Gottingen in Mathematisch-Physikalische Klasse. Venderhoeck and Ruprecht, Gottingen, 1959.

4. Tousey, R.: Optical Problems of the Satellite. J. Opt. Soc. Amer, vol. XLVII, 1957, p 261.

5. Tousey, R.: The Visibility of an Earth Satellite. Astronautic Acta, vol II, No. 2, 1956, p. 101-12.

6. Russell, H.N.: On the Albedo of the Planets and Their Satellites. Astrophysical Journal, vol. XLIII, April 1916, p. 173.

7. Emmons, Richard H.: An Indicated Specular Degradation Rate for Aluminized Mylar Surfaces in Near-Earth Orbit from Recent Photometric Observations of the Echo I Satellite. GER-11521, Rev A, Goodyear Aerospace Corp, 17 June 1964.

8. Hardie, R.H.: Photoelectric Reductions. Ch. 8 of Astronomical Techniques, W.A. Hiltner, ed., University of Chicago Press, 1960, p. 178.

9. Iriarte, B.; Johnson, H.L.; Mitchell, R.I.; and Wisniewski, W.K.: Five-Color Photometry of Bright Stars. (Includes the Arizona-Tonantzintla Catalog of 1325 Stars.) Sky and Telescope, July, 1965, p. 21-31.

10. Anon: Ground-Based Photometric Surveillance of the Passive Geodetic Satellite. GER 12762, Goodyear Aerospace Corp. for NASA-Langley Research Center, Hampton, Va., 1966.

11. Hiltner, W.A.: Polarization Measurements. Ch. 10 of Astronomical Techniques, W.A. Hiltner, ed., University of Chicago Press, 1960, p. 229.

12. Treanor, P.J.: The Reduction of Astronomical Polarization Measurements. Ch. 11 of Astronomical Techniques, W.A. Hiltner, ed., University of Chicago Press, 1960, p. 247.

13. Mehr, Morton H.: Engineering Report ER-7071. Measurement Systems, Inc. 140 Water St., Norwalk, Conn.

14. Richart, F.E.: Foundation Vibrations. J. Soil Mech and Foundations, ASCE, vol. 86; SM4, Aug. 1960, p. 1.

15. Arnold, Bycroft, Warburton: Forced Vibrations of a Body on an Infinite Elastic Solid. J. Appl. Mech., ASME, vol. 77, 1955, p. 391-401.

16. Jones, R.: In-Site Measurements of the Dynamic Properties of Soil by Vibration Methods. Geotechnique, vol. VIII, No. 1, March 1953, p. 1-21.

17. Niles, A.S.; and Newell, J.S.: Airplane Structures. Third ed., vol. I, John Wiley and Sons, Inc., 1943.